CRUISE REPORT: RF18-05

Created: June 2024

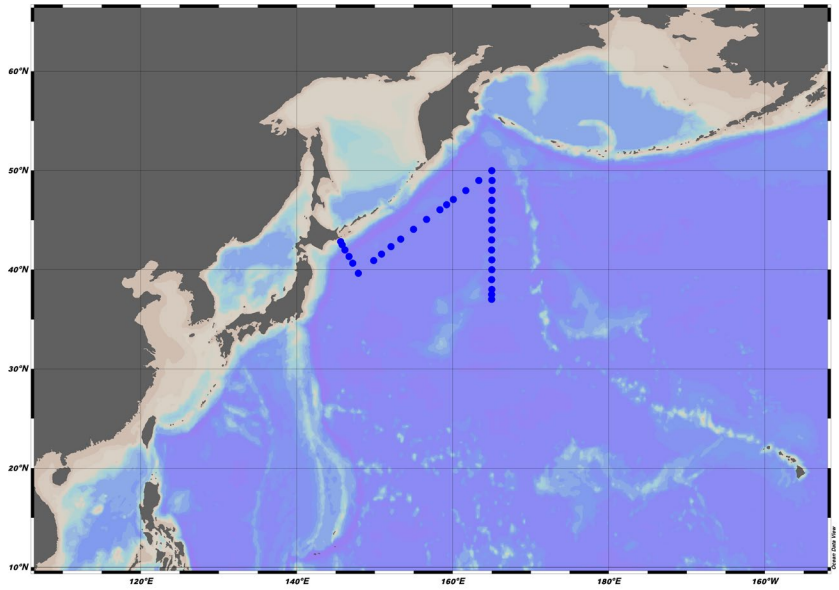

Highlights

Cruise Summary Information

Section Designation	P13
Expedition Designation (ExpoCode)	**49UP20180614**
Chief Scientist	**Keizo SAKURAI / JMA**
Dates	Leg 1: 14 June– 4 July, 2018 Leg 2: 8 July – 22 July, 2018
Ship	R/V *Ryofu Maru*
Ports of Call	Leg 1: Tokyo, JP – Hakodate, JP Leg 2: Hakodate, JP – Tokyo, JP
Geographic Boundaries	49° 99”N 145° 68”E 165° 02”E 37° 02”N
Stations	33
Floats and Drifters Deployed	0
Moorings Deployed and Recovered	0

Contact Information:

Toshiya NAKANO
Marine Division • Global Environment and Marine Department • Japanese Meteorological Agency (JMA)
1-3-4, Otemachi, Chiyoda-ku, Tokyo 100-8122, JAPAN
Phone: +81-3-3212-8341 Ext. 5131• Email:seadata@met.kishou.go.jp

Report assembled by Savannah Lewis

Contents

A. Cruise narrative

1. Highlights

Cruise designation: RF18-05, RF18-06 (WHP-P13 revisit)

a. EXPOCODE: RF18-05 49UP20180614
RF18-06 49UP20180806

b. Chief scientist: Keizo SAKURAI
Marine Division
Global Environment and Marine Department
Japan Meteorological Agency (JMA)

c. Ship name: R/V Ryofu Maru

d. Ports of call: RF18-05: Leg 1: Tokyo (Japan) – Hakodate (Japan)
Leg 2: Hakodate (Japan) – Tokyo (Japan)
RF18-06: Leg 1: Tokyo (Japan) – Pohnpei (FSM)
Leg 2: Pohnpei (FSM) – Tokyo (Japan)
*FSM: Federated States of Micronesia

e. Cruise dates (JST): RF18-05: Leg 1: 14 June 2018 – 4 July 2018
Leg 2: 8 July 2018 – 22 July 2018
RF18-06: Leg 1: 6 August 2018 – 30 August 2018
Leg 2: 3 September 2018 – 27 September 2018

f. Principal Investigator (Contact person):
Toshiya NAKANO
Marine Division
Global Environment and Marine Department
Japan Meteorological Agency (JMA)
1-3-4, Otemachi, Chiyoda-ku, Tokyo 100-8122, JAPAN
Phone: +81-3-3212-8341 Ext. 5131
E-mail: seadata@met.kishou.go.jp

2. Cruise Summary

RF18-05 and RF18-06 cruises were carried out during the period from June 14 to September 27, 2018. The cruise started from the south of Hokkaido, Japan, and sailed southeastern line along the Kuril Islands, thereafter from 50°N to 8°S along approximately 165°E meridian. This line (WHP-P13) was observed by JMA in 2011 as CLIVER (Climate Variability and Predictability Project) / GO-SHIP (Global Ocean Ship-based Hydrographic Investigations Program).

A total of 103 stations were occupied using a Sea-Bird Electronics (SBE) 36 position carousel equipped with 10-liter Niskin water sample bottles, a CTD system (SBE911plus) equipped with SBE35 deep ocean standards thermometer, JFE Advantech oxygen sensor (RINKO III), Teledyne Benthos altimeter (PSA-916D), and Teledyne RD Instruments L-ADCP (300kHz). To examine consistency of data, we carried out the observation repeatedly twice at stations of 47°N, 165°E (Stn.21 and 22), 37°N, 165°E (Stn.33 and 34) and 8°N, 165°E (Stn.73 and 74). Cruise track and station location are shown in Figure A.1.

At each station, full-depth $CTDO_2$ (temperature, conductivity (salinity) and dissolved oxygen) profile were taken, and up to 36 water samples were taken and analyzed. Water samples were obtained from 10 dbar to approximately 10 m above the bottom. In addition, surface water was sampled by a stainless steel bucket at each station. Sampling layer is designed as so-called staggered mesh as shown in Table A.1 (*Swift*, 2010). The bottle depth diagram is shown in Figure A.2.

Water samples were analyzed for salinity, dissolved oxygen, nutrients, dissolved inorganic carbon (DIC), total alkalinity (TA), pH, CFCs (CFC-11, CFC-12, and CFC-113) and phytopigments (chlorophyll-*a* and phaeopigment). Underway measurements of partial pressure of carbon dioxide (pCO_2), temperature, salinity, chlorophyll-*a*, subsurface current, bathymetry and meteorological parameters were conducted along the cruise track.

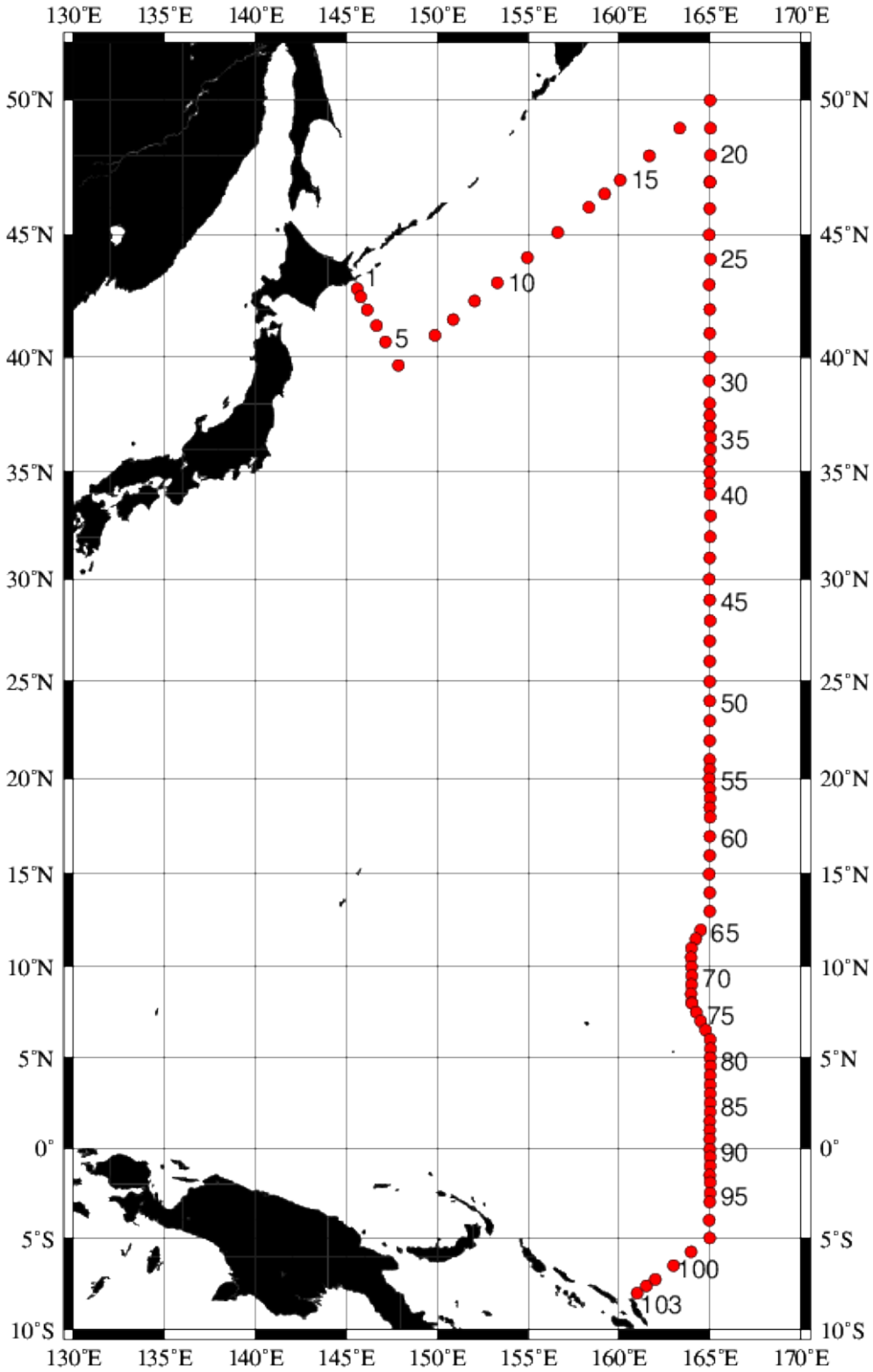

Figure A.1. Location of hydrographic stations of RF18-05 and RF18-06.

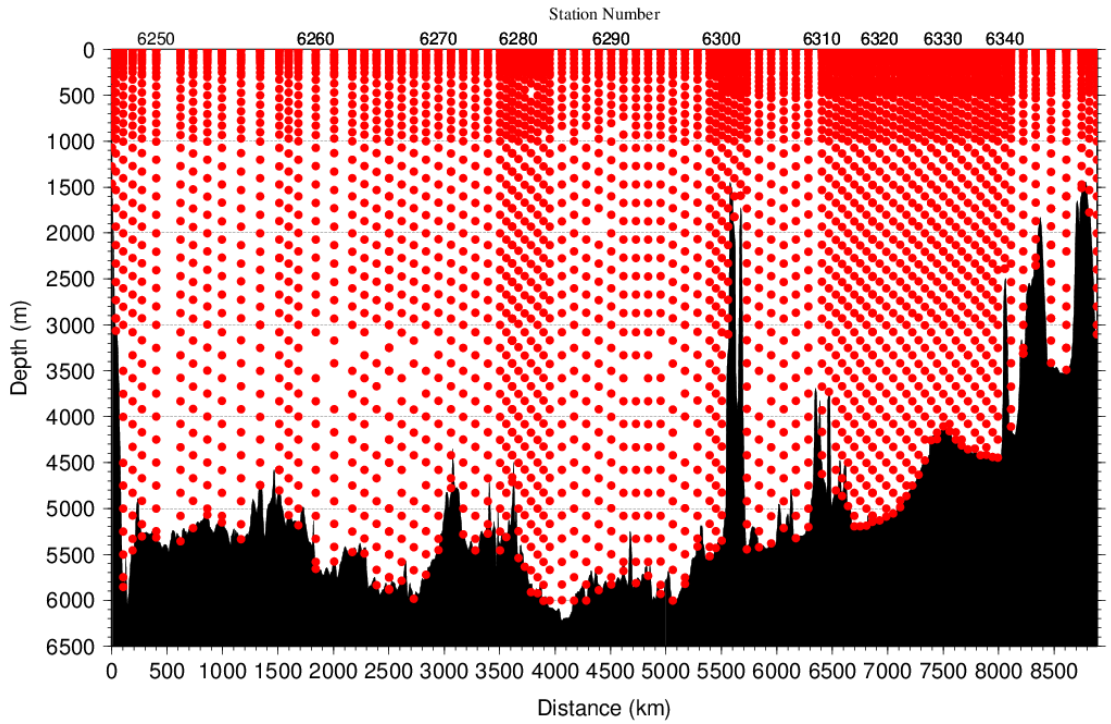

Figure A.2. The bottle depth diagram for WHP-P13 revisit.

Table A.1. The scheme of sampling layer in meters.

Bottle count	***Scheme 1***	***Scheme 2***	***Scheme 3***	***Scheme 4***	***Scheme 5***	***Scheme 6***
1	10	10	10	10	10	10
2	*25*	*25*	*25*	*25*	*25*	*25*
3	50	50	50	50	50	50
4	*75*	*75*	*75*	*75*	*75*	*75*
5	100	100	100	100	100	100
6	*125*	*125*	*125*	*125*	*125*	*125*
7	150	150	150	150	150	150
8	200	200	200	200	200	200
9	250	250	250	250	250	250
10	300	330	280	300	330	280
11	400	430	370	350	380	320
12	500	530	470	400	430	370
13	600	630	570	450	480	420
14	700	730	670	500	530	470
15	800	830	770	600	630	570
16	900	930	870	700	730	670
17	1000	1070	970	800	830	770
18	1200	1270	1130	900	930	870
19	1400	1470	1330	1000	1070	970
20	1600	1670	1530	1200	1270	1130
21	1800	1870	1730	1400	1470	1330
22	2000	2070	1930	1600	1670	1530
23	2200	2270	2130	1800	1870	1730
24	2400	2470	2330	2000	2070	1930
25	2600	2670	2530	2200	2270	2130
26	2800	2870	2730	2400	2470	2330
27	3000	3080	2930	2600	2670	2530
28	*3250*	*3330*	*3170*	*2800*	*2870*	*2730*
29	3500	3580	3420	3000	3080	2930
30	*3750*	*3830*	*3670*	*3250*	*3330*	*3170*
31	4000	4080	3920	3500	3580	3420
32	*4250*	*4330*	*4170*	*3750*	*3830*	*3670*
33	4500	4580	4420	4000	4080	3920
34	*4750*	*4830*	*4670*	*4250*	*4330*	*4170*
35	5000	5080	4920	4500	4580	4420
36	5250	5330	5170	4750	4830	4670
37	5500	5580	5420	5000	5080	4920
38	5750	5830	5670	5250	5330	5170
39	6000	6000	6000	5500	5580	5420
40				5750	5830	5670
41				6000	6000	6000

Scheme 1 to Scheme 3 are applied to the area north of 20°N, while Scheme 4 to Scheme 6 are applied to the area south of 20°N. At some deep stations over 36 layers, some layers shown in italic may be skipped.

Table A.2(a). Station lists of RF18-05 cruise. The 'RF' column indicates the JMA station identification number.

Leg	***Station***		***Location***	
	Stn.	*RF*	*Latitude*	*Longitude*
1	1	6245	42-50.18 N	145-36.48 E
1	2	6246	42-30.93 N	145-48.32 E
1	3	6247	41-59.72 N	146-09.29 E
1	4	6248	41-20.12 N	146-40.60 E
1	5	6249	40-39.71 N	147-09.18 E
1	6	6250	39-39.35 N	147-52.95 E
1	7	6251	40-55.78 N	149-52.16 E
1	8	6252	41-35.03 N	150-52.31 E
1	9	6253	42-20.57 N	152-04.61 E
1	10	6254	43-05.28 N	153-19.20 E
1	11	6255	44-05.06 N	154-57.09 E
1	12	6256	45-04.97 N	156-38.26 E
1	13	6257	46-03.67 N	158-20.28 E
1	14	6258	46-33.33 N	159-12.29 E
1	15	6259	47-04.83 N	160-04.44 E
1	16	6260	47-59.29 N	161-39.94 E
1	17	6261	48-59.67 N	163-20.29 E
1	18	6262	49-59.35 N	165-00.16 E
1	19	6263	48-59.63 N	165-01.21 E
1	20	6264	48-00.63 N	165-01.01 E
1	21	6265	47-00.05 N	164-59.97 E
2	22	6266	47-00.27 N	165-00.42 E
2	23	6267	46-00.05 N	164-59.38 E
2	24	6268	44-59.99 N	164-58.23 E
2	25	6269	44-01.34 N	165-01.00 E
2	26	6270	43-00.88 N	164-58.46 E
2	27	6271	42-00.07 N	164-59.10 E
2	28	6272	41-00.30 N	164-59.99 E
2	29	6273	40-00.45 N	164-59.62 E
2	30	6274	39-00.60 N	164-58.51 E
2	31	6275	38-01.41 N	164-59.87 E
2	32	6276	37-30.89 N	164-59.08 E
2	33	6277	37-01.36 N	164-59.17 E

Table A.2(b). Station lists of RF18-06 cruise.

Leg	Station		Location		Leg	Station		Location	
	Stn.	RF	Latitude	Longitude		Stn.	RF	Latitude	Longitude
1	34	6279	37-01.10 N	164-59.37 E	1	69	6314	9-59.43 N	163-59.60 E
1	35	6280	36-31.46 N	165-02.19 E	1	70	6315	9-29.76 N	164-00.44 E
1	36	6281	36-00.82 N	165-02.64 E	1	71	6316	9-00.61N	163-59.05 E
1	37	6282	35-29.80 N	164-59.61 E	1	72	6317	8-29.99 N	163-58.81 E
1	38	6283	34-57.76 N	164-59.29 E	1	73	6318	8-01.13 N	164-00.75 E
1	39	6284	34-28.57 N	164-59.41 E	2	74	6319	7-59.79 N	164-00.79 E
1	40	6285	33-58.88 N	165-00.20 E	2	75	6320	7-30.04 N	164-15.50 E
1	41	6286	32-59.67 N	165-01.43 E	2	76	6321	7-00.04 N	164-30.19 E
1	42	6287	32-00.36 N	165-00.79 E	2	77	6322	6-30.33 N	164-45.50 E
1	43	6288	31-00.64 N	164-59.94 E	2	78	6323	6-00.75 N	165-00.92 E
1	44	6289	29-59.62 N	164-58.36 E	2	79	6324	5-29.47 N	165-01.23 E
1	45	6290	28-59.54 N	164-59.41 E	2	80	6325	5-00.37 N	165-00.81 E
1	46	6291	27-59.85 N	165-00.41 E	2	81	6326	4-31.00 N	165-01.17 E
1	47	6292	26-59.58 N	164-59.01 E	2	82	6327	4-00.80 N	165-00.88 E
1	48	6293	25-59.32 N	164-59.49 E	2	83	6328	3-30.31 N	165-00.81 E
1	49	6294	24-59.17 N	164-59.86 E	2	84	6329	3-00.18 N	165-00.54 E
1	50	6295	24-00.22 N	164-59.80 E	2	85	6330	2-29.86 N	165-00.30 E
1	51	6296	22-59.72 N	164-59.23 E	2	86	6331	1-59.65 N	165-00.06 E
1	52	6297	21-59.24 N	164-59.56 E	2	87	6332	1-29.73 N	164-59.08 E
1	53	6298	20-59.43 N	164-59.39 E	2	88	6333	0-59.75 N	164-59.58 E
1	54	6299	20-29.87 N	164-59.51 E	2	89	6334	0-29.57 N	164-59.58 E
1	55	6300	20-00.28 N	164-58.05 E	2	90	6335	0-04.44 S	164-59.83 E
1	56	6301	19-30.08 N	164-59.05 E	2	91	6336	0-30.66 S	165-00.40 E
1	57	6302	19-00.14 N	165-00.08 E	2	92	6337	1-00.02 S	165-00.42 E
1	58	6303	18-30.12 N	164-59.52 E	2	93	6338	1-30.10 S	164-59.89 E
1	59	6304	17-59.46 N	165-00.31 E	2	94	6339	1-55.60 S	165-00.83 E
1	60	6305	16-59.60 N	164-59.83 E	2	95	6340	2-29.73 S	165-00.00 E
1	61	6306	15-59.92 N	164-59.51 E	2	96	6341	2-59.05 S	164-59.92 E
1	62	6307	14-59.39 N	164-58.80 E	2	97	6342	3-59.50 S	164-58.84 E
1	63	6308	13-59.54 N	164-59.68 E	2	98	6343	4-59.62 S	164-59.62 E
1	64	6309	12-59.46 N	164-59.51 E	2	99	6344	5-44.17 S	163-58.36 E
1	65	6310	11-59.28 N	164-29.83 E	2	100	6345	6-30.64 S	163-00.11 E
1	66	6311	11-29.56 N	164-14.31 E	2	101	6348	7-15.47 S	162-00.13 E
1	67	6312	10-59.71 N	163-59.29 E	2	102	6347	7-37.42 S	161-30.45 E
1	68	6313	10-29.44 N	163-58.69 E	2	103	6346	8-00.17 S	160-59.70 E

3. List of Principal Investigators for Measurements

The principal investigators for each parameter are listed in Table A.3.

Table A.3. List of principal investigators for each parameter.

Hydrography	$CTDO_2$	Keizo SHUTTA
	Salinity	Keizo SHUTTA
	Dissolve oxygen	Kazuhiro SAITO
	Nutrients	Kazuhiro SAITO
	Phytopigments	Kazuhiro SAITO
	DIC	Kazutaka ENYO
	TA	Kazutaka ENYO
	pH	Kazutaka ENYO
	CFCs	Kazutaka ENYO
	LADCP	Keizo SHUTTA
Underway	Meteorology	Keizo SAKURAI
	Thermo-Salinograph	Kazutaka ENYO
	pCO_2	Kazutaka ENYO
	Chlorophyll *a*	Kazuhiro SAITO
	ADCP	Keizo SHUTTA
	Bathymetry	Keizo SHUTTA

Reference

Swift, J. H. (2010): Reference-quality water sample data: Notes on acquisition, record keeping, and evaluation. *IOCCP Report No.**14**, ICPO Pub. 134, 2010 ver.1*

5. Underway chlorophyll-a

10 October 2021

(1) Personnel

RF18-05

Kazuhiro SAITO (GEMD/JMA)
Daisuke SASANO (GEMD/JMA)
Yoichi IMAI (GEMD/JMA)
Ryoma SUZUKI (GEMD/JMA)
Risa FUJIMOTO (GEMD/JMA)

RF18-06

Yoshihiro SHINODA (GEMD/JMA)
Yoichi IMAI (GEMD/JMA)
Ryoma SUZUKI (GEMD/JMA)
Takuya SASAKI (GEMD/JMA)
Takahiro OKA (GEMD/JMA)

(2) Method

The Continuous Sea Surface Water Monitoring System of fluorescence (Nippon Kaiyo, Japan) automatically had been continuously measured seawater which is pumped from a depth of about 4.5 m below the maximum load line to the laboratory. The flow rate of the surface seawater was controlled by several valves and adjusted to about 0.6 L min^{-1}. The sensor in this system is a fluorometer 10-AU (S/N: 6721, Turner Designs, United States).

(3) Observation log

The chlorophyll-*a* continuous measurements were conducted during the entire cruise; from 14 Jun. to 3 Jul., 2018 in RF 18-05 Leg 1, and from 8 Jul. to 21 Jul., 2018 RF 18-05 in Leg 2, and from 6 Aug. to 26 Aug., 2018 RF 18-06 in Leg 1, and from 4 Sep. to 25 Sep., 2018 RF 18-06 in Leg 2.

(4) Water sampling

Surface seawater was corrected from outlet of water line of the system at nominally 1 day intervals. The seawater sample was measured in the same procedure as hydrographic samples of chlorophyll-*a* (see Chapter C5 “Phytopigments”).

(5) Calibration

At the beginning and the end of legs, a raw fluorescence value of sensor was adjusted in sensitivity of the sensor using deionized water and a rhodamine 0.1ppm solution measured. After the cruise, the fluorescence value was converted to chlorophyll-*a* concentration by programs in the system based on nearby water sampling data (chlorophyll-*a* concentration and distance from location of sensor data).

(6) Data

Underway fluorescence and chlorophyll-*a* data is distributed in JMA format in “49UP20180614_P13_underway_chl.csv”. The record structure of the format is as follows;

Column1 DATE: Date (YYYYMMDD) [JST]
Column2 TIME: Time (HHMM) [JST] (= UTC + 9h)
Column3 LATITUDE: Latitude
Column4 LONGITUDE: Longitude
Column5 FLUOR: Fluorescence value (RFU)
Column6 CHLORA: Chlorophyll-*a* concentration (μg L^{-1})
Column7 BTLCHL: Chlorophyll-*a* concentration of water sampling (μg L^{-1}).

C. Hydrographic Measurement Techniques and Calibration

4. $CTDO_2$ Measurements

8 June 2020

(1) Personnel

RF18-05

Keizo SHUTTA (GEMD/JMA)
Masafumi KASAISHI (GEMD/JMA)
Sho HIBINO (GEMD/JMA)
Keita KAKUYA (GEMD/JMA)
Mitsuho OE (GEMD/JMA)
Yuma KAWAKAMI(GEMD/JMA)

RF18-06

Noriyuki OKUNO(GEMD/JMA)
Kazuaki MINAMI(GEMD/JMA)
Sho HIBINO(GEMD/JMA)
Keita KAKUYA(GEMD/JMA)
Kanako ISSHIKI(GEMD/JMA)

(2) $CTDO_2$ measurement system

(*Software*: SEASAVEwin32 ver7.23.2)

Deck unit	***Serial Number***	***Station***
SBE 11plus (SBE)	0683	RF6245 – 6348
Under water unit	***Serial Number***	***Station***
SBE 9plus (SBE)	69709 (Pressure: 1103)	RF6245 – 6348
Temperature	***Serial Number***	***Station***
SBE 3plus (SBE)	6159 (primary)	RF6245 – 6348
	5632 (secondary)	RF6245 – 6265
	4437 (secondary)	RF6266 – 6348
SBE 35 (SBE)	0062	RF6245 – 6348
Conductivity	***Serial Number***	***Station***
SBE 4C (SBE)	4316 (primary)	RF6245 – 6348
	3697 (secondary)	RF6245 – 6348
Pump	***Serial Number***	***Station***
SBE 5T (SBE)	6021 (primary)	RF6245 – 6348
	5501 (secondary)	RF6245 – 6348
Oxygen	***Serial Number***	***Station***
RINKO III (JFE)	025 (foil number:164313A)	RF6245 – 6348
	283 (foil numner:141304A)	RF6245 – 6348
Water sampler (36 position)	***Serial Number***	***Station***
SBE 32 (SBE)	0734	RF6245 – 6348
Altimeter	***Serial Number***	***Station***
PSA-916D (TB)	43854	RF6245 – 6348
Water Sampling Bottle		***Station***
Niskin Bottle (GO)		RF6245 – 6348

SBE: Sea- Bird Electronics, Inc., USA
TB: Teledyne Benthos, Inc., USA
JFE: JFE Advantech Co., Ltd., Japan
GO: General Oceanics, Inc., USA

(3) Pre-cruise calibration

(3.1) Pressure

S/N 1103, 04 May 2018

c_1	=	–4.282684e+004	t_1	=	3.006702e+001
c_2	=	5.097742e–001	t_2	=	–8.607997e–005
c_3	=	1.312000e–002	t_3	=	3.727820e–006
d_1	=	3.583800e–002	t_4	=	3.699030e–009
d_2	=	0.000000e+000	t_5	=	0.000000e+000

Formula:

$$c = c_1 + c_2 \times U + c_3 \times U^2$$

$$d = d_1 + d_2 \times U$$

$$t_0 = t_1 + t_2 \times U + t_3 \times U^2 + t_4 \times U^3 + t_5 \times U^4$$

U (*degrees Celsius*) = *M* × (*12-bit pressure temperature compensation word*) + *B*

U: temperature in degrees Celsius

S/N 1103 coefficients in SEASOFT (configuration sheet dated on 04 *May 2018)*

M = 1.28040e–002, B = –9.31868e+000

Finally, pressure is computed as

$$P(psi) = c \times (1 - t_0^2 / t^2) \times \left\{1 - d \times (1 - t_0^2 / t^2)\right\}$$

t: pressure period (μsec)

The drift-corrected pressure is computed as

$$Drift\ corrected\ pressure(dbar) = slope \times (computed\ pressure\ in\ dbar) + offset$$

Slope = 1.00000, Offset = −0.4119

(3.2) Temperature (ITS-90): SBE 3plus

S/N 6159(primary), 16 May 2018

g	=	4.32888740e–003	j	=	2.00420537e–006
h	=	6.34148869e–004	f_0	=	1000.0
i	=	2.15687440e–005			

S/N 5632(secondary), 16 May 2018

g	=	4.34075986e–003	j	=	1.39026467e–006
h	=	6.28137960e–004	f_0	=	1000.0
i	=	1.94640009e–005			

S/N 4437(secondary), 16 May 2018

g	=	4.33416905e–003	j	=	1.84196906e–006
h	=	6.37365010e–004	f_0	=	1000.0
i	=	2.11934235e–005			

Formula:

$$Temperature(ITS-90) = \frac{1}{g + h \times \ln(f_0/f) + i \times \ln^2(f_0/f) + j \times \ln^3(f_0/f)} - 273.15$$

f: Instrument freq.[Hz]

(3.3) Deep Ocean Standards Thermometer Temperature (ITS-90): SBE 35

S/N 0062, 25 Mar. 2006

a_0	=	4.41977256e–003	a_3	=	–1.01508095e–005
a_1	=	–1.19652517e–003	a_4	=	2.17345047e–007
a_2	=	1.82077469e–004			

Formula:

$$Linearized\ temperature(ITS{-}90) = 1/\left\{a_0 + a_1 \times \ln(n) + a_2 \times \ln^2(n) + a_3 \times \ln^3(n) + a_4 \times \ln^4(n)\right\} - 273.15$$

n: instrument output

The slow time drift of the SBE 35

S/N 0062, 05 Feb. 2018 (2nd step: fixed point calibration)

Slope = 1.000007, Offset = –0.001105

Formula:

$$Temperature(ITS{-}90) = slope \times (Linearized\ temperature) + offset$$

(3.4) Conductivity: SBE 4C

S/N 4316(primary), 08 May 2018

g	=	–9.86914496e+000	j	=	2.38966478e–004
h	=	1.29073035e+000	CP_{cor}	=	–9.5700e–008
i	=	–2.50542998e–003	CT_{cor}	=	3.2500e–006

S/N 3697(secondary), 08 May 2018

g	=	–9.72827359e+000	j	=	3.65435078e–005
h	=	1.24373812e+000	CP_{cor}	=	–9.5700e–008
i	=	2.22892626e–004	CT_{cor}	=	3.2500e–006

Conductivity of a fluid in the cell is expressed as:

$$C(S/m) = \left(g + h \times f^2 + i \times f^3 + j \times f^4\right) \Big/ \left\{10 \times \left(1 + CT_{cor} \times t + CP_{cor} \times p\right)\right\}$$

f: instrument frequency (kHz)
t: water temperature (degrees Celsius)
p: water pressure (dbar).

(3.5) Oxygen (RINKO III)

RINKO III (JFE Advantech Co., Ltd., Japan) is based on the ability of selected substance to act as dynamic fluorescence quenchers. RINKO III model is designed to use with a CTD system which accept an auxiliary analog sensor, and is designed to operate down to 7000 m.

RINKO III output is expressed in voltage from 0 to 5 V.

(4) Data correction and Post-cruise calibration

(4.1) Temporal change of deck pressure and Post-cruise calibration

S/N 1103, 28 Nov. 2018

c_1	=	–4.282536e+004	t_1	=	3.006750e+001
c_2	=	5.290200e–001	t_2	=	–7.981460e–005
c_3	=	1.312000e–002	t_3	=	3.727820e–006
d_1	=	3.583800e–002	t_4	=	3.699030e–009
d_2	=	0.000000e+000	t_5	=	0.000000e+000

Formula:

$$c = c_1 + c_2 \times U + c_3 \times U^2$$

$$d = d_1 + d_2 \times U$$

$$t_0 = t_1 + t_2 \times U + t_3 \times U^2 + t_4 \times U^3 + t_5 \times U^4$$

U (*degree Celsius*) = *M* × (*12-bit pressure temperature compensation word*) + *B*

U: temperature in degrees Celsius

S/N 1103 coefficients in SEASOFT (configuration sheet dated on 28 *Nov. 2018)*

M = 1.28963e–002, B = –8.30041e+000

Finally, pressure is computed as

$$P(psi) = c \times (1 - t_0^2 / t^2) \times \left\{1 - d \times (1 - t_0^2 / t^2)\right\}$$

t: pressure period (μsec)

The drift-corrected pressure of post-cruise is computed as

$$Drift\ corrected\ pressure(dbar) = slope \times (computed\ pressure\ in\ dbar) + offset$$

S/N 1103, 28 *Nov. 2018*

Slope = 1.00004, Offset = −1.0955

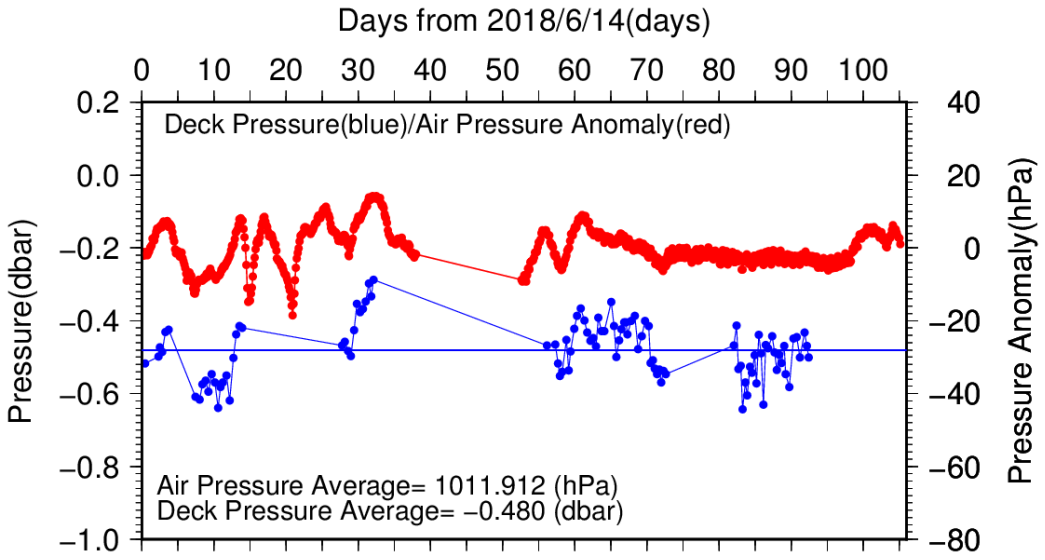

Figure C.1.1. Time series of the CTD deck pressure. Red line indicates atmospheric pressure anomaly. Blue line and dots indicate pre-cast deck pressure and average.

(4.2) Temperature sensor (SBE 3plus)

The practical corrections for CTD temperature data can be made by using a SBE 35, correcting the SBE 3plus to agree with the SBE 35 (*McTaggart et al., 2010*; *Uchida et al., 2007*).

CTD temperature is corrected as

$$Corrected\,temperature = T - (c_0 + c_1 \times P + c_2 \times P^2)$$

T: the CTD temperature (degrees Celsius), *P:* pressure (dbar) and c_0, c_1, c_2: coefficients

Table C.1.1. Temperature correction summary (Pressure ≥ 2000dbar). (Bold: accepted sensor)

S/N	*Num*	c_0*(K)*	c_1*(K/dbar)*	C_2*(K/dbar²)*	*Stations*
6159	**296**	**1.5317030e–3**	**0.0000000e+0**	**0.0000000e+0**	**RF6245 – 6265**
6159	**181**	**1.5547784e–3**	**0.0000000e+0**	**0.0000000e+0**	**RF6266 – 6277**
6159	**582**	**1.2756246e–3**	**0.0000000e+0**	**0.0000000e+0**	**RF6279 – 6318**
6159	**311**	**1.2444344e–3**	**0.0000000e+0**	**0.0000000e+0**	**RF6319 – 6348**
5632	296	1.8070953e–3	–8.6239675e–7	1.3857811e–10	RF6245 – 6265
4437	181	8.2228788e–4	1.9428346e–7	0.0000000e+0	RF6266 – 6277
4437	582	5.3299013e–4	2.0442098e–7	0.0000000e+0	RF6279 – 6318
4437	311	6.6802004e–3	1.6993226e–7	0.0000000e+0	RF6319 – 6348

Table C.1.2. Temperature correction summary for S/N 6159.

Stations	Pressure < 2000dbar			Pressure ≥ 2000 dbar		
	Num	Average (K)	Std (K)	Num	Average (K)	Std (K)
RF6245 – 6265	438	–0.0002	0.0096	296	0.0000	0.0001
RF6266 – 6277	250	–0.0006	0.0059	181	0.0000	0.0001
RF6279 – 6318	803	–0.0002	0.0096	582	0.0000	0.0001
RF6319 – 6348	698	–0.0001	0.0086	311	0.0000	0.0001

Table C.1.3. Temperature correction summary for S/N 5632.

Stations	Pressure < 2000dbar			Pressure ≥ 2000 dbar		
	Num	Average (K)	Std (K)	Num	Average (K)	Std (K)
RF6245 – 6265	438	–0.0016	0.0132	296	0.0000	0.0002

Table C.1.4. Temperature correction summary for S/N 4437.

Stations	Pressure < 2000dbar			Pressure ≥ 2000 dbar		
	Num	Average (K)	Std (K)	Num	Average (K)	Std (K)
RF6266 – 6277	250	0.0000	0.0148	181	0.0000	0.0001
RF6279 – 6318	803	–0.0013	0.0108	582	0.0000	0.0002
RF6319 – 6348	698	–0.0003	0.0087	311	0.0000	0.0002

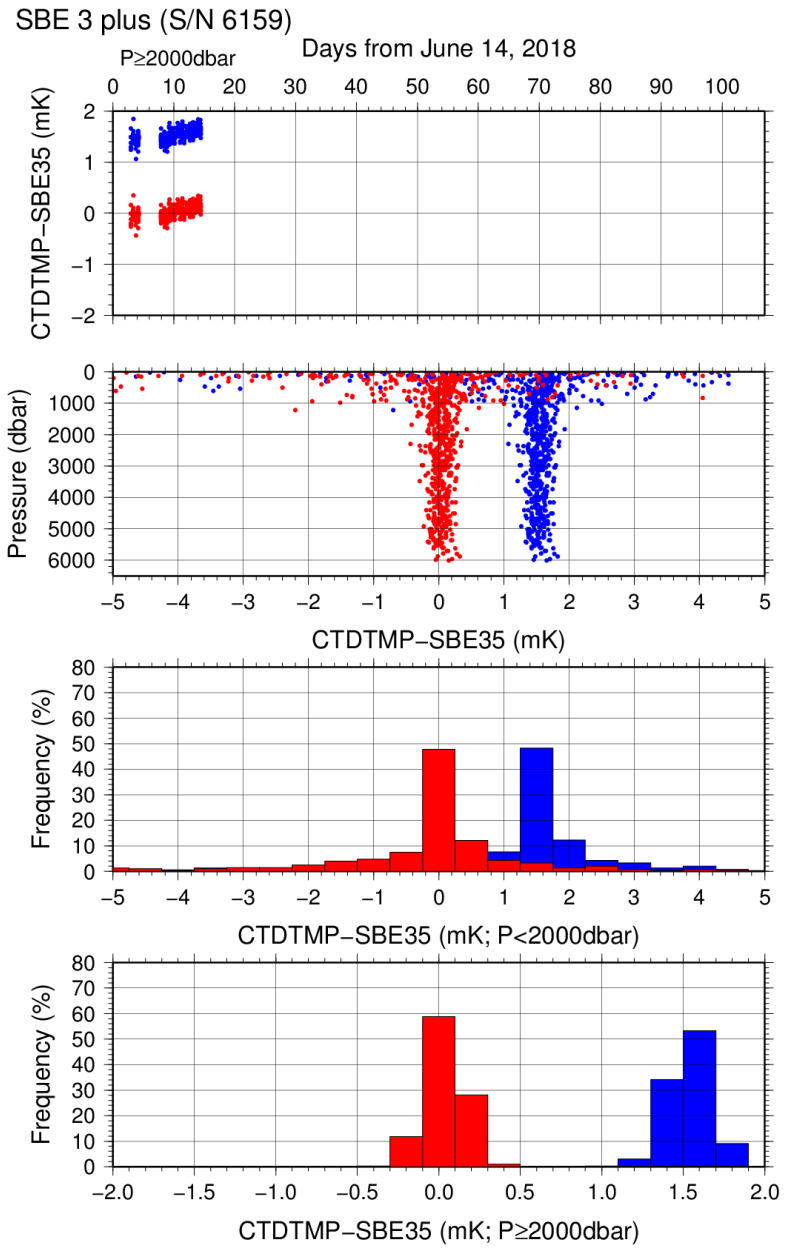

Figure C.1.2. Difference between the CTD temperature (*S/N 6159*) and the Deep Ocean Standards thermometer (SBE 35) at RF18-05 Leg 1. Blue and red dots indicate before and after the correction using SBE 35 data respectively. Lower two panels show histogram of the difference after correction.

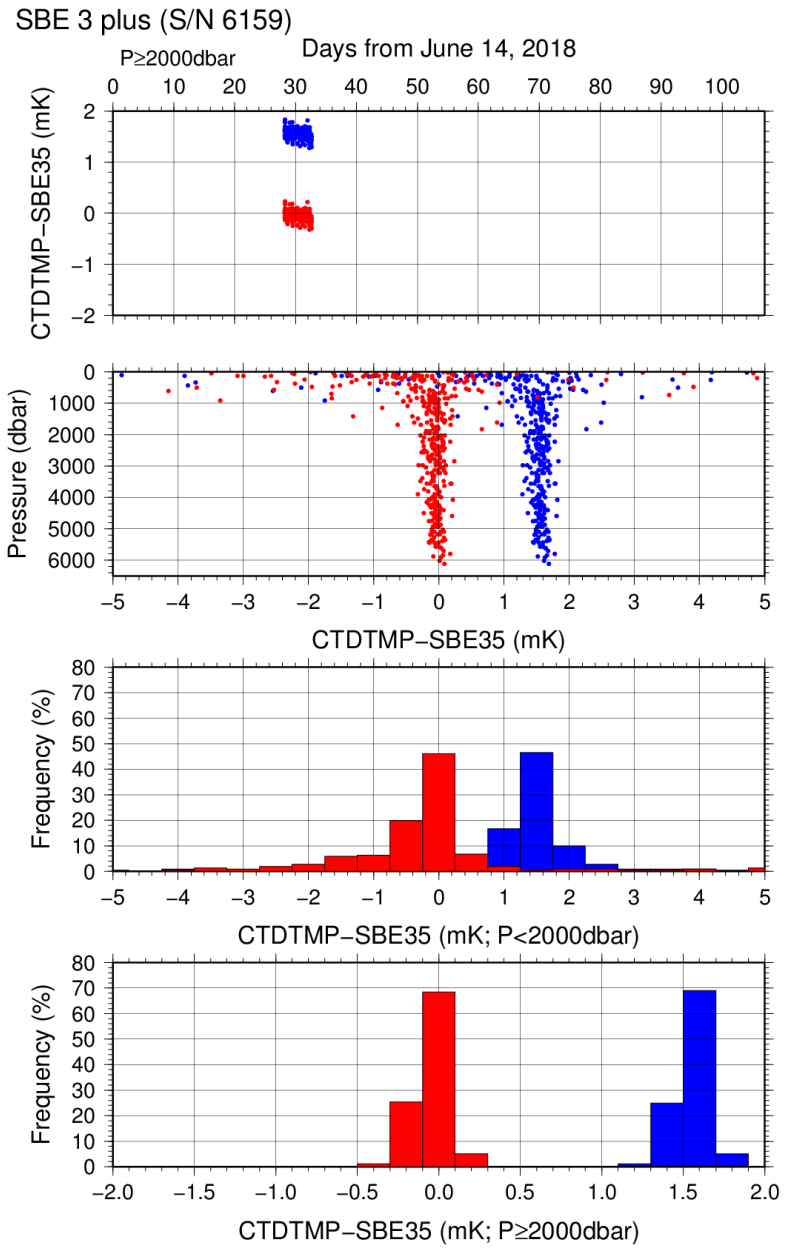

Figure C.1.3. Difference between the CTD temperature (*S/N 6159*) and the Deep Ocean Standards thermometer (SBE 35) at RF18-05 Leg 2. Blue and red dots indicate before and after the correction using SBE 35 data respectively. Lower two panels show histogram of the difference after correction.

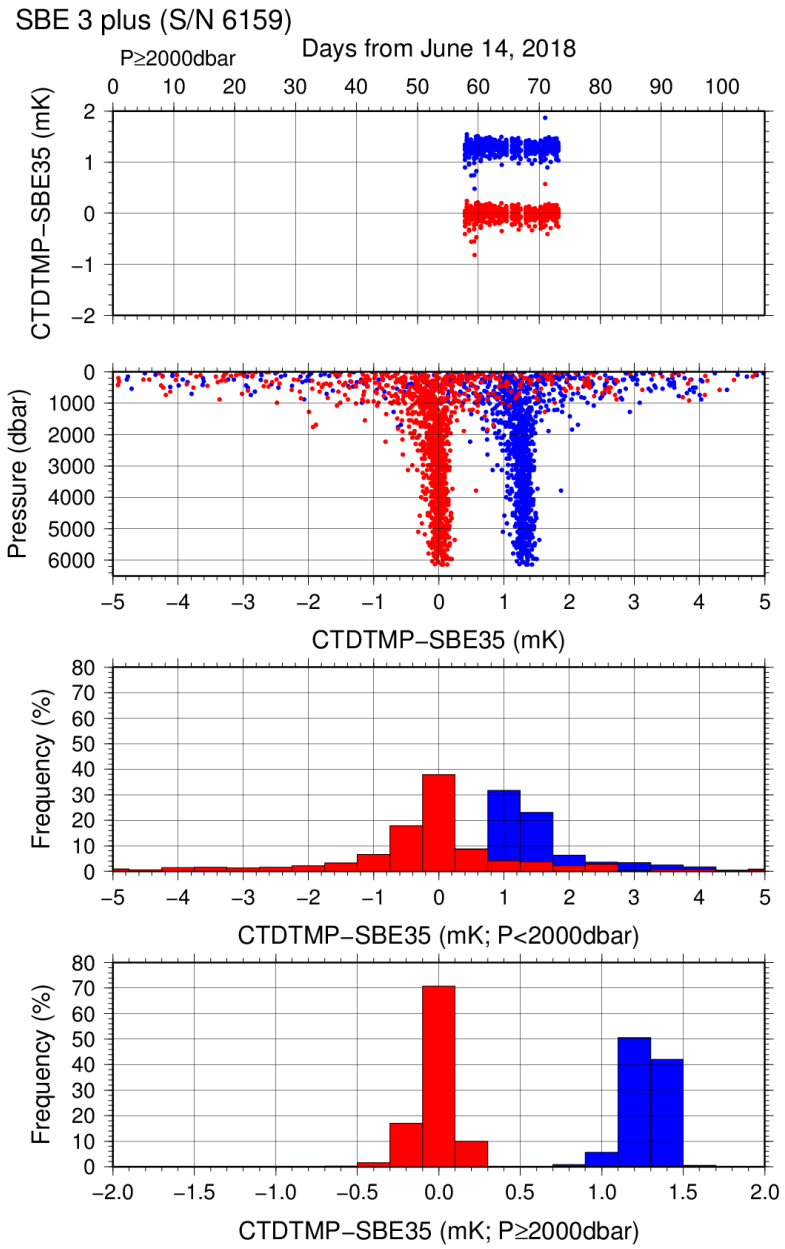

Figure C.1.4. Difference between the CTD temperature (*S/N 6159*) and the Deep Ocean Standards thermometer (SBE 35) at RF18-06 Leg 1. Blue and red dots indicate before and after the correction using SBE 35 data respectively. Lower two panels show histogram of the difference after correction.

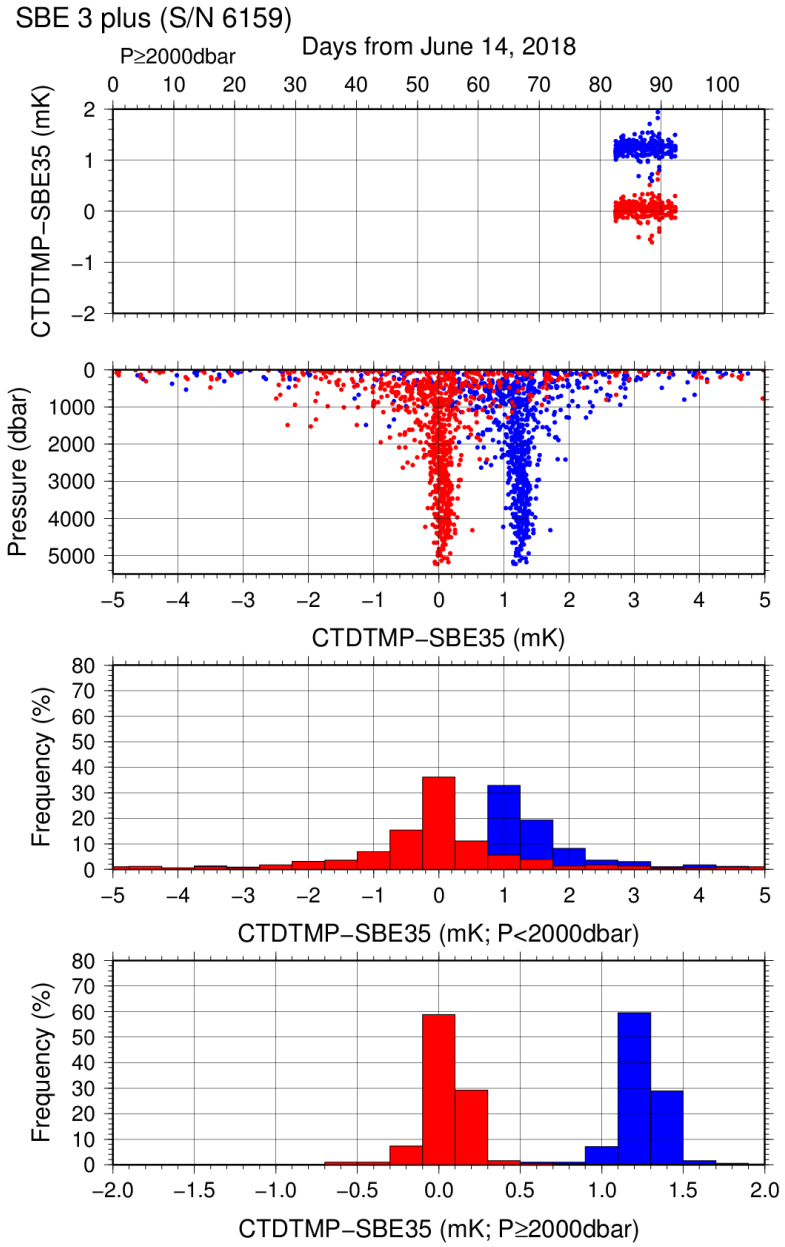

Figure C.1.5. Difference between the CTD temperature (*S/N 6159*) and the Deep Ocean Standards thermometer (SBE 35) at RF18-06 Leg 2. Blue and red dots indicate before and after the correction using SBE 35 data respectively. Lower two panels show histogram of the difference after correction.

Post-cruise sensor calibration for the SBE 3plus

S/N 6159(secondary), 07 Nov. 2018

g	=	4.32895976e–003	j	=	2.03770980e–006
h	=	6.34318807e–004	f_0	=	1000.0
i	=	2.17012423e–005			

S/N 5632(secondary), 07 Nov. 2018

g	=	4.34069736e–003	j	=	1.37997556e–006
h	=	6.28031070e–004	f_0	=	1000.0
i	=	1.94048382e–005			

$$Temperature(ITS-90) = \frac{1}{g + h \times \ln(f_0/f) + i \times \ln^2(f_0/f) + j \times \ln^3(f_0/f)} - 273.15$$

f: Instrument freq.[Hz]

(4.3) Conductivity sensor (SBE 4C)

The practical corrections for CTD conductivity data can be made by using a bottle salinity data, correcting the SBE 4C to agree with measured conductivity (*McTaggart et al., 2010*).

CTD conductivity is corrected

$$Corrected\ Conductivity = C - (\sum_{i=0}^{I} c_i \times C^i + \sum_{j=1}^{J} p_j \times P^j)$$

C: CTD conductivity, c_i and p_j: calibration coefficients
i, j: determined by referring to AIC (*Akaike*, 1974). According to *McTaggart et al.* (2010), maximum of I and J are 2.

Table C.1.5. Conductivity correction coefficient summary. (Bold: accepted sensor)

S/N	*Num*	c_0(S/m)	c_1	c_2(m/S)	*Stations*
			p_1(S/m/dbar)	p_2(S/m/dbar^2)	
4316	**737**	**6.8376e–5**	**0.0000e+0**	**0.0000e+0**	**RF6245 – 6265**
			1.0051e–7	**–8.7310e–12**	
4316	**444**	**4.1046e–3**	**–2.1478e–3**	**2.7719e–4**	**RF6266 – 6277**
			6.0074e–8	**0.0000e+0**	
4316	**1425**	**4.1099e–3**	**–2.0082e–3**	**2.4479e–4**	**RF6279 – 6318**
			4.0697e–8	**0.0000e+0**	
4316	**1082**	**2.0665e–3**	**–1.0976e–3**	**1.4965e–4**	**RF6319 – 6348**
			5.5960e–8	**0.0000e+0**	
3697	737	1.3995e–4	0.0000e+0	0.0000e+0	RF6245 – 6265
			2.9761e–8	–4.7258e–12	
3697	442	2.2821e–3	1.0481e–2	1.1829e–3	RF6266 – 6277
			7.4386e–9	0.0000e+0	
3697	1425	3.6248e–3	–1.6768e–3	1.7908e–4	RF6279 – 6318
			5.2588e–9	0.0000e+0	
3697	1082	–2.7818e–5	–2.2536e–5	0.0000e+0	RF6319 – 6348
			5.7845e–8	–3.0030e–12	

Table C.1.6. Conductivity correction and salinity correction summary for S/N 4316.

Stations	Pressure < 1900dbar					
	Conductivity			Salinity		
	Num	Average (S/m)	Std (S/m)	Num	Average	Std
RF6245 – 6265	418	0.0000	0.0002	418	0.0001	0.0019
RF6266 – 6277	241	0.0000	0.0001	241	0.0001	0.0016
RF6279 – 6318	805	0.0000	0.0002	805	0.0001	0.0022
RF6319 – 6348	705	0.0000	0.0004	705	0.0000	0.0031
Stations	Pressure ≥ 1900 dbar					
	Conductivity			Salinity		
	Num	Average (S/m)	Std (S/m)	Num	Average	Std
RF6245 – 6265	319	0.0000	0.0000	319	–0.0001	0.0005
RF6266 – 6277	203	0.0000	0.0000	203	0.0000	0.0005
RF6279 – 6318	620	0.0000	0.0000	620	0.0000	0.0006
RF6319 – 6348	377	0.0000	0.0000	377	–0.0001	0.0006

Table C.1.7. Conductivity correction and salinity correction summary for S/N 3697.

Stations	Pressure < 1900dbar					
	Conductivity			Salinity		
	Num	Average (S/m)	Std (S/m)	Num	Average	Std
RF6245 – 6265	418	0.0000	0.0002	418	0.0001	0.0019
RF6266 – 6277	239	0.0000	0.0001	239	0.0000	0.0015
RF6279 – 6318	805	0.0000	0.0002	805	0.0000	0.0022
RF6319 – 6348	705	0.0000	0.0004	705	0.0000	0.0031
Stations	Pressure ≥ 1900 dbar					
	Conductivity			Salinity		
	Num	Average (S/m)	Std (S/m)	Num	Average	Std
RF6245 – 6265	319	0.0000	0.0000	319	–0.0001	0.0005
RF6266 – 6277	203	0.0000	0.0000	203	0.0000	0.0005
RF6279 – 6318	620	0.0000	0.0001	620	–0.0001	0.0007
RF6319 – 6348	377	0.0000	0.0000	377	0.0000	0.0006

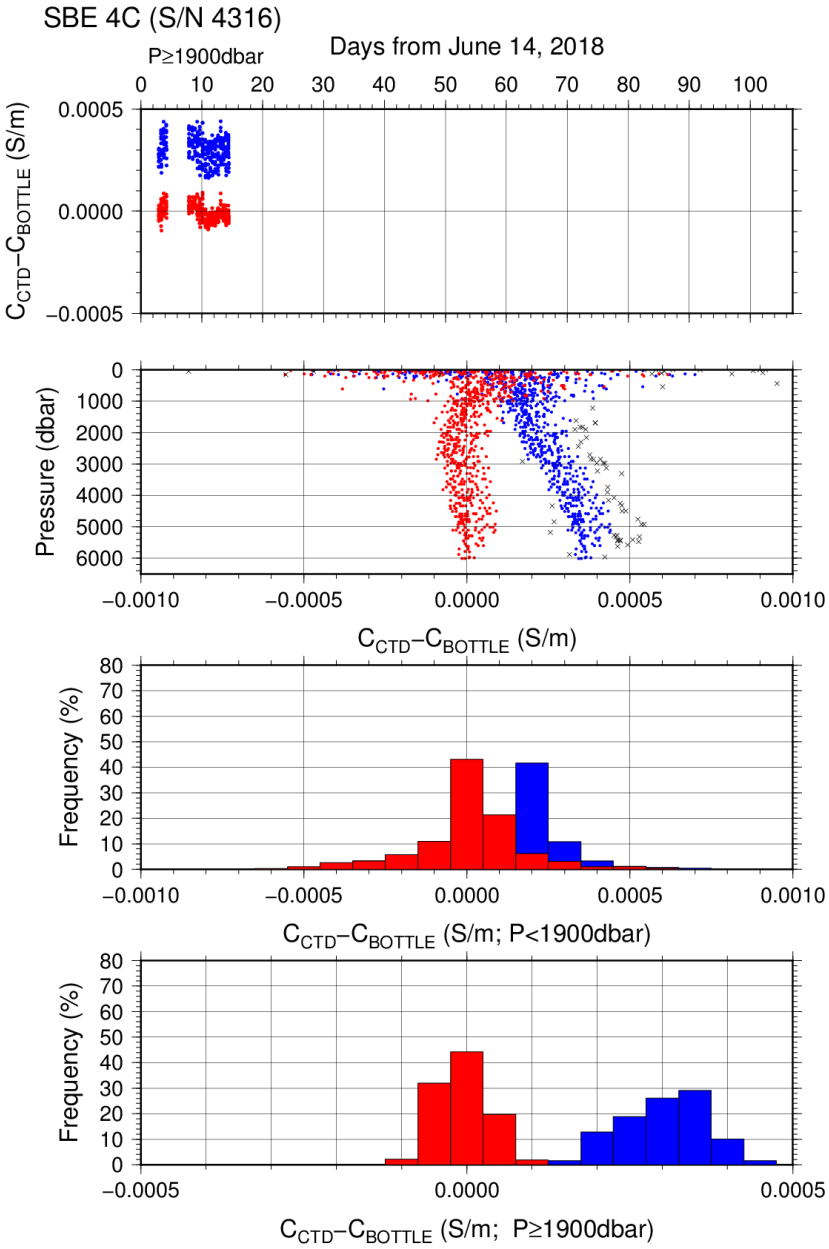

Figure C.1.6. Difference between the CTD conductivity (*S/N 4316*) and the bottle conductivity at RF18-05 Leg 1. Blue and red dots indicate before and after the calibration using bottle data respectively. Lower two panels show histogram of the difference before and after calibration.

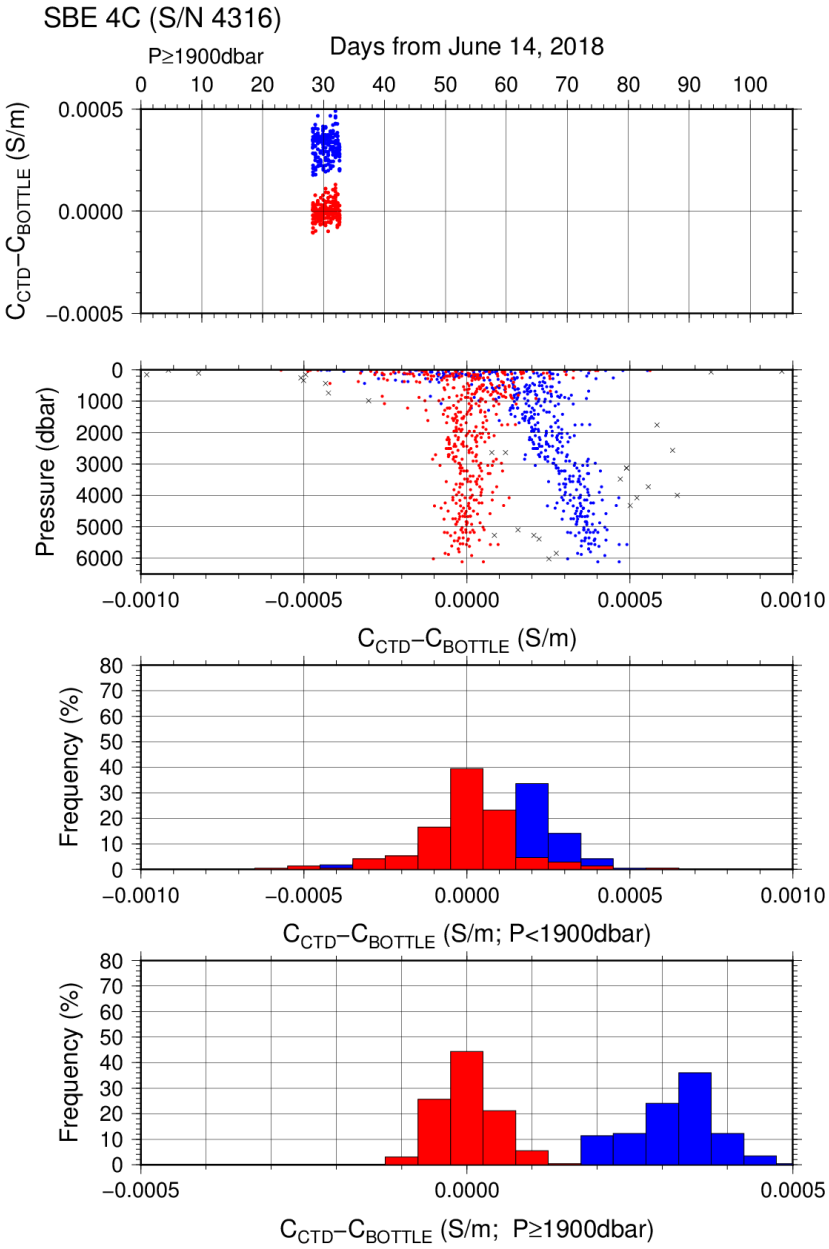

Figure C.1.7. Difference between the CTD conductivity (*S/N 4316*) and the bottle conductivity at RF18-05 Leg 2. Blue and red dots indicate before and after the calibration using bottle data respectively. Lower two panels show histogram of the difference before and after calibration.

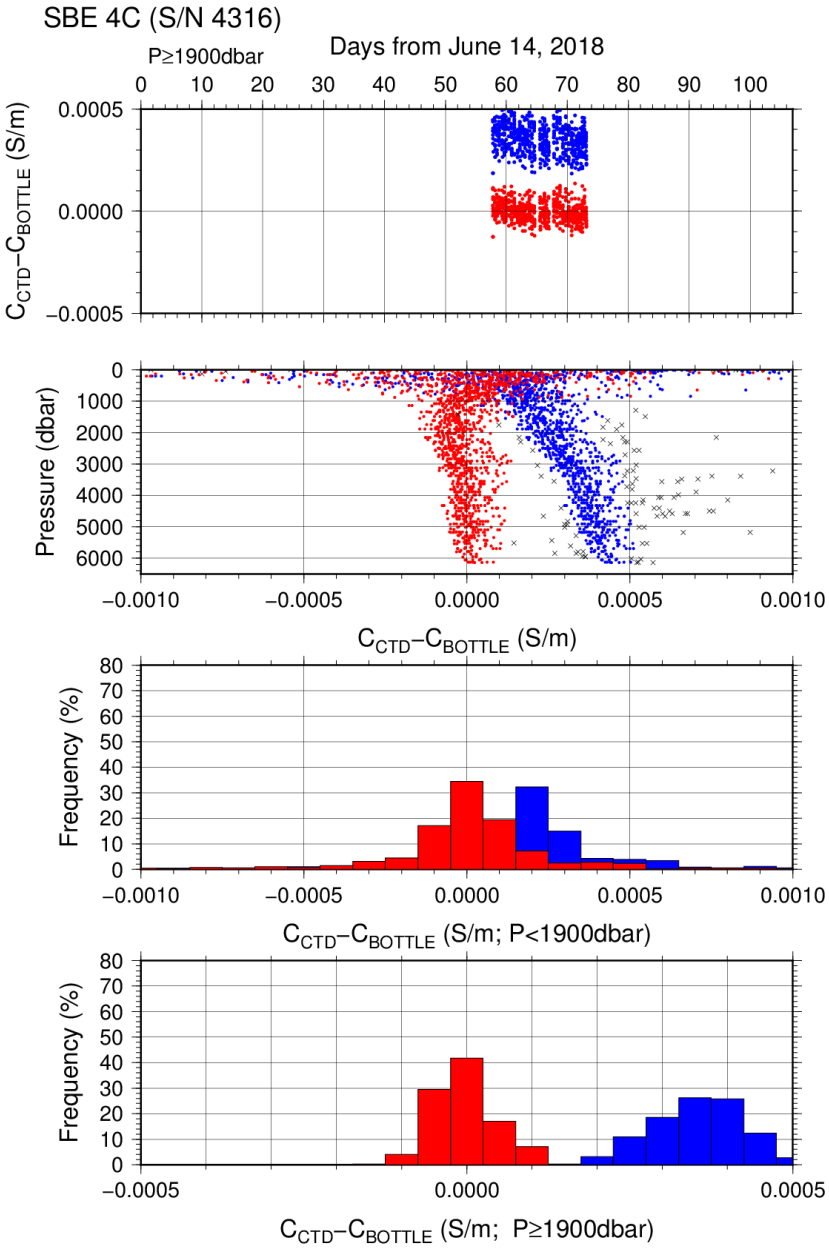

Figure C.1.8. Difference between the CTD conductivity (*S/N 4316*) and the bottle conductivity at RF18-06 Leg 1. Blue and red dots indicate before and after the calibration using bottle data respectively. Lower two panels show histogram of the difference before and after calibration.

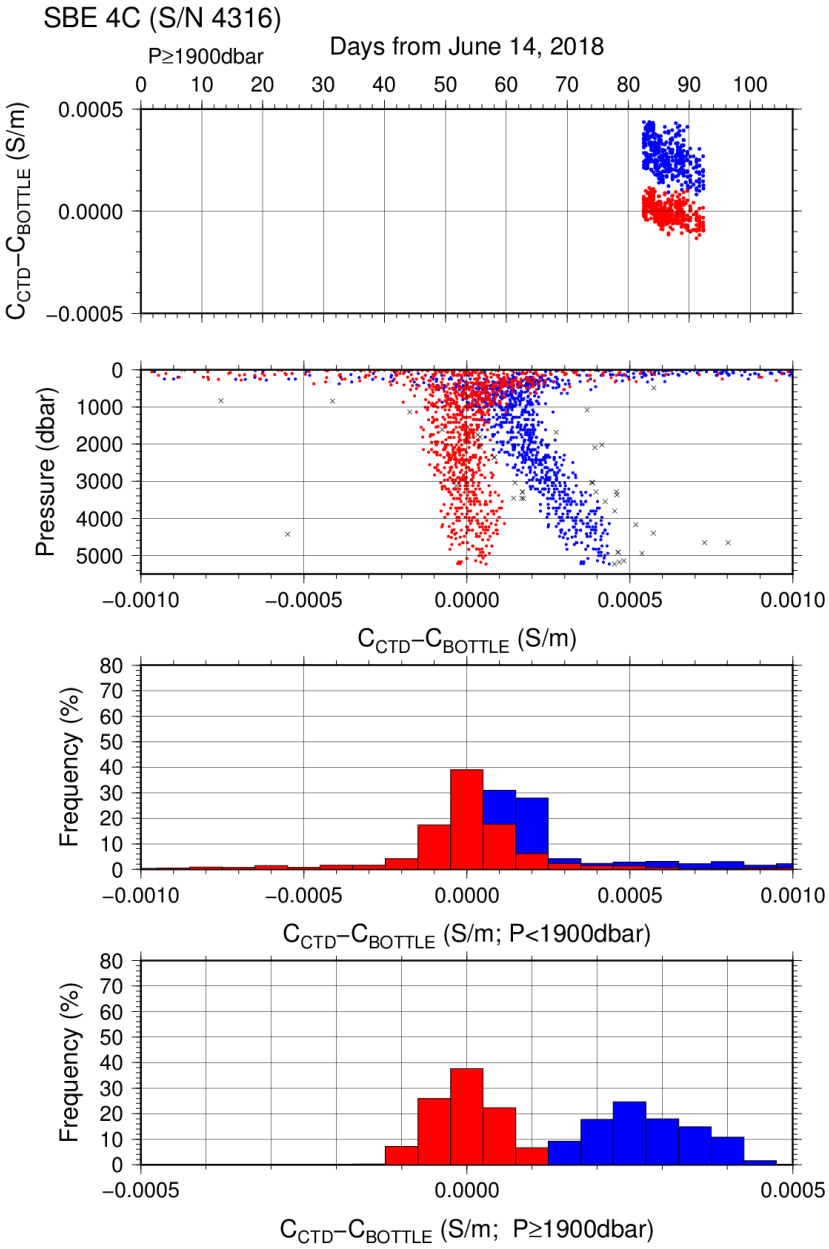

Figure C.1.9. Difference between the CTD conductivity (*S/N 4316*) and the bottle conductivity at RF18-06 Leg 2. Blue and red dots indicate before and after the calibration using bottle data respectively. Lower two panels show histogram of the difference before and after calibration.

Post-cruise sensor calibration for the SBE 4C

S/N 4316(primary), 26 Oct. 2018

g	=	–9.87493388e+000	j	=	2.65931934e–004
h	=	1.29237672e+000	CP_{cor}	=	–9.5700e–008
i	=	–2.90530737e–003	CT_{cor}	=	3.2500e–006

S/N 3697(secondary), 26 Oct. 2018

g	=	–9.73127203e+000	j	=	5.76368338e–005
h	=	1.24473240e+000	CP_{cor}	=	–9.5700e–008
i	=	-4.11024108e–005	CT_{cor}	=	3.2500e–006

Conductivity of a fluid in the cell is expressed as:

$$C(S/m) = \left(g + h \times f^2 + i \times f^3 + j \times f^4\right) \Big/ \left\{10 \times \left(1 + CT_{cor} \times t + CP_{cor} \times p\right)\right\}$$

f: instrument frequency (kHz)
t: water temperature (degrees Celsius)
p: water pressure (dbar).

(4.4) Oxygen sensor (RINKO III)

The CTD oxygen is calculated using RINKO III output (voltage) by the Stern-Volmer equation, according to a method by *Uchida et al. (2008)* and *Uchida et al. (2010)*. The pressure hysteresis for the RINKO III output (voltage) is corrected according to a method by *Sea-bird Electornics (2009)* and *Uchida et al. (2010).* The formulas are as follows:

$$P_0 = 1.0 + c_4 \times t$$
$$P_c = c_5 + c_6 \times v + c_7 \times T + c_8 \times T \times v$$
$$K_{sv} = c_1 + c_2 \times t + c_3 \times t^2$$
$$coef = (1.0 + c_9 \times P/1000)^{1/3}$$
$$[O_2] = O_2^{sat} \times \{(P_0/P_c - 1.0)/K_{sv} \times coef\}$$

P: pressure (dbar), t: potential temperature, v: RINKO output voltage (volt)
T: elapsed time of the sensor from the beginning of first station in calculation group in day
O_2^{sat}: dissolved oxygen saturation by *Garcìa and Gordon* (1992) (μmol/kg)
$[O_2]$: dissolved oxygen concentration (μmol/kg)
c_1–c_9: determined by minimizing difference between CTD oxygen and bottle dissolved oxygen by quasi-newton method (*Shanno, 1970*).

Table C.1.8. Dissolved oxygen correction coefficient summary. (Bold: accepted sensor)

S/N	*Stations*	c_1	c_2	c_3	c_4	c_5
		c_6	c_7	c_8	c_9	
025	**RF6245 – 6265**	**1.71349e+0**	**1.71180e–2**	**5.23123e–4**	**–1.36118e–3**	**–1.38551e–1**
		3.14815e–1	**–1.56393e–3**	**1.20367e–3**	**6.54144e–2**	
025	**RF6266 – 6277**	**1.71603e+0**	**2.79165e–2**	**2.24068e–4**	**2.32347e–4**	**–1.48937e–1**
		3.19390e–1	**7.75061e–4**	**2.35448e–4**	**6.57689e–2**	
025	**RF6279 – 6318**	**1.74597e+0**	**2.58007e–2**	**2.62547e–4**	**2.39261e–4**	**-1.42934e–1**
		3.18774e–1	**1.20856e–5**	**5.42330e–4**	**7.70425e–2**	
025	**RF6319 – 6348**	**1.72812e+0**	**2.40085e–2**	**1.23049e–4**	**–3.74261e–4**	**–1.25593e–1**
		3.13255e–1	**–3.17918e–4**	**5.53393e–4**	**8.27147e–2**	
283	RF6245 – 6265	1.61299e+0	2.02649e–2	4.51603e–4	–7.31222e–4	–1.26457e–1
		3.11516e–1	–1.72303e–3	8.30994e–4	7.67659e–2	
283	RF6266 – 6277	1.60589e+0	3.02712e–2	2.21919e–4	1.01718e–3	–1.40601e–1
		3.16815e–1	1.50408e–3	–2.07557e–4	7.55489e–2	
283	RF6279 – 6318	1.65631e+0	2.60455e–2	2.69784e–4	4.00513e–4	–1.30487e–1
		3.13763e–1	–1.03207e–4	3.23402e–4	8.69710e–2	
283	RF6319 – 6348	1.64977e+0	2.60491e–2	1.51475e–4	2.51229e–5	–1.22723e–1
		3.11717e–1	-6.06506e–5	2.09785e–4	8.97008e–2	

Table C.1.9. Dissolved oxygen correction summary for S/N 025.

Stations	Pressure < 950dbar			Pressure ≥ 950 dbar		
	Num	Average (μmol/kg)	Std (μmol/kg)	Num	Average (μmol/kg)	Std (μmol/kg)
RF6245 – 6265	324	0.01	1.64	378	–0.01	0.34
RF6266 – 6277	184	–0.04	0.81	221	–0.03	0.36
RF6279 – 6318	587	0.00	0.71	733	0.00	0.37
RF6319 – 6348	535	0.10	0.91	460	–0.01	0.32

Table C.1.10. Dissolved oxygen correction summary for S/N 283.

Stations	Pressure < 950dbar			Pressure ≥ 950 dbar		
	Num	Average (μmol/kg)	Std (μmol/kg)	Num	Average (μmol/kg)	Std (μmol/kg)
RF6245 – 6265	324	–0.02	1.59	378	–0.01	0.38
RF6266 – 6277	184	–0.05	0.77	221	–0.01	0.39
RF6279 – 6318	587	0.00	0.69	733	0.00	0.37
RF6319 – 6348	535	0.15	0.90	460	–0.02	0.34

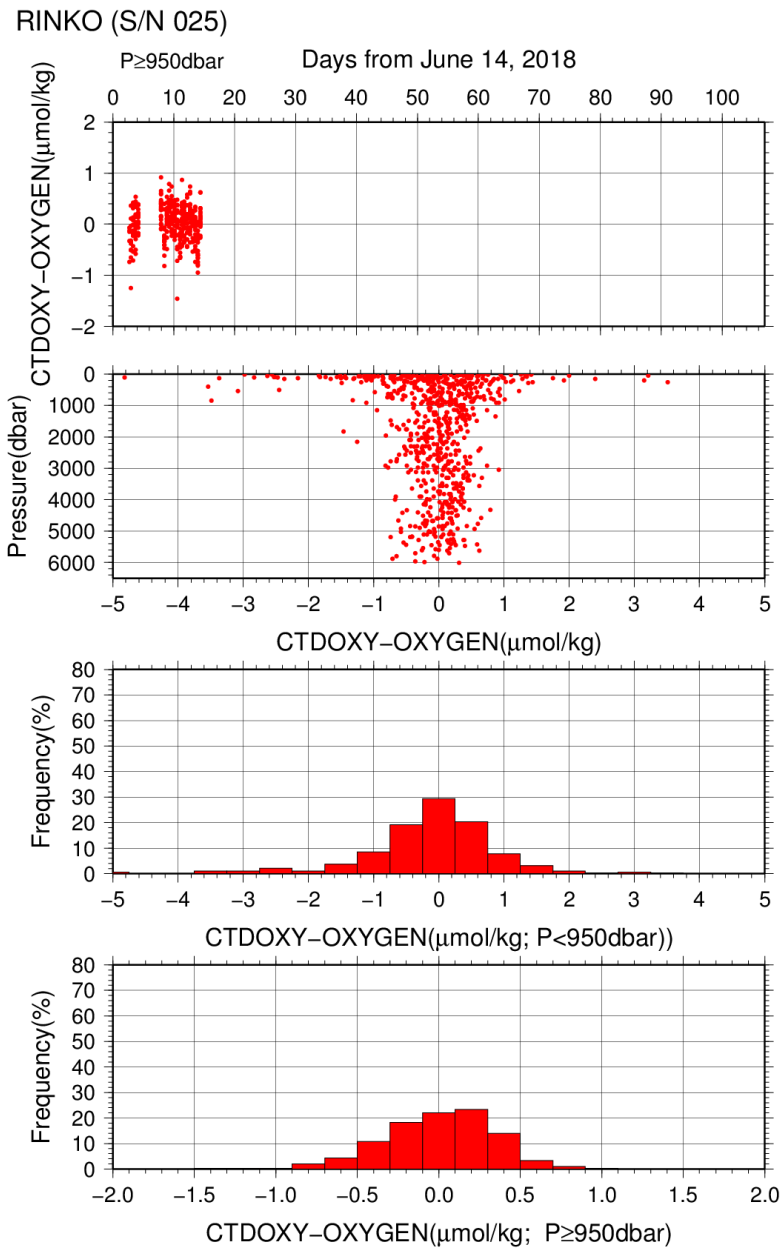

Figure C.1.10. Difference between the CTD oxygen (*S/N 025*) and bottle dissolved oxygen at RF18-05 Leg 1. Red dots in upper two panels indicate the result of calibration. Lower two panels show histogram of the difference between calibrated oxygen and bottle oxygen.

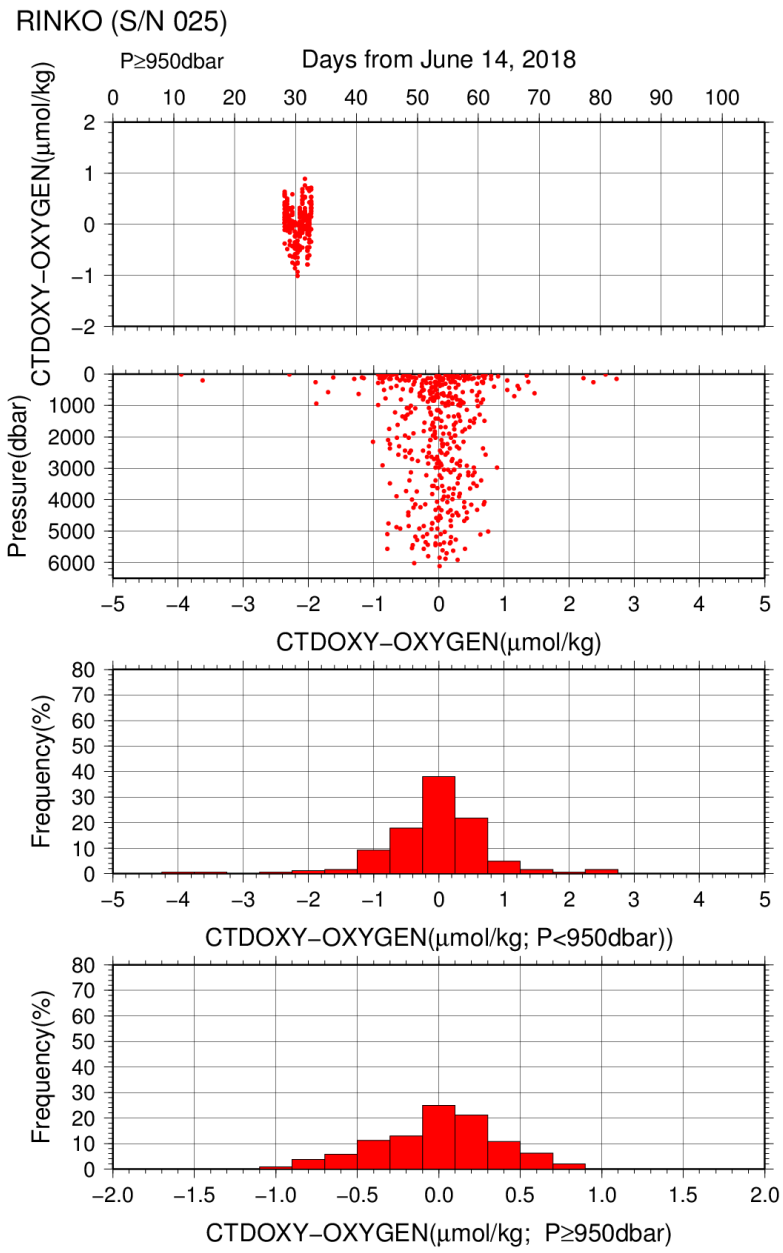

Figure C.1.11. Difference between the CTD oxygen (*S/N 025*) and bottle dissolved oxygen at RF18-05 Leg 2. Red dots in upper two panels indicate the result of calibration. Lower two panels show histogram of the difference between calibrated oxygen and bottle oxygen.

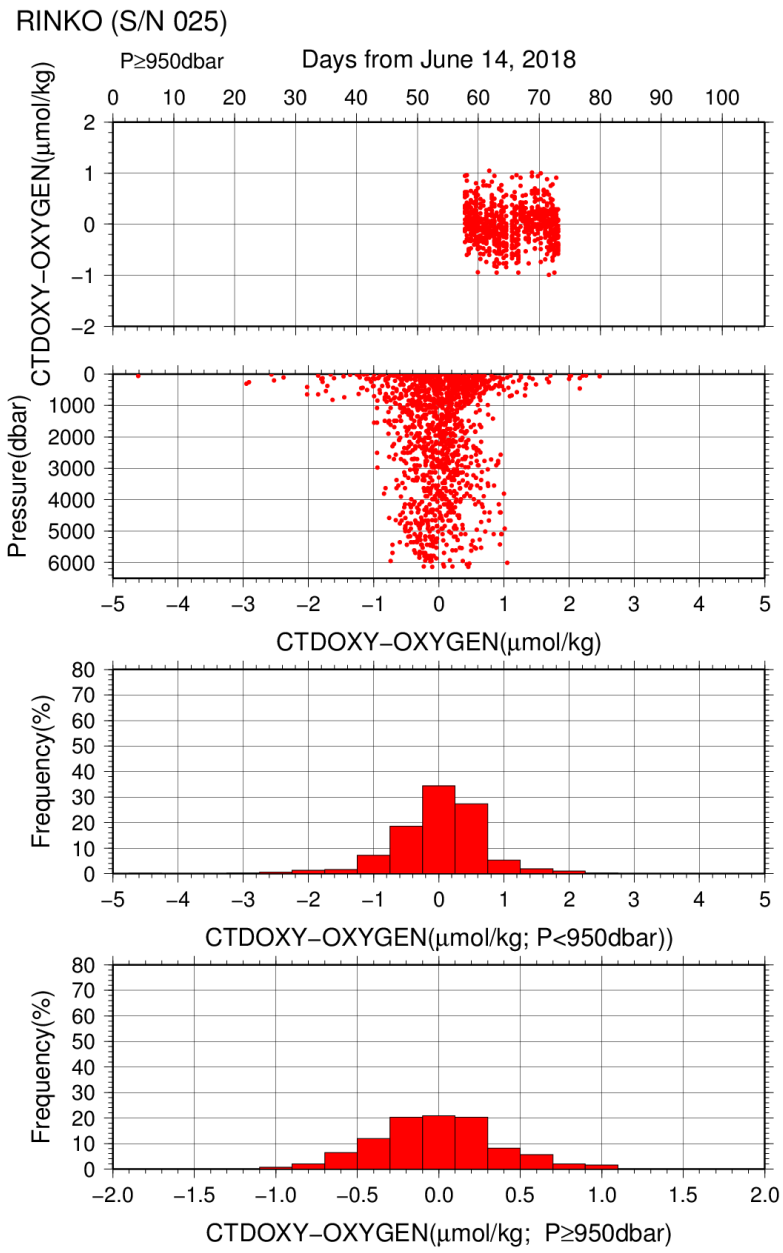

Figure C.1.12. Difference between the CTD oxygen (*S/N 025*) and bottle dissolved oxygen at RF18-06 Leg 1. Red dots in upper two panels indicate the result of calibration. Lower two panels show histogram of the difference between calibrated oxygen and bottle oxygen.

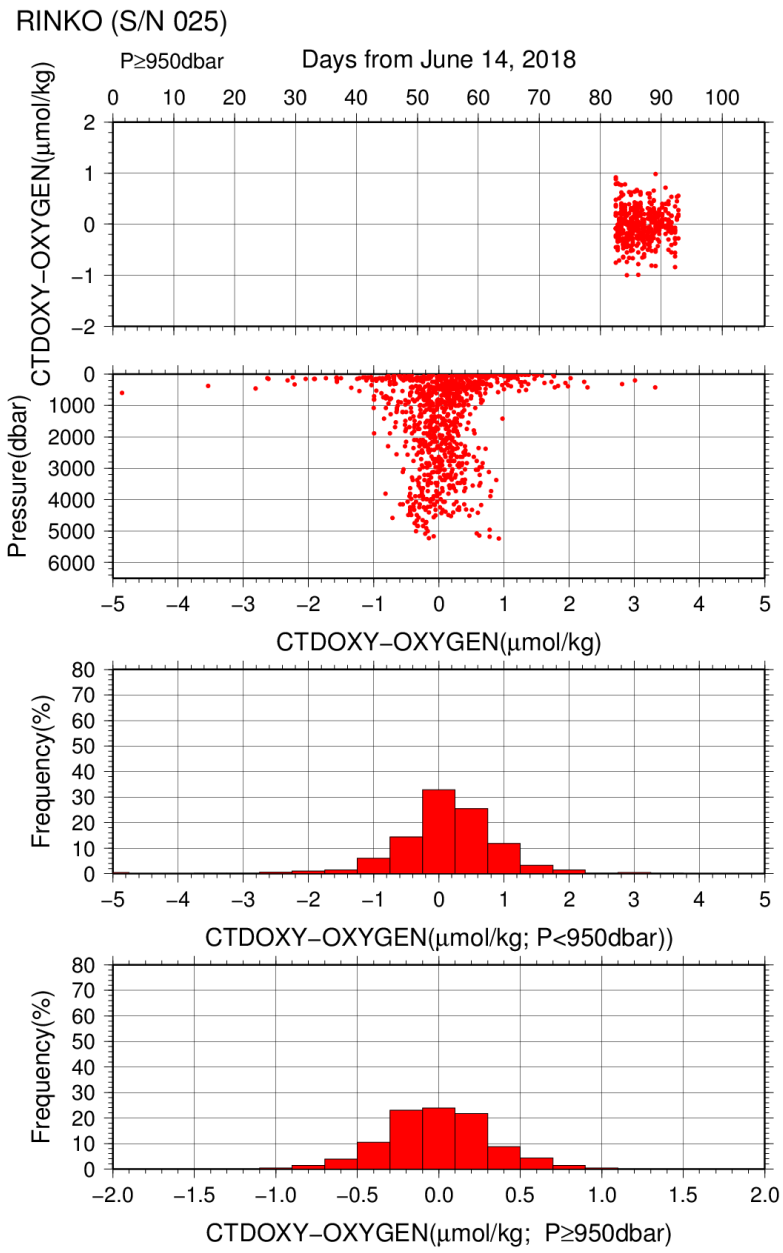

Figure C.1.13. Difference between the CTD oxygen (*S/N 025*) and bottle dissolved oxygen at RF18-06 Leg 2. Red dots in upper two panels indicate the result of calibration. Lower two panels show histogram of the difference between calibrated oxygen and bottle oxygen.

(4.5) Results of detection of sea floor by the altimeter (PSA-916D)

The altimeter detected the sea floor at 97 of 103 stations, the average distance of beginning detecting the sea floor was 36.1 m, and that of final detection of sea floor was 12.9 m. The summary of detection of PSA-916D was shown in Figure C.1.8.

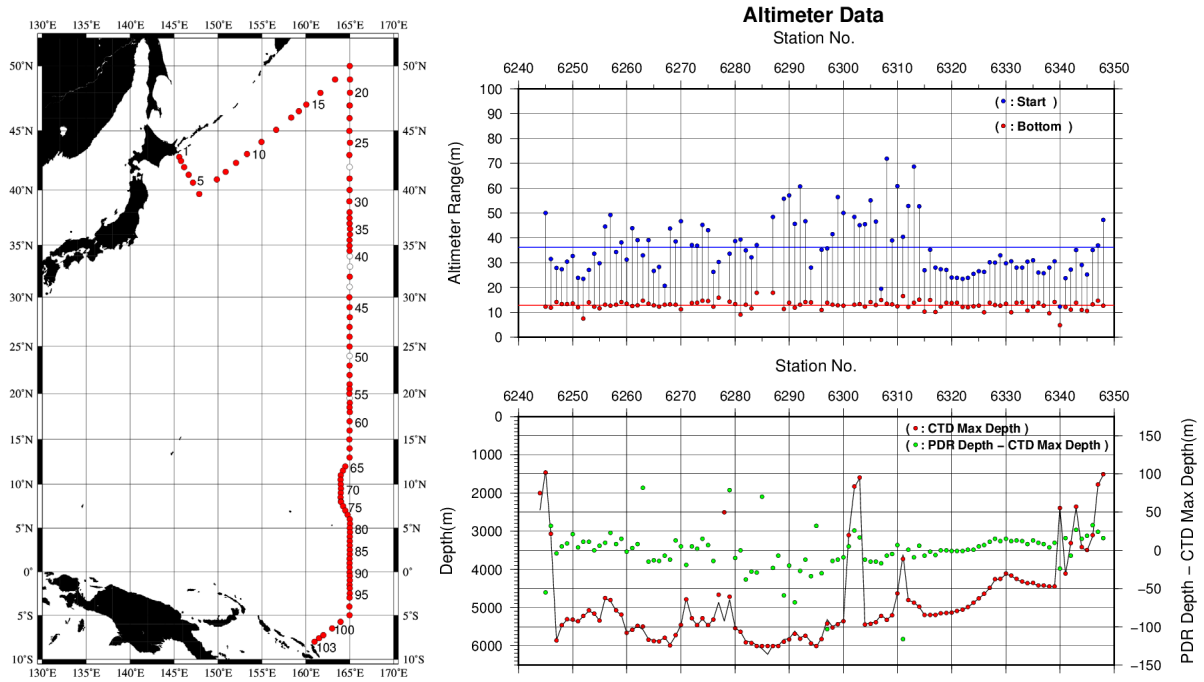

Figure C.1.14. The summary of detection of PSA-916D. The left panel shows the stations of detection, the right panel shows the relationship among PSA-916D, bathymetry and CTD depth. In the left panel, closed and open circles indicate react and no-react stations, respectively.

References

Akaike, H. (1974): A new look at the statistical model identification. *IEEE Transactions on Automatic Control, **19**:716–722.*

Garcìa, H. E., and L. I. Gordon (1992): Oxygen solubility in seawater: Better fitting equations. *Limnol. Oceanogr., **37**, 1307–1312*.

McTaggart, K. E., G. C. Johnson, M. C. Johnson, F. M. Delahoyde, and J. H. Swift (2010): The GO-SHIP Repeat Hydrography Manual: A Collection of Expert Reports and guidelines. IOCCP Report No ***14***, ICPO Publication Series No. 134, version 1, 2010.

Sea-Bird Electronics (2009): SBE 43 dissolved oxygen (DO) sensor – hysteresis corrections, *Application note no. 64-3, 7 pp.*

Shanno, David F. (1970): Conditioning of quasi-Newton methods for function minimization. *Math. Comput. **24**, 647–656. MR 42 #8905.*

Uchida, H., G. C. Johnson, McTaggart, K. E. (2010): CTD oxygen sensor calibration procedures. In: The GO-SHIP repeat hydrography manual: A Collection of Expert Reports and guidelines. IOCCP Report No ***14***, ICPO Publication Series No. 134, version 1, 2010.

Uchida, H., K. Ohyama, S. Ozawa, and M. Fukasawa (2007): In-situ calibration of the Sea-Bird 9plus CTD thermometer. *J. Atmos. Oceanic Technol., **24**, 1961–1967.*

Uchida, H., T. Kawano, I. Kaneko, and M. Fukasawa (2008): In-situ calibration of optode-based oxygen sensors. *J. Atmos. Oceanic Technol., **25**, 2271–2281*.

5. Bottle Salinity

8 June 2020

(1) Personnel

RF 18-05

Keizo SHUTTA (GEMD/JMA)
Masafumi KASAISHI (GEMD/JMA)
Sho HIBINO (GEMD/JMA)
Keita KAKUYA (GEMD/JMA)
Mitsuho OE (GEMD/JMA)
Yuma KAWAKAMI(GEMD/JMA)

RF 18-06

Noriyuki OKUNO(GEMD/JMA)
Kazuaki MINAMI(GEMD/JMA)
Sho HIBINO(GEMD/JMA)
Keita KAKUYA(GEMD/JMA)
Kanako ISSHIKI(GEMD/JMA)

(2) Salinity measurement

Salinometer: AUTOSAL 8400B (S/N68614; Guildline Instruments Ltd., Canada)
Thermometer: Guildline platinum thermometers model 9450 (to monitor an ambient temperature and bath temperature)
IAPSO Standard Sea Water: P161 (K15=0.99987)

(3) Sampling and measurement

The measurement system was almost same as *Kawano* (2010).
Algorithm for practical salinity scale, 1978 (PSS-78; *UNESCO*, 1981) was employed to convert the conductivity ratios to salinities.

(4) Station occupied

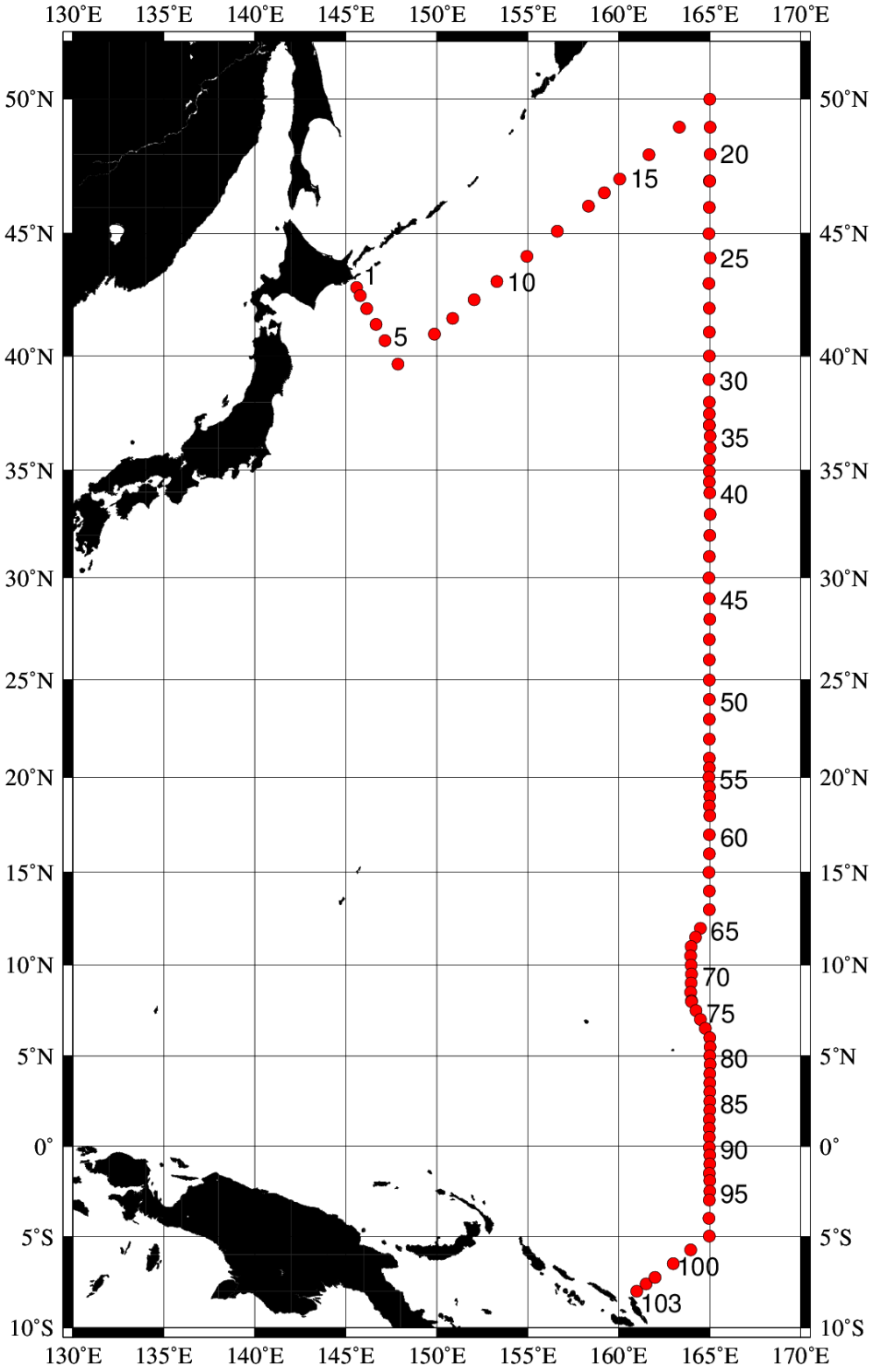

Figure C.2.1. Location of observation stations of bottle salinity.

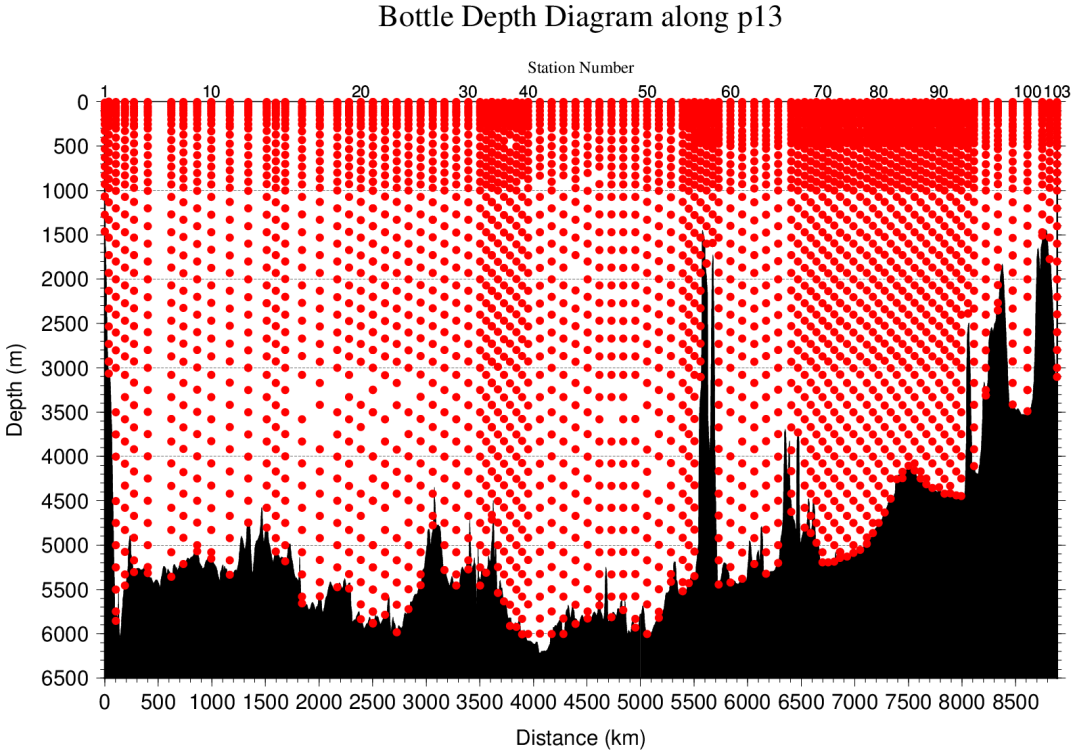

Figure C.2.2. Distance-depth distribution of sampling layers of bottle salinity.

(5) Result

(5.1) Ambient temperature, bath temperature and SSW measurements

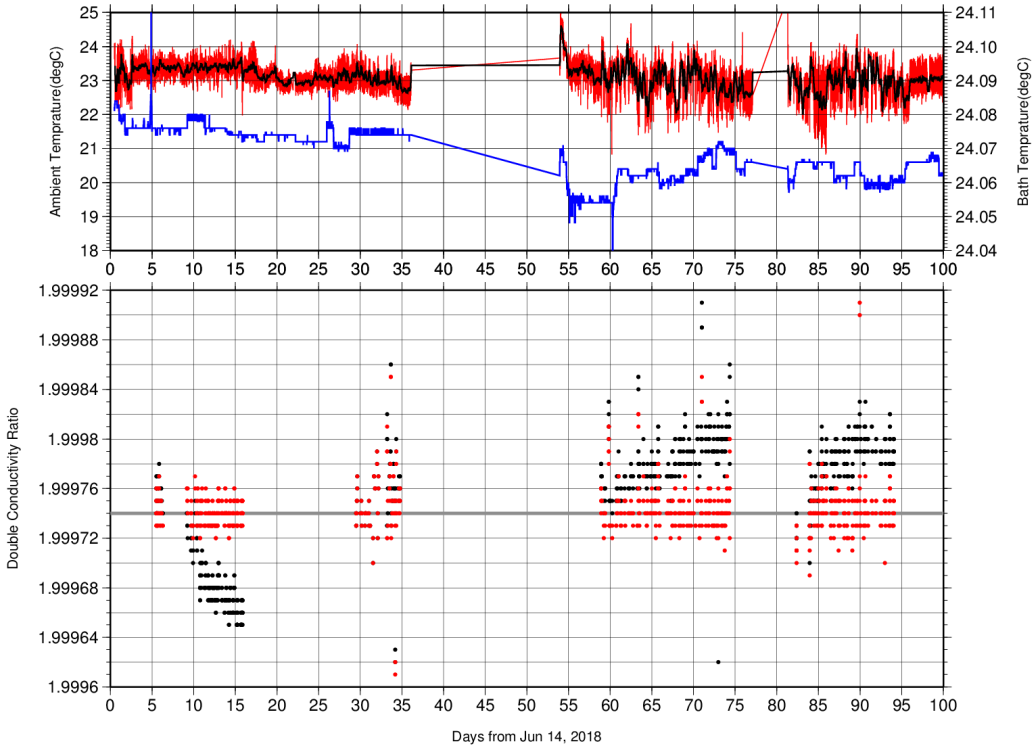

Figure C.2.3. The upper panel, red line, black line and blue line indicate time-series of ambient temperature, ambient temperature average and bath temperature during cruise. The lower panel, black dots and red dots indicate raw and corrected time-series of the double conductivity ratio of the standard sea water (P161).

(5.2) Replicate and Duplicate Samples

We took replicate (pair of water samples taken from a single Niskin bottle) and duplicate (pair of water samples taken from different Niskin bottles closed at the same depth) samples of bottle salinity through the cruise. Results of the analyses are summarized in Table C.2.1. Detailed results of them are shown in Figure C.2.4. The calculation of the standard deviation from the difference of sets was based on a procedure (SOP 23) in *DOE* (1994).

Table C.2.1. Summary of replicate and duplicate analyses.

Measurement	Ave. ± S.D.
Replicate	0.0003±0.0003 (N=355)
Duplicate	0.0009±0.0011 (N=47)

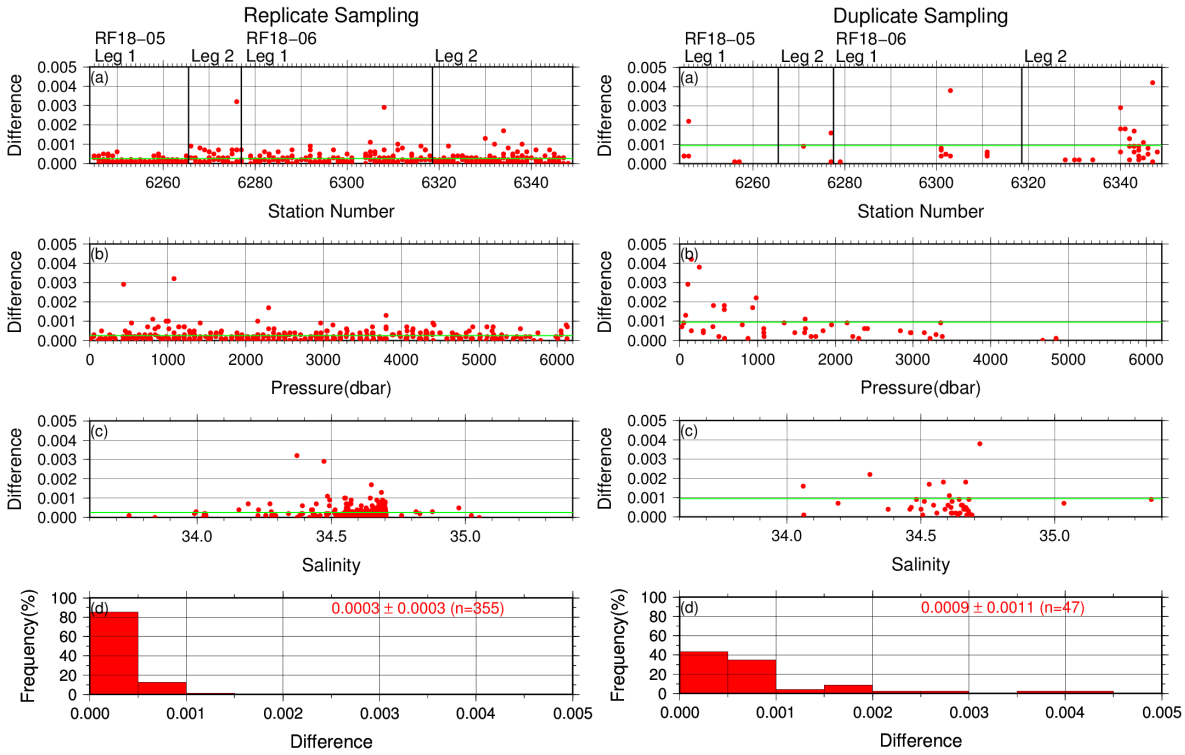

Figure C.2.4. Result of (left) replicate and (right) duplicate analyses during the cruise against (a) station number, (b) pressure and (c) salinity, and (d) histogram of the measurements. Green line indicates the mean of the differences of salinity of replicate/duplicate.

(5.3) Summary of assigned quality control flags

Table C.2.2. Summary of assigned quality control flags

Flag	Definition	Salinity
2	Good	3036
3	Questionable	0
4	Bad (Faulty)	239
5	Not reported	2
6	Replicate measurements	365
Total number of samples		3642

References

DOE (1994), Handbook of methods for the analysis of the various parameters of the carbon dioxide system in sea water; version 2. *A. G. Dickson and C. Goyet (eds), ORNL/CDIAC-74.*

Kawano (2010), The GO-SHIP Repeat Hydrography Manual: A Collection of Expert Reports and Guidelines. *IOCCP Report No. 14, ICPO Publication Series No. 134, Version 1.*

UNESCO (1981), Tenth report of the Joint Panel on Oceanographic Tables and Standards. *UNESCO Tech. Papers in Mar. Sci.,* ***36****, 25 pp.*

6. Bottle Oxygen

8 June 2020

(1) Personnel

RF18-05

Kazuhiro SAITO (GEMD/JMA)
Daisuke SASANO (GEMD/JMA)
Yoichi IMAI (GEMD/JMA)
Ryoma SUZUKI (GEMD/JMA)
Risa FUJIMOTO (GEMD/JMA)

RF18-06

Yoshihiro SHINODA (GEMD/JMA)
Yoichi IMAI (GEMD/JMA)
Ryoma SUZUKI (GEMD/JMA)
Takuya SASAKI (GEMD/JMA)
Takahiro OKA (GEMD/JMA)

(2) Station occupied

A total of 103 stations (RF 18-05 Leg 1: 21, Leg 2: 12, RF 18-06 Leg 1: 40, Leg 2: 30) were occupied for dissolved oxygen measurements. Station location and sampling layers of bottle oxygen are shown in Figures C.3.1 and C.3.2, respectively.

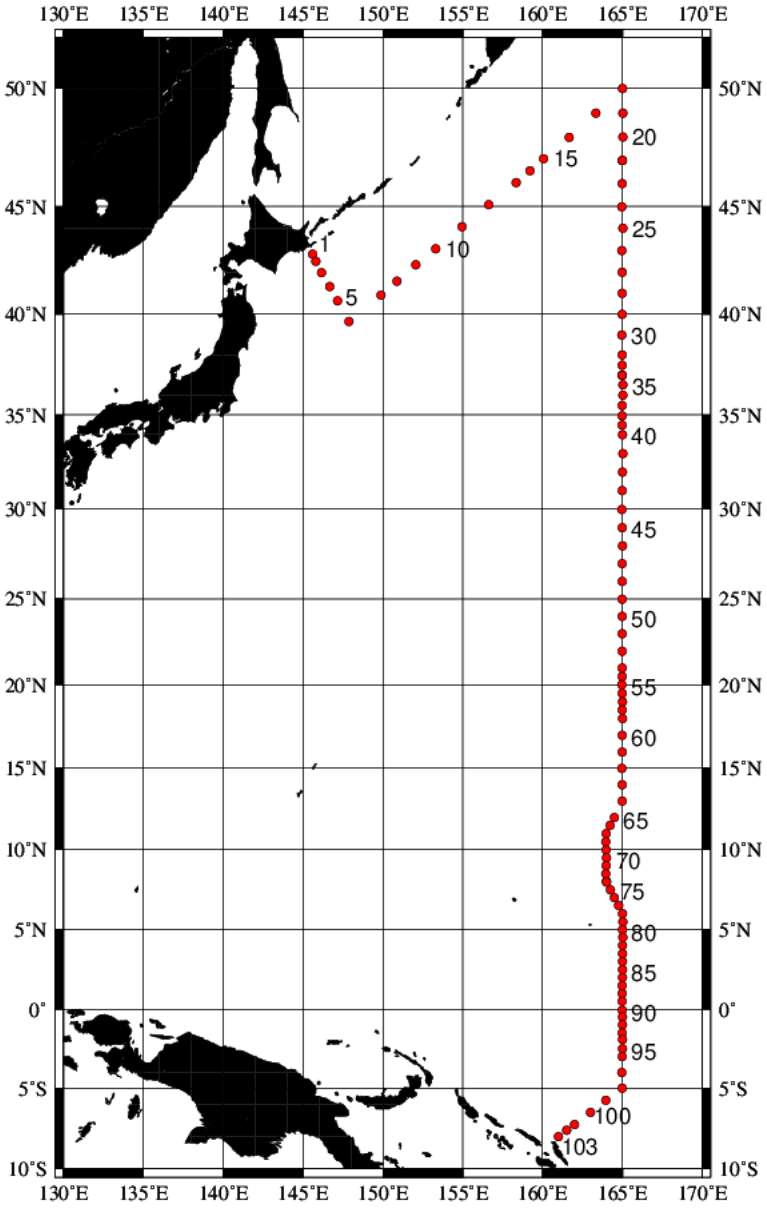

Figure C.3.1. Location of observation stations of bottle oxygen.

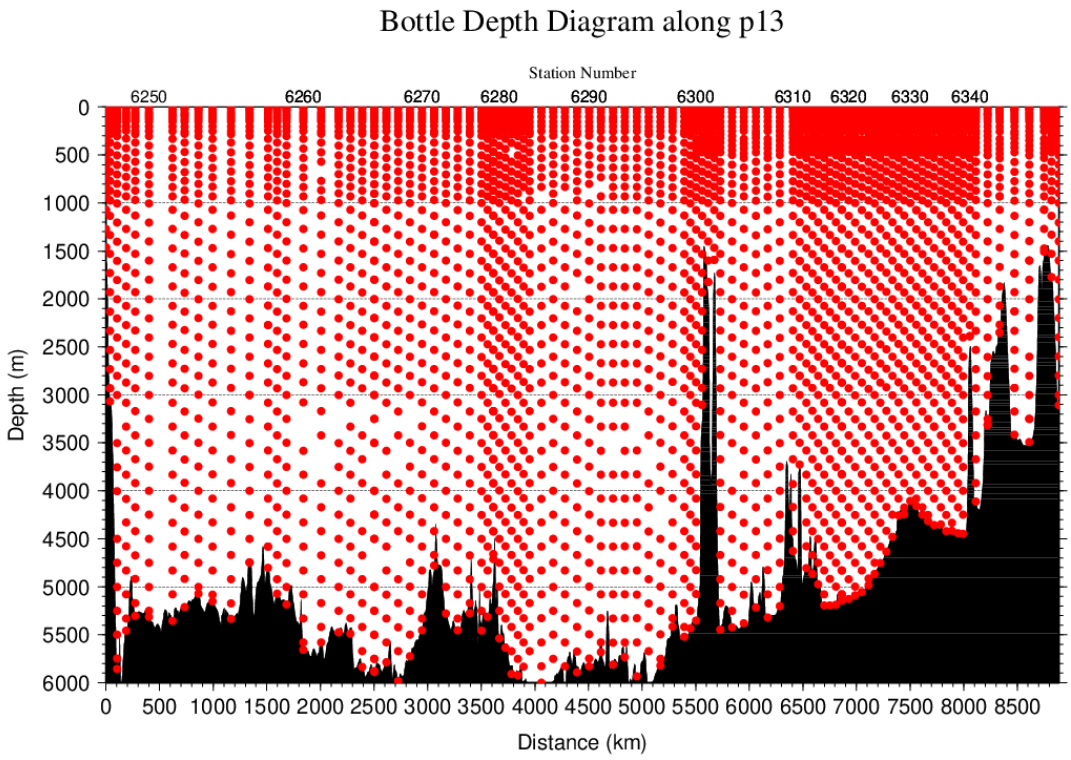

Figure C.3.2. Distance-depth distribution of sampling layers of bottle oxygen.

(3) Instrument

Detector: DOT-15X (Kimoto Electronic, Japan)

Burette: APB-610 (Kyoto Electronic, Japan)

(4) Sampling and measurement

Methods of seawater sampling, measurement, and calculation of dissolved oxygen concentration were based on IOCCP Report (Langdon, 2010). Details of the methods are shown in Appendix A1.

The reagents for the measurement were prepared according to recipes described in Appendix A2. It is noted that standard KIO_3 solutions were prepared gravimetrically using the highest purity standard substance KIO_3 (Lot. No. KPK3283 for RF18-05, and KPK3283 and ECG4358 for RF18-06, Wako Pure Chemical, Japan). Batch list of prepared standard KIO_3 solutions is shown in Table C.3.1.

Table C.3.1. Batch list of the standard KIO_3 solutions.

KIO_3 batch	**Lot**	**Cruise**	**Concentration and uncertainty (k=2) at 20 °C. Unit is mol L^{-1}.**	**Purpose of use**
20171120-2	KPK3283	RF18-05	0.0016670±0.0000003	Standardization (main use)
20171212-3	KPK3283	RF18-05	0.0016668±0.0000003	Mutual comparison
20171212-1	KPK3283	RF18-06	0.0016667±0.0000003	Standardization (main use)
20180329-1	ECG4358	RF18-06	0.0016666±0.0000003	Mutual comparison

(5) Standardization

Concentration of $Na_2S_2O_3$ titrant was determined with the standard KIO_3 solution "20171120-2" and "20171212-1", for RF18-05 and RF18-06, respectively, based on the methods of IOCCP Report (Langdon, 2010). The results of standardization during the cruise are shown in Figure C.3.3. Standard deviation of its concentration at 20 °C determined through standardization was used in calculation of an uncertainty.

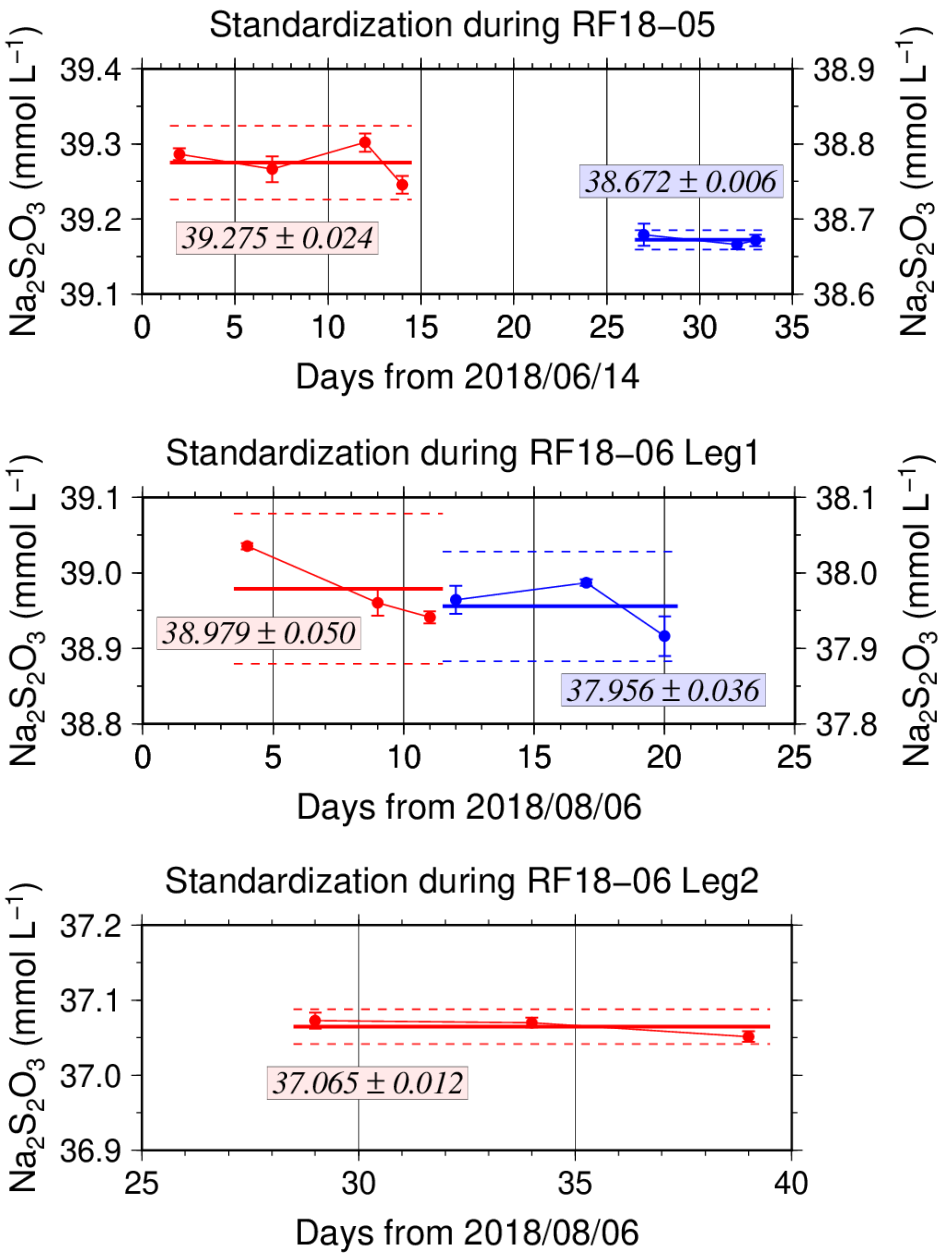

Figure C.3.3. Calculated concentration of $Na_2S_2O_3$ solution at 20 °C in standardization during RF18-05 (top) and RF18-06 Leg 1 (middle), RF18-06 Leg 2 (bottom). Different colors of plots indicate different batches of $Na_2S_2O_3$ solution; red (blue) plots correspond to the left (right) y-axis. Error bars of plots show standard deviation of concentration of $Na_2S_2O_3$ in the measurement. Thick and dashed lines denote the mean and 2 times of standard deviations for the batch measurements, respectively.

(6) Blank

(6.1) Reagent blank

Blank in oxygen measurement (reagent blank; V_{blk}) can be represented as follows;

$$V_{blk} = V_{blk\text{-}ep} + V_{blk\text{-}reg} \qquad \text{(C3.1)}$$

where $V_{blk\text{-}ep}$ represents a blank due to differences between the measured end-point and the equivalence point, and $V_{blk\text{-}reg}$ a blank associated with oxidants or reductants in the reagent. The reagent blank V_{blk} was determined by the methods described in IOCCP Report (Langdon, 2010) using pure water. Because we used two sets (set A and B) of pickling reagent-I and -II, the blanks in each set were determined (Figure C.3.4).

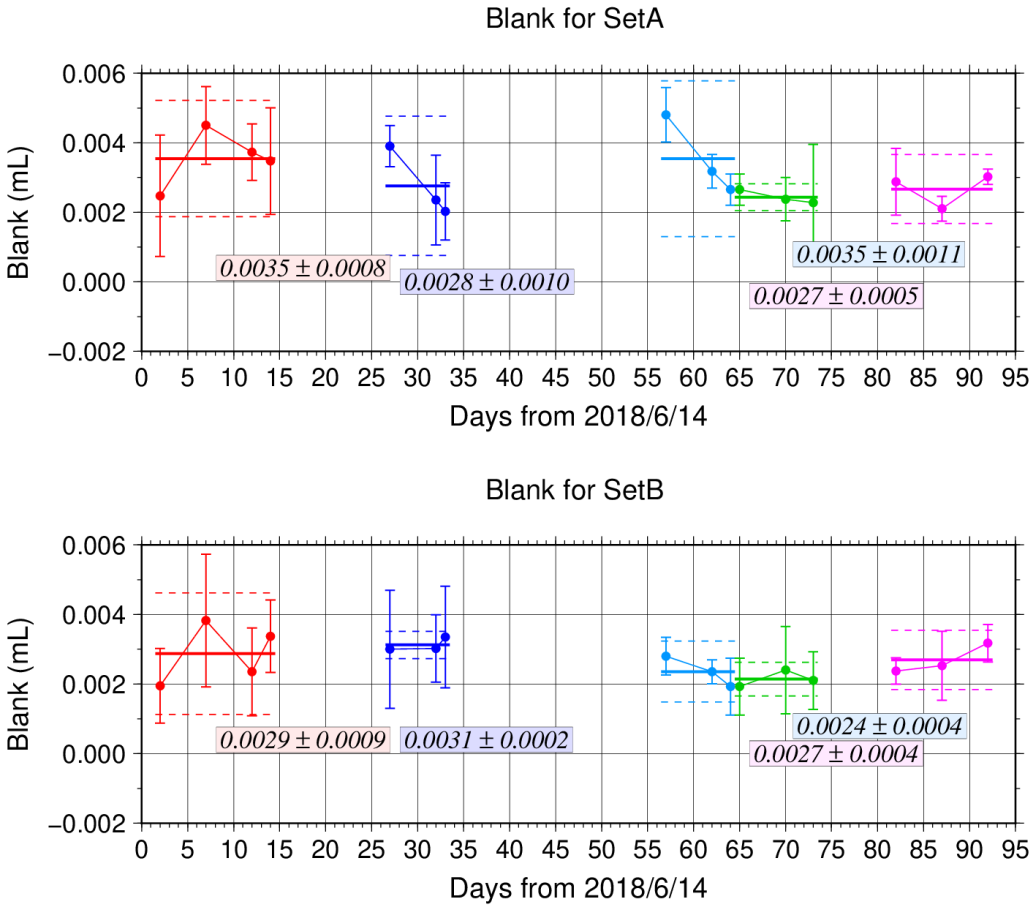

Figure C.3.4. Reagent blank (V_{blk}) determination for set A (top) and set B (bottom). Error bars of plots show standard deviation of the measurement. Thick and dashed lines denote the mean and 2 times of standard deviations for the batch measurement, respectively.

(6.2) Seawater blank

We also determined seawater blank ($V_{sw\text{-}blk}$) which reflects interfering substances in seawater. Although this blank is not included in determination of oxygen concentration, measurement of the blank would be necessary to improve traceability and comparability in dissolved oxygen concentration. Details are described in Appendix A3.

(7) Quality Control

(7.1) Replicate and duplicate analyses

We took replicate (pair of water samples taken from a single Niskin bottle) and duplicate (pair of water samples taken from different Niskin bottles closed at the same depth) samples of dissolved oxygen through the cruise. Results of the measurements are summarized in Table C.3.2. Detailed results of them are shown in Figure C.3.5. The calculation of the standard deviation from the difference of sets was based on a procedure (SOP 23) in DOE (1994).

Table C.3.2. Summary of replicate and duplicate measurements.

Measurement	Ave. ± S.D. (μmol kg^{-1})
Replicate	0.19±0.18 (N=381)
Duplicate	0.26±0.24 (N=48)

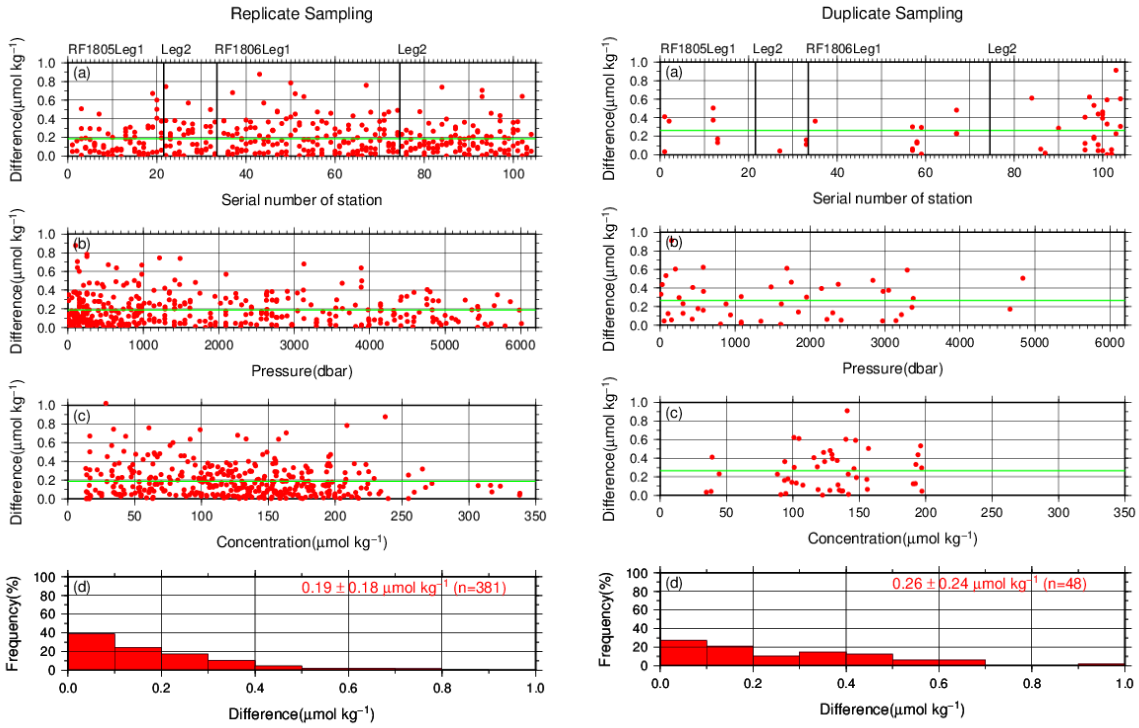

Figure C.3.5. Results of (left) replicate and (right) duplicate measurements during the cruise against (a) station number, (b) pressure and (c) concentration of dissolved oxygen. Green line denotes the average of the measurements. Bottom panels (d) show histogram of the measurements.

(7.2) Mutual comparison between each standard KIO_3 solution

During the cruise, mutual comparison between different lots of standard KIO_3 solution was performed to confirm the accuracy of our oxygen measurement and the bias of a standard KIO_3 solution. A concentration of the standard KIO_3 solutions "20171212-3" and "20180329-1" was determined using $Na_2S_2O_3$ solution standardized with the KIO_3 solution "20171120-2" and "20171212-1", respectively, and the difference between measurement value and theoretical one. A good agreement among two standards confirmed that there was no systematic shift in our oxygen measurements during the cruise (Figure C.3.6).

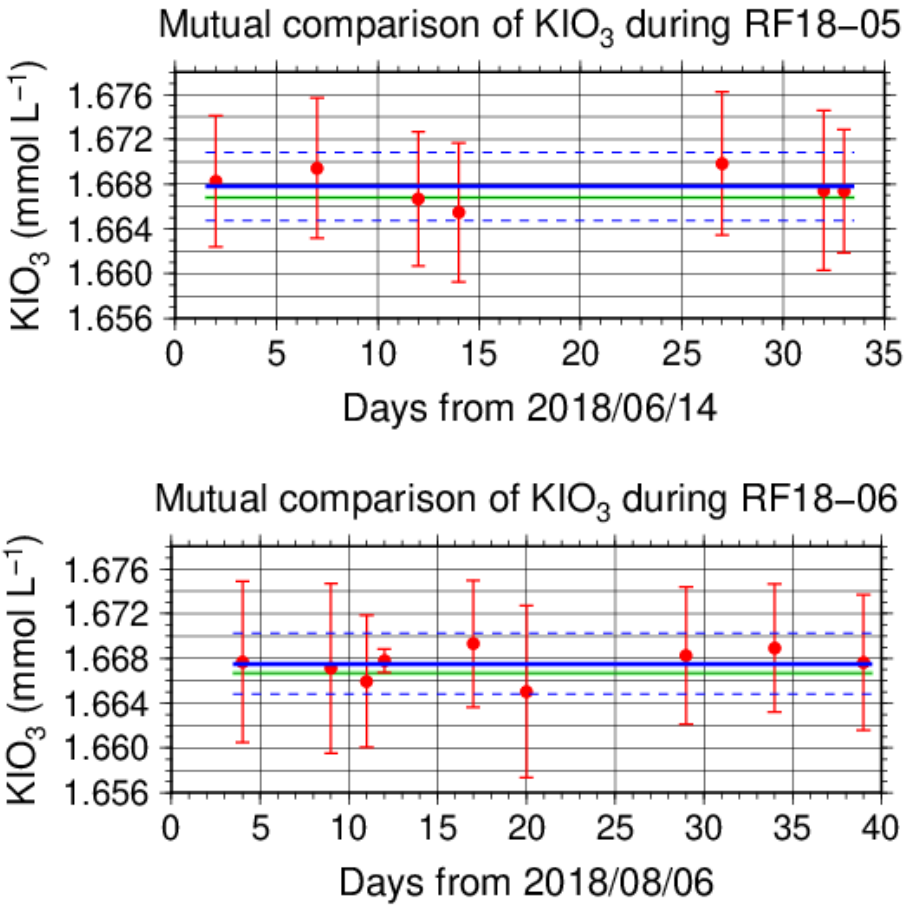

Figure C.3.6. Result of mutual comparison of standard KIO_3 solutions during RF18-05 (top) and RF18-06 (bottom). Circles and error bars show mean of the measurement value and its uncertainty (k=2), respectively. Thick and dashed lines in blue denote the mean and 2 times of standard deviations, respectively, for the measurement through the cruise. Green thin line and light green thick line denote nominal concentration and its uncertainty (k=2) of standard KIO_3 solutions "20171212-3" and "20180329-1", for RF18-05 and RF18-06, respectively.

(7.3) Quality control flag assignment

Quality flag value was assigned to oxygen measurements as shown in Table C.3.3, using the code defined in IOCCP Report No.14 (Swift, 2010).

Table C.3.3. Summary of assigned quality control flags.

Flag	Definition	Number of samples
2	Good	3210
3	Questionable	63
4	Bad (Faulty)	9
5	Not reported	2
6	Replicate measurements	381
Total number of samples		3665

(8) Uncertainty

Oxygen measurement involves various uncertainties; determination of glass bottles volume, repeatability and systematic error of burette discharge, repeatability of pickling reagents discharge, determination of reagent blank, standardization of $Na_2S_2O_3$ solution, and uncertainty of KIO_3 concentration. Considering evaluable uncertainties as above, expanded uncertainty of bottle oxygen concentration (T=20, S=34.5) was estimated as shown in Table C.3.4. However, it is difficult to determine a strict uncertainty for oxygen concentration because there is no reference material for oxygen measurement.

Table C.3.4. Expanded uncertainty (k=2) of bottle oxygen in the cruise.

O_2 conc. (μmol kg^{-1})	Uncertainty (μmol kg^{-1})
20	0.33
30	0.34
50	0.36
70	0.39
100	0.45
150	0.56
200	0.69
250	0.82
300	0.96
400	1.25

Appendix

A1. Methods

(A1.1) Seawater sampling

Following procedure is based on a determination method in IOCCP Report (Langdon, 2010). Seawater samples were collected from 10-liters Niskin bottles attached the CTD-system and a stainless steel bucket for the surface. Seawater for bottle oxygen measurement was transferred from the Niskin bottle and a stainless steel bucket to a volumetrically calibrated dry glass bottles. At least three times the glass volume water was overflowed. Then, pickling reagent-I 1 mL and reagent-II 1mL were added immediately, and sample temperature was measured using a thermometer. After a stopper was inserted carefully into the glass, it was shaken vigorously to mix the content and to disperse the precipitate finely. After the precipitate has settled at least halfway down the glass, the glass was shaken again. The sample glasses containing pickled samples were stored in a laboratory until they were titrated. To prevent air from entering the glass, deionized water (DW) was added to its neck after sampling.

(A1.2) Sample measurement

At least 15 minutes after the re-shaking, the samples were measured on board. Added 1 mL H_2SO_4 solution and a magnetic stirrer bar into the sample glass, samples were titrated with $Na_2S_2O_3$ solution whose molarity was determined with KIO_3 solution. During the titration, the absorbance of iodine in the solution was monitored using a detector. Also, temperature of $Na_2S_2O_3$ solution during the titration was recorded using a thermometer. Dissolved oxygen concentration (μmol kg^{-1}) was calculated from sample temperature at the fixation, CTD salinity, glass volume, and titrated volume of the $Na_2S_2O_3$ solution, and oxygen in the pickling reagents-I (1 mL) and II (1 mL) (7.6×10^{-8} mol; Murray *et al.*, 1968).

A2. Reagents recipes

Pickling reagent-I; Manganous chloride solution (3 mol L^{-1})

Dissolve 600 g of $MnCl_2 \cdot 4H_2O$ in DW, then dilute the solution with DW to a final volume of 1 L.

Pickling reagent-II; Sodium hydroxide (8 mol L^{-1}) / sodium iodide solution (4 mol L^{-1})

Dissolve 320 g of NaOH in about 500 mL of DW, allow to cool, then add 600 g NaI and dilute with DW to a final volume of 1 L.

H_2SO_4 solution; Sulfuric acid solution (5 mol L^{-1})

Slowly add 280 mL concentrated H_2SO_4 to roughly 500 mL of DW. After cooling the final volume should be 1 L.

$Na_2S_2O_3$ solution; Sodium thiosulfate solution (0.04 mol L^{-1})

Dissolve 50 g of $Na_2S_2O_3 \cdot 5H_2O$ and 0.4 g of Na_2CO_3 in DW, then dilute the solution with DW to a final volume of 5 L.

KIO_3 solution; Potassium iodate solution (0.001667 mol L^{-1})

Dry high purity KIO_3 for two hours in an oven at 130 °C. After weight out accurately KIO_3, dissolve it in DW in a 5 L flask. Concentration of potassium iodate is determined by a gravimetric method.

A3. Seawater blank

Blank due to redox species other than oxygen in seawater ($V_{sw\text{-}blk}$) can be a potential source of measurement error. Total blank ($V_{tot\text{-}blk}$) in seawater measurement can be represented as follows;

$$V_{tot\text{-}blk,} = V_{blk} + V_{sw\text{-}blk}. \quad \text{(C3.A1)}$$

Because the reagent blank (V_{blk}) determined for pure water is expected to be equal to that in seawater, the difference between blanks for seawater ($V_{tot\text{-}blk}$) and for pure water (V_{blk}) gives the $V_{sw\text{-}blk}$.

Here, $V_{sw\text{-}blk}$ was determined by following procedure. Seawater was collected in the calibrated volumetric glass without the pickling solution. Then 1 mL of the standard KIO_3 solution, H_2SO_4 solution, and reagent solution-II and I each were added in sequence into the glass. After that, the sample was titrated to the end-point by $Na_2S_2O_3$ solution. Similarly, a glass contained 100 mL of DW added with 1 mL of the standard KIO_3 solution, H_2SO_4 solution, pickling reagent solution-II and I were titrated with $Na_2S_2O_3$ solution. The difference of the titrant volume of the seawater and DW glasses gave $V_{sw\text{-}blk}$.

The seawater blank has been reported from 0.4 to 0.8 μmol kg^{-1} in the previous study (Culberson *et al*., 1991). Additionally, these errors are expected to be the same to all investigators and not to affect the comparison of results from different investigators (Culberson, 1994). However, the magnitude and variability of the seawater blank have not yet been documented. Understanding of the magnitude and variability is important to improve traceability and comparability in oxygen concentration. The determined seawater blanks are shown in Table C.3.A1.

Table C.3.A1. Results of seawater blank determinations.

Station: RF6262 49°-59′N/165°-00′E	
Depth (m)	Blank (μmol kg^{-1})
51	1.18
300	0.62
600	0.82
600	0.64
1001	0.72
1401	0.72
2001	0.96
3002	0.76
4001	0.73
5000	0.88
5000	0.80
5476	0.71

Station: RF6265 47°-00′N/165°-00′E	
Depth (m)	Blank (μmol kg^{-1})
11	1.33
50	2.71
50	0.79
125	0.78
401	0.65
803	0.67
803	0.60
1599	0.66
3001	0.67
4250	0.66
5750	0.63
5876	1.73

Station: RF6286 33°-00′N/165°-01′E	
Depth (m)	Blank (μmol kg^{-1})
101	0.63
330	0.67
631	0.92
631	1.44
1072	0.82
1472	0.72
2074	0.68
3082	0.76
4082	0.72
5077	0.81
5077	0.71
6000	0.82

Station: RF6345 6°-31′N/163°-00′E	
Depth (m)	Blank (μmol kg^{-1})
53	0.66
126	1.21
126	1.27
250	0.84
350	0.67
502	0.71
702	0.81
1001	0.81
2001	0.79
3002	0.74
3492	0.85
3492	1.29

Reference

Culberson, A.H. (1994), Dissolved oxygen, in WHPO Pub. 91-1 Rev. 1, November 1994, Woods Hole, Mass., USA.

Culberson, A.H., G. Knapp, M.C. Stalcup, R.T. Williams, and F. Zemlyak (1991), A comparison of methods for the determination of dissolved oxygen in seawater, WHPO Pub. 91-2 , August 1991, Woods Hole, Mass., USA.

DOE (1994), Handbook of methods for the analysis of the various parameters of the carbon dioxide system in sea water; version 2. *A. G. Dickson and C. Goyet (eds), ORNL/CDIAC-74*.

Langdon, C. (2010), Determination of dissolved oxygen in seawater by Winkler titration using the amperometric technique, *IOCCP Report No.14, ICPO Pub. 134, 2010 ver.1*

Murray, C. N., J. P. Riley and T. R. S. Wilson (1968), The solubility of oxygen in Winkler reagents used for the determination of dissolved oxygen. *Deep-Sea Res*. 15, 237–238.

Swift, J. H. (2010), Reference-quality water sample data: Notes on acquisition, record keeping, and evaluation. *IOCCP Report No.14, ICPO Pub. 134, 2010 ver.1*.

7. Nutrients

10 June 2020

(1) Personnel

RF18-05

Kazuhiro SAITO (GEMD/JMA)
Daisuke SASANO (GEMD/JMA)
Yoichi IMAI (GEMD/JMA)
Ryoma SUZUKI (GEMD/JMA)
Risa FUJIMOTO (GEMD/JMA)

RF18-06

Yoshihiro SHINODA (GEMD/JMA)
Yoichi IMAI (GEMD/JMA)
Ryoma SUZUKI (GEMD/JMA)
Takuya SASAKI (GEMD/JMA)
Takahiro OKA (GEMD/JMA)

(2) Station occupied

A total of 99 stations (RF 18-05 Leg 1: 21, Leg 2: 12, RF 18-06 Leg 1: 36, Leg 2: 30) were occupied for nutrients measurements. Station location and sampling layers of nutrients are shown in Figures C.4.1 and C.4.2.

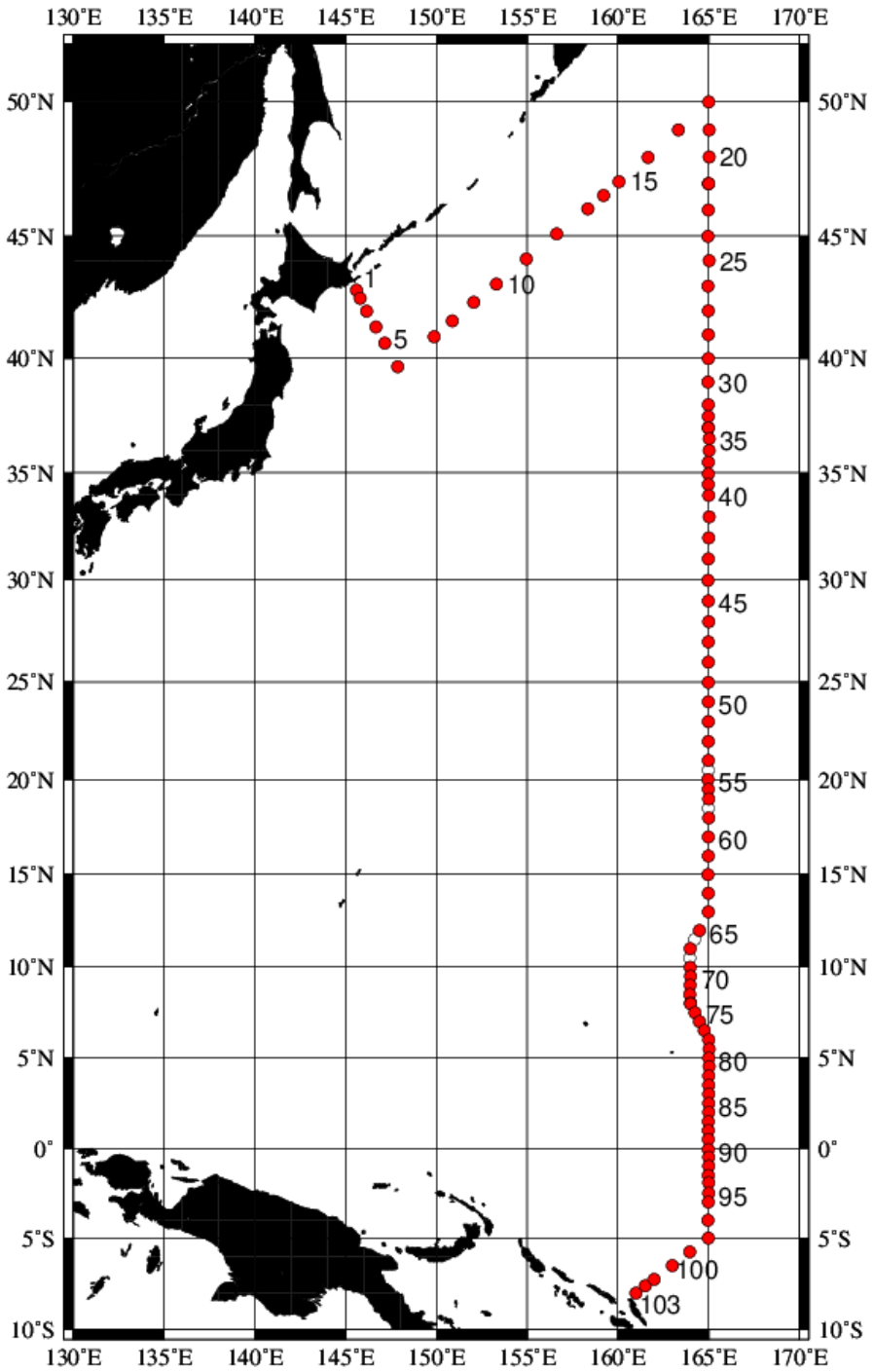

Figure C.4.1. Location of observation stations of nutrients.

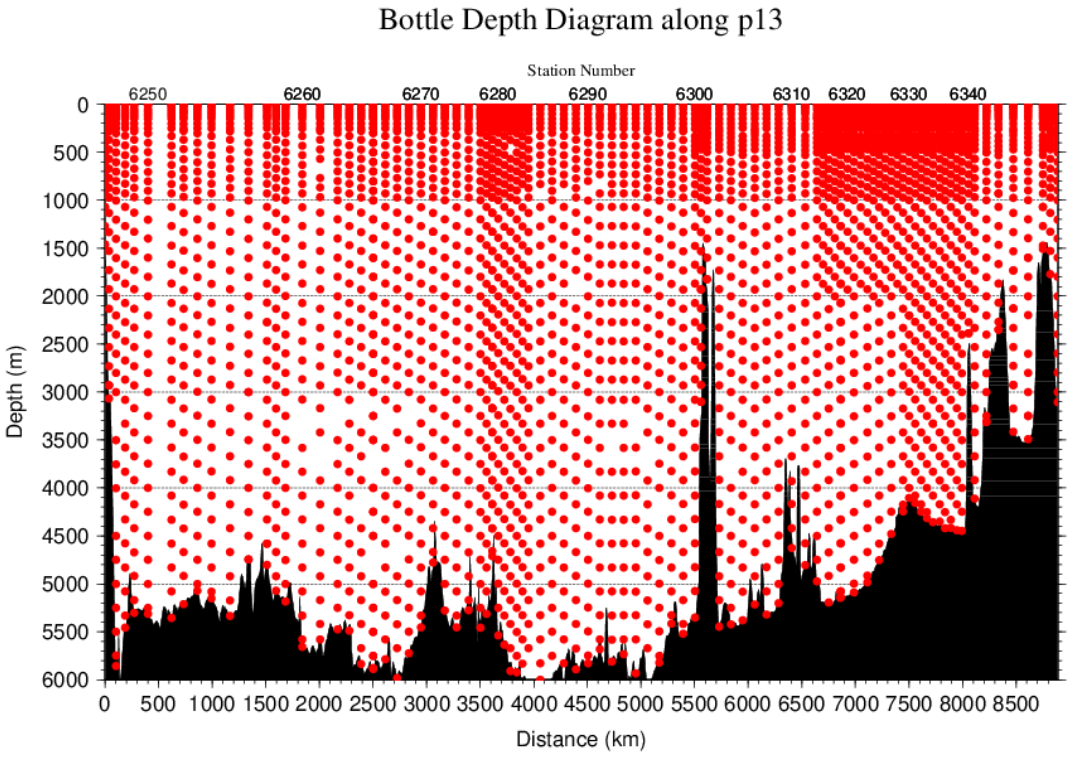

Figure C.4.2. Distance-depth distributions of sampling layers of nutrients.

(3) Instrument

The nutrients analysis was carried out on 4-channel Auto Analyzer III (BL TEC K.K., Japan) for 4 parameters; nitrate+nitrite, nitrite, phosphate, and silicate.

(4) Sampling and measurement

Methods of seawater sampling, measurement, and data processing of nutrient concentration were described in Appendixes A1, A2, and A3, respectively. The reagents for the measurement were prepared according to recipes shown in Appendix A4.

(5) Nutrients standards

(5.1) Volumetric laboratory ware of in-house standards

All volumetric wares were gravimetrically calibrated. The weights obtained in the calibration weighing were corrected for the density of water and for air buoyancy. Polymethylpenten volumetric flasks were gravimetrically calibrated at the temperature of use within 4–6 °C. All pipettes have nominal calibration tolerances of 0.1 % or better. These were gravimetrically calibrated in order to verify and improve upon this nominal tolerance.

(5.2) Reagents of standard

The batches of the reagents used for standard are listed in Table C.4.1.

Table C.4.1. List of reagents of standard used in the cruise.

	Name	CAS No	Lot. No	Industries
Nitrate	potassium nitrate 99.995 suprapur®	7757-79-1	B0993065	Merck KGaA
Nitrite	sodium nitrite GR for analysis ACS, Reag. Ph Eur	7632-00-0	A0723349	Merck KGaA
Phosphate	potassium dihydrogen phosphate anhydrous 99.995 suprapur®	7778-77-0	B1501008	Merck KGaA
Silicate	Silicon standard solution 1000 mg/l Si*	-	HC73014836	Merck KGaA

* Traceable to NIST-SRM3150

(5.3) Low nutrient seawater (LNSW)

Surface water with sufficiently low nutrient concentration was taken and filtered using 10 μm pore size membrane filter in our previous cruise. This water was stored in 20 liter flexible container with paper box.

(5.4) In-house standard solutions

Nutrient concentrations for A, B and C standards were set as shown in Table C.4.2. A and B standards were prepared with deionized water (DW). C standard (full scale of working standard) was mixture of B-1 and B-2 standards, and was prepared with LNSW. C-1 standard, whose concentrations of nutrient were nearly zero, was prepared as LNSW slightly added with DW to be equal with mixing ratio of LNSW and DW in C standard. The C-2 to -5 standards were prepared with mixture of C-1 and C standards in stages as 1/4, 2/4, 3/4, and 4/4 (i.e., pure “C standard”) concentration for full scale, respectively. The actual concentration of nutrients in each standard was calculated based on the solution temperature and factors of volumetric laboratory wares calibrated prior to use. Nominal zero concentration of nutrient was determined in measurement of DW after refraction error correction. The calibration curves for each run were obtained using 5 levels of C-1 to -5 standards. These standard solutions were periodically renewed as shown in Table C.4.3.

Table C.4.2. Nominal concentrations of nutrients for A, B, and C standards at 20 °C. Unit is μmol L^{-1}.

	A	B	C
Nitrate	28750*	574*	45.9*
	27502	549	43.9
Nitrite	12505	250	2.0
Phosphate	2189*	43.7*	3.49*
	2121	42.4	3.39
Silicate	35606	2312*	185*
		2134	171

* Use in the south of 40°N

Table C.4.3. Schedule of renewal of in-house standards.

Standard	Renewal
A-1 std. (NO_3)	No renewal
A-2 std. (NO_2)	No renewal
A-3 std. (PO_4)	No renewal
A-4 std. (Si)	Commercial prepared solution
B-1 std. (mixture of A-1, A-3, and A-4 stds.)	Maximum 8 days
B-2 std. (diluted A-2 std.)	Maximum 15 days
C-std. (mixture of B-1 and B-2 stds.)	Every measurement
C-1 to -5 stds.	Every measurement

(6) Certified reference material

Certified reference material for nutrients in seawater (hereafter CRM), which was prepared by the General Environmental Technos (KANSO Technos, Japan), was used every analysis at each hydrographic station. Using CRMs for the analysis of seawater, stable comparability and uncertainty of our data are secured.

CRMs used in the cruise are shown in Table C.4.4.

Table C.4.4. Certified concentration and uncertainty (k=2) of CRMs. Unit is μmol kg^{-1}.

	Nitrate	Nitrite	Phosphate	Silicate
CRM-BY	0.024±0.019*	0.019±0.0085*	0.039±0.010*	1.763±0.063
CRM-CJ	16.2±0.2	0.031±0.007	1.19±0.02	38.5±0.4
CRM-CB	35.79±0.27	0.116±0.0057	2.520±0.022	109.2±0.62
CRM-BZ	43.35±0.33	0.215±0.011	3.056±0.033	161.0±0.93

* Reference value because concentration is under limit of quantitation

The CRM-BY and -CB were analyzed every runs using newly opened CRM bottle at each hydrographic station. The CRM-CJ and -BZ were also analyzed every runs but were newly opened every 2 or 3 runs. Although this usage of CRM might be less common, we have confirmed a stability of the opened CRM bottles to be tolerance in our observation. The CRM bottles were stored at a laboratory in the ship, where the temperature was maintained around 25 °C.

It is noted that nutrient data in our report are calibrated not on CRM but on in-house standard solutions. Therefore, to calculate data based on CRM, it is necessary that values of nutrient concentration in our report are correlated with CRM values measured in the same analysis run. The result of CRM measurements is attached as 49UP20180614_P13_nut_CRM_measurement.csv.

(7) Quality Control

(7.1) Replicate and duplicate analyses

We took replicate (pair of water samples taken from a single Niskin bottle) and duplicate (pair of water samples taken from different Niskin bottles closed at the same depth) samples of nutrient through the cruise. Results of the measurements are summarized in Table C.4.5. Detailed results of them are shown in Figures C.4.3–C.4.5. The calculation of the standard deviation from the difference of sets was based on a procedure (SOP 23) in DOE (1994).

Table C.4.5. Average and standard deviation of difference of replicate and duplicate measurements through the cruise for data of flag 2 and for flag 2 and 3. Unit is μmol kg^{-1}.

Measurement	Flag	Nitrate+nitrite	Phosphate	Silicate
Replicate	2	0.040±0.037 (N=372)	0.002±0.003 (N=73)	0.102±0.115 (N=100)
	2 & 3	-	0.004±0.005 (N=371)	0.171±0.209 (N=371)
Duplicate	2	0.039±0.035 (N=45)	0.003±0.002 (N=8)	0.149±0.155 (N=9)
	2 & 3	-	0.006±0.006 (N=45)	0.226±0.284 (N=45)

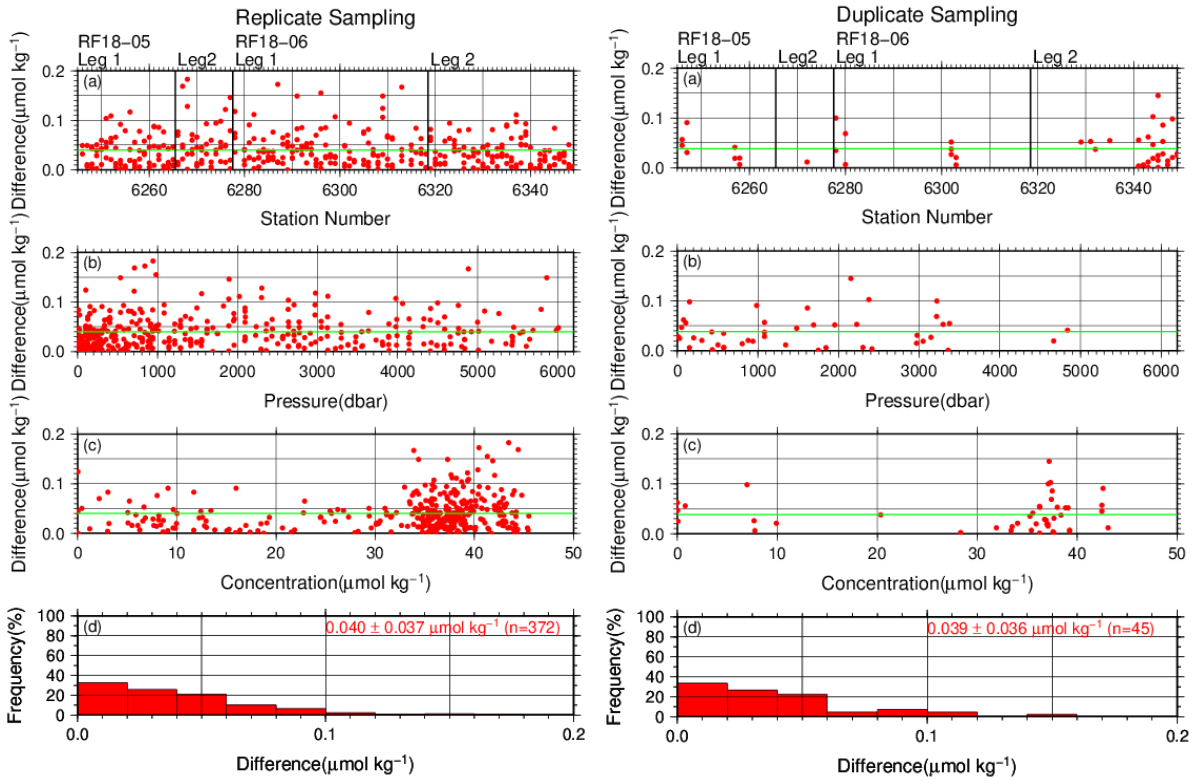

Figure C.4.3. Result of (left) replicate and (right) duplicate measurements of nitrate+nitrite through the cruise versus (a) station number, (b) sampling pressure, (c) concentration, and (d) histogram of the measurements. Green line indicates the mean of the differences of concentration of replicate/duplicate measurements for data flag 2.

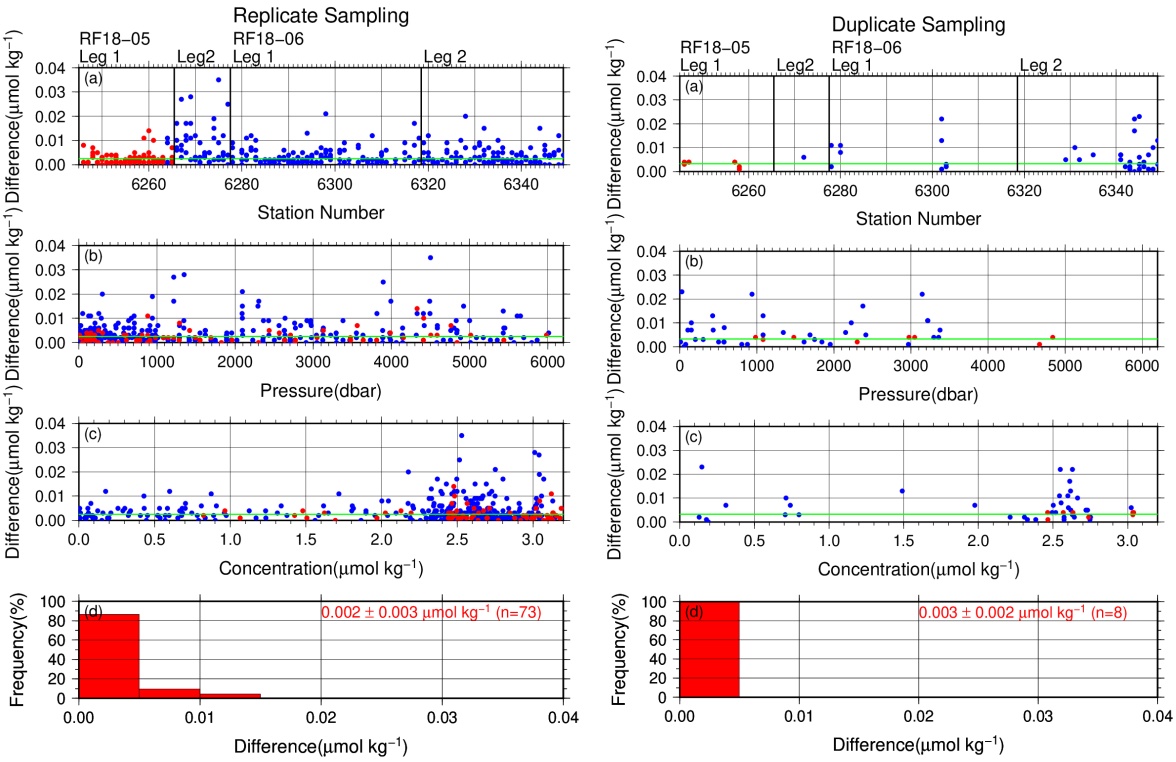

Figure C.4.4. Same as Figure C.4.3 but for phosphate. Red (blue) plots denote data flag 2 (3).

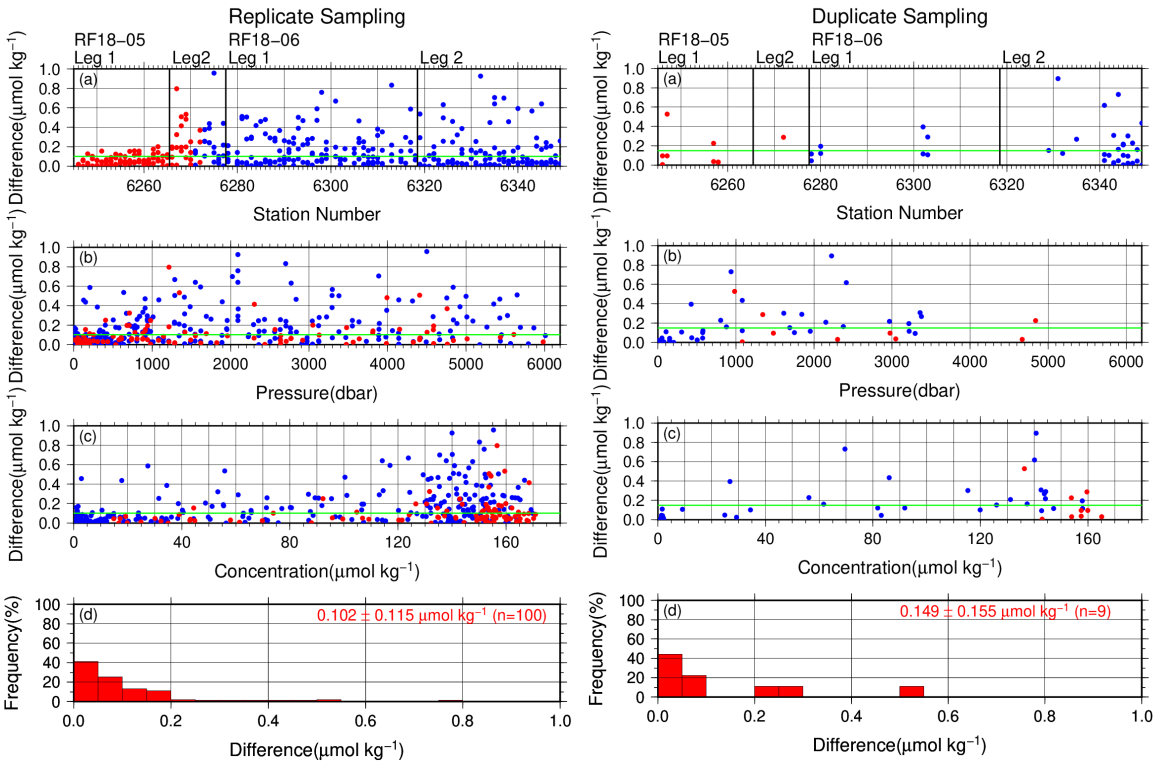

Figure C.4.5. Same as Figure C.4.4 but for silicate.

(7.2) Measurement of CRMs

CRM measurements during the cruise are summarized in Table C.4.6, whose concentrations were assigned with in-house standard solutions. The measured concentrations of CRM-BZ through the cruise are shown in Figures C.4.6–C.4.9.

Table C.4.6. Summary of (upper) mean concentration and its standard deviation (unit: μmol kg^{-1}), (middle) coefficient of variation (%), and (lower) total number of CRMs measurements through the cruise for data of flag 2 and for flag 2 and 3.

	Flag	Nitrate+nitrite	Nitrite	Phosphate	Silicate
CRM-BY	2	0.034±0.062 182.33 % (N=196)	0.025±0.002 8.27 % (N=194)	0.032±0.004 11.84 % (N=37)	1.89±0.08 4.34 % (N=51)
	2 & 3	-	-	0.032±0.007 20.24 % (N=196)	1.87±0.23 12.21 % (N=196)
CRM-CJ	2	16.17±0.06 0.38 % (N=150)	0.042±0.002 3.87 % (N=149)	1.18±0.003 0.24 % (N=27)	38.84±0.12 0.32 % (N=38)
	2 & 3	-	-	1.18±0.01 1.14 % (N=150)	38.85±0.50 1.28 % (N=150)
CRM-CB	2	35.89±0.10 0.27 % (N=196)	0.131±0.003 2.07 % (N=195)	2.51±0.004 0.16 % (N=37)	110.47±0.18 0.16 % (N=51)
	2 & 3	-	-	2.51±0.02 0.73 % (N=196)	110.59±0.83 0.75 % (N=196)
CRM-BZ	2	43.59±0.11 0.25 % (N=150)	0.226±0.006 2.77 % (N=149)	3.04±0.004 0.15 % (N=27)	162.55±0.23 0.14 % (N=38)
	2 & 3	-	-	3.05±0.02 0.62 % (N=150)	162.66±1.00 0.61 % (N=150)

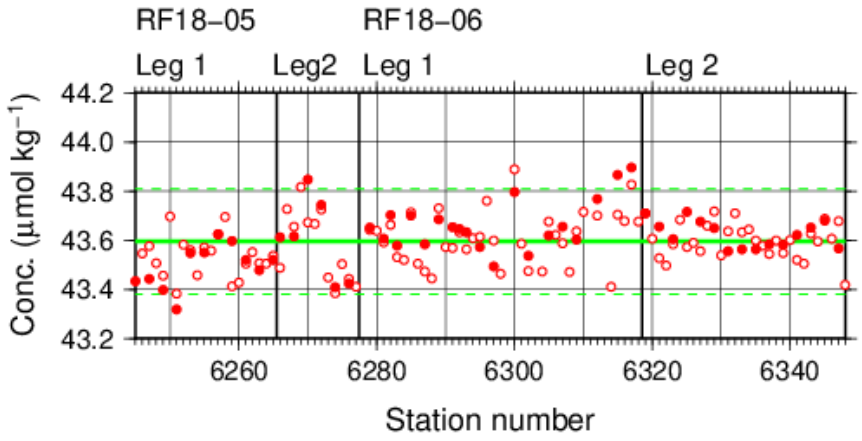

Figure C.4.6. Time-series of measured concentration of nitrate+nitrite of CRM-BZ through the cruise. Closed and open circles indicate the newly and previously opened bottle, respectively. Thick and dashed lines denote the mean and 2 times of standard deviations of the measurements for data flag 2 through the cruise, respectively.

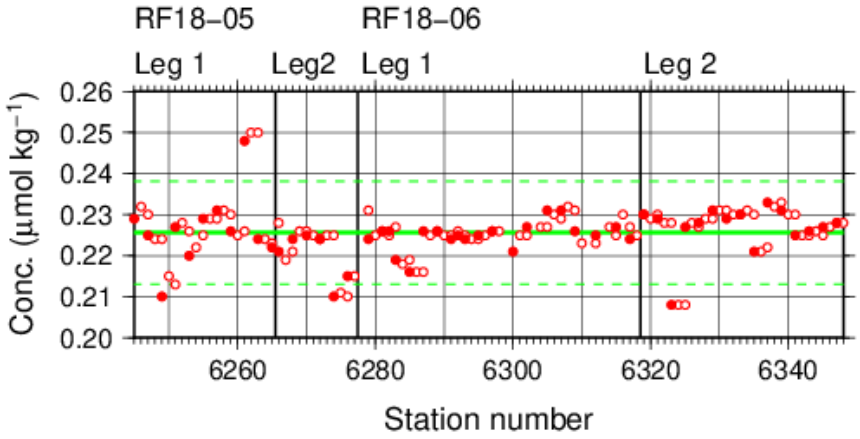

Figure C.4.7. Same as Figure C.4.6 but for nitrite.

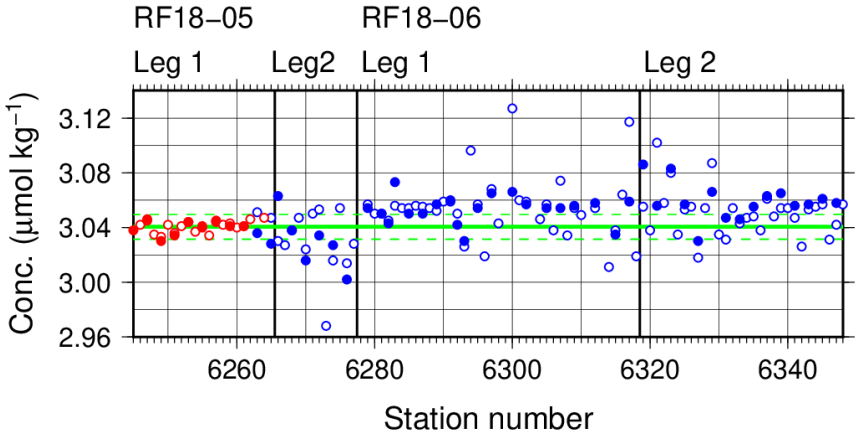

Figure C.4.8. Same as Figure C.4.6 but for phosphate. Red (blue) plots denote data flag 2 (3).

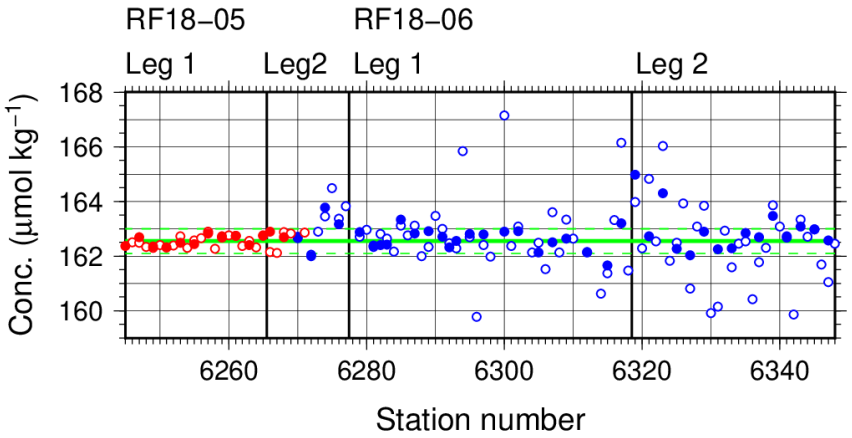

Figure C.4.9. Same as Figure C.4.8 but for silicate.

(7.3) Precision of analysis in a run

To monitor precision of analysis, the same samples were repeatedly measured in a sample array in a run. For this, C-5 standard solutions were randomly arrayed in every 2–10 samples as “check standard” (the number of the standard is about 8–9) in the run. The precision was estimated as coefficient of variation of the measurements. The results are summarized in Table C.4.7. The time series are shown in Figures C.4.10–C.4.13.

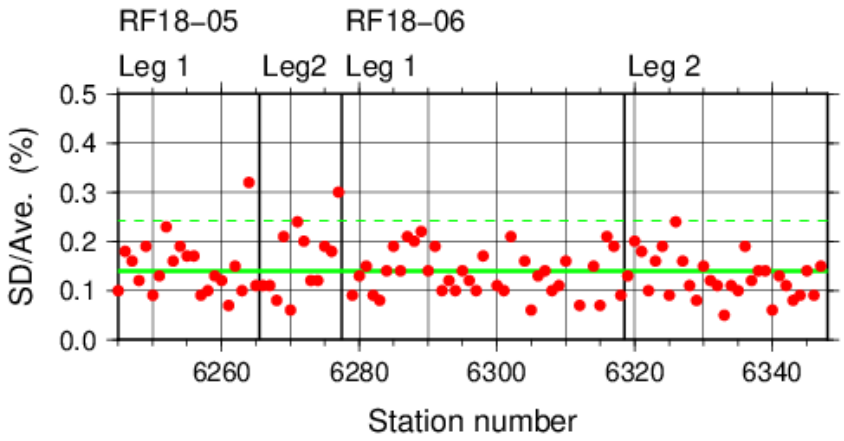

Figure C.4.10. Time-series of coefficient of variation of “check standard” measurement of nitrate+nitrite through the cruise. Thick and dashed lines denote the mean and 2 times of standard deviations of the measurements through the cruise, respectively.

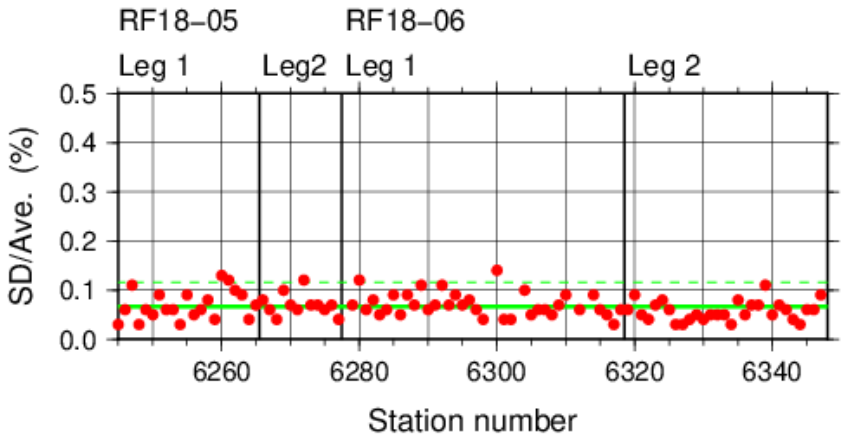

Figure C.4.11. Same as Figure C.4.10 but for nitrite.

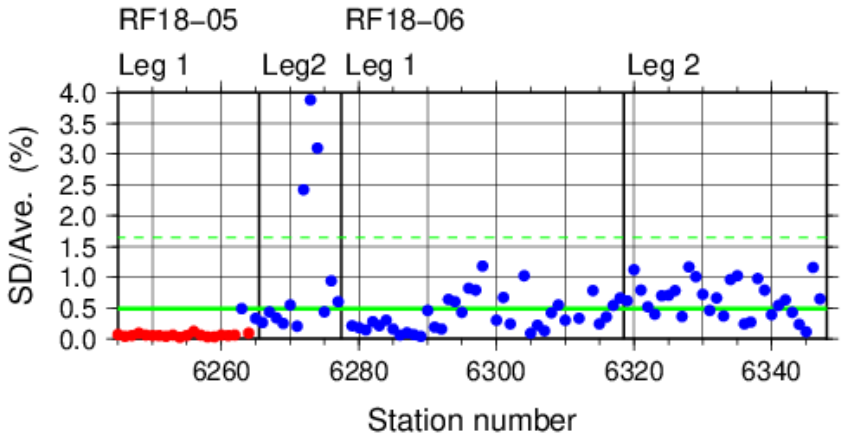

Figure C.4.12. Same as Figure C.4.10 but for phosphate. Red (blue) plots denote data flag 2 (3).

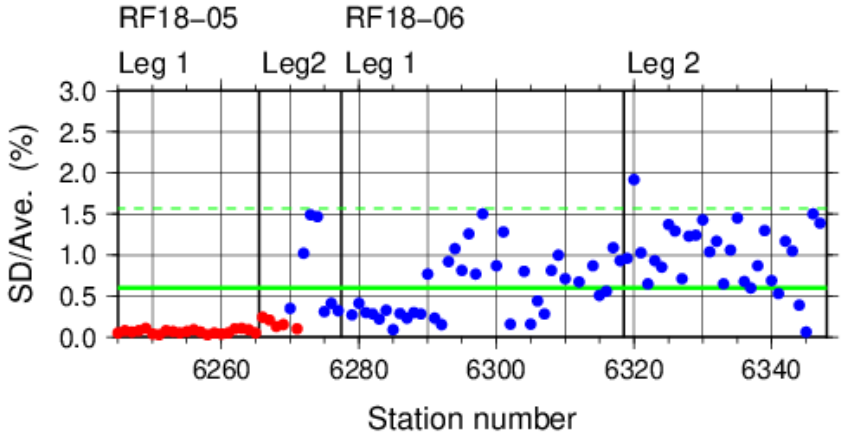

Figure C.4.13. Same as Figure C.4. 12 but for silicate.

Table C.4.7. Summary of precisions during the cruise. Numbers in parentheses indicate the summary with good measurement as data flag 2 (see (9)).

	Nitrate+nitrite	Nitrite	Phosphate	Silicate
Median	0.13 %	0.06 %	0.35 % (0.05 %)	0.48 % (0.08 %)
Mean	0.14 %	0.07 %	0.49 % (0.06 %)	0.60 % (0.09 %)
Minimum	0.05 %	0.03 %	0.02 % (0.02 %)	0.03 % (0.03 %)
Maximum	0.32 %	0.14 %	3.88 % (0.12 %)	1.92 % (0.24 %)
Number	98	98	98 (19)	98 (26)

(7.4) Carryover

Carryover coefficients were determined in each analysis run, using C-5 standard (high standard) followed by two C-1 standards (low standard). Time series of the carryover coefficients are shown in Figures C.4.14–17.

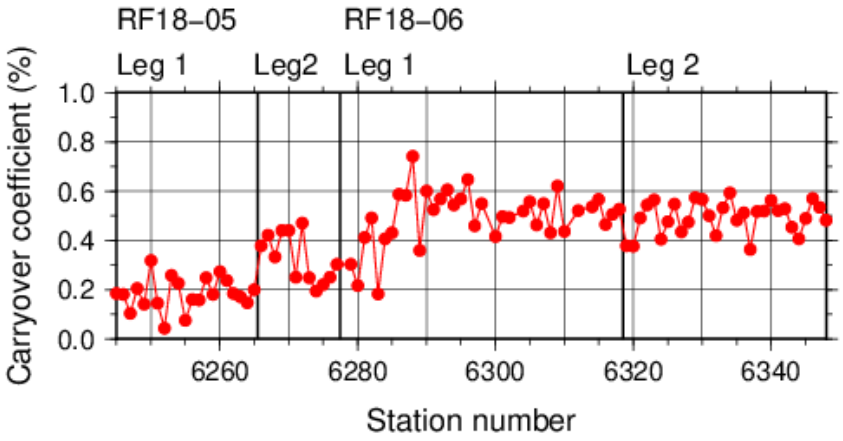

Figure C.4.14. Time-series of carryover coefficients in measurement of nitrate+nitrite through the cruise.

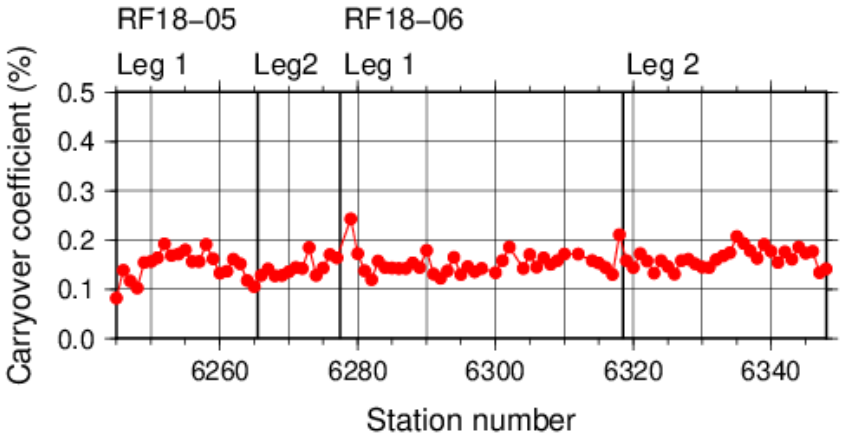

Figure C.4.15. Same as Figure C.4.14 but for nitrite.

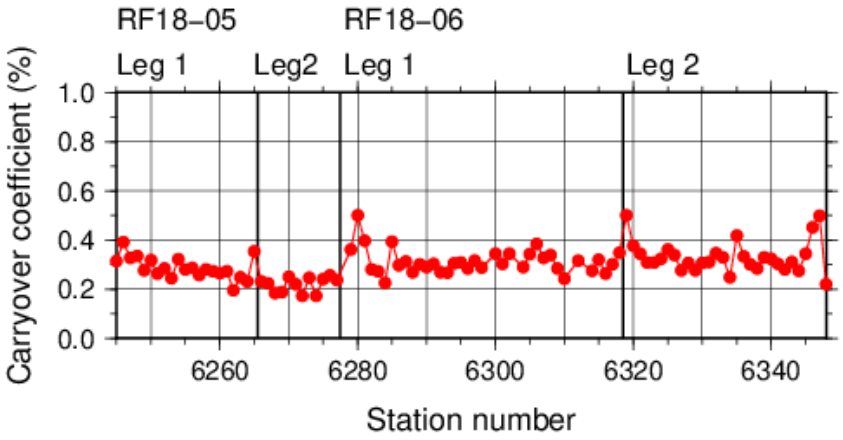

Figure C.4.16. Same as Figure C.4.14 but for phosphate.

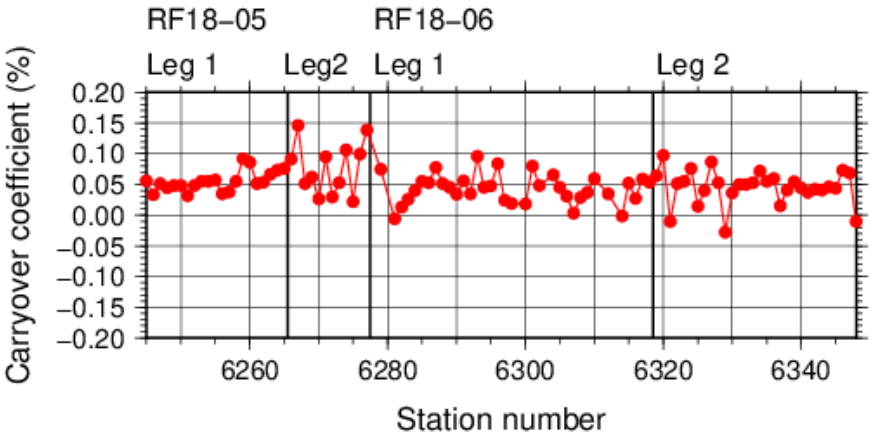

Figure C.4.17. Same as Figure C.4.14 but for silicate.

(7.5) Limit of detection/quantitation of measurement

Limit of detection (LOD) and quantitation (LOQ) of nutrient measurement were estimated from standard deviation (σ) of repeated measurements of nutrients concentration in C-1 standard as 3σ and 10σ, respectively. Summary of LOD and LOQ are shown in Table C.4.8.

Table C.4.8. Limit of detection (LOD) and quantitation (LOQ) of nutrient measurement in the cruise. Unit is μmol kg^{-1}.

	LOD	LOQ
Nitrate+nitrite	0.159	0.530
Nitrite	0.003	0.010
Phosphate	0.002	0.008
Silicate	0.127	0.424

(7.6) Quality control flag assignment

Quality flag value was assigned to nutriment measurements as shown in Table C.4.9, using the code defined in IOCCP Report No.14 (Swift, 2010).

Table C.4.9. Summary of assigned quality control flags.

Flag	Definition	Nitrate+nitrite	Nitrite	Phosphate	Silicate
2	Good	3061	3062	608	839
3	Questionable	1	0	2753	2489
4	Bad (Faulty)	4	4	4	10
5	Not reported	0	0	0	0
6	Replicate measurements	372	372	73	100
Total number of samples		3438	3438	3438	3438

(8) Uncertainty

(8.1) Uncertainty associated with concentration level

Generally, an uncertainty of nutrient measurement is expressed as a function of its concentration level which reflects that some components of uncertainty are relatively large in low concentration. Empirically, the uncertainty associated with concentrations level (U_c) can be expressed as follows;

$$U_c\ (\%) = a + b \cdot (1/C_x) + c \cdot (1/C_x)^2, \qquad \text{(C4.1)}$$

where C_x is the concentration of sample for parameter X.

Using the coefficients of variation of the CRM measurements throughout the cruise, uncertainty associated with concentrations of nitrate+nitrite, phosphate, and silicate were determined as follows:

$$U_{c\text{-}no3}\ (\%) = 0.171 + 3.414 \times (1/C_n) - 0.093 \times (1/C_n)^2 \qquad \text{(C4.2)}$$

$$U_{c\text{-}po4}\ (\%) = 0.091 + 0.168 \times (1/C_p) \qquad \text{(C4.3)}$$

$$U_{c\text{-}sil}\ (\%) = 0.080 + 9.39 \times (1/C_s) - 2.53 \times (1/C_s)^2, \qquad \text{(C4.4)}$$

where C_n, C_p, and C_s represent concentrations of nitrate+nitrite, phosphate, and silicate, respectively, in μmol kg^{-1}. For phosphate and silicate, uncertainty was evaluated with good measurement as data flag 2. Figures C.4.18–C.4.20 show the calculated uncertainty graphically.

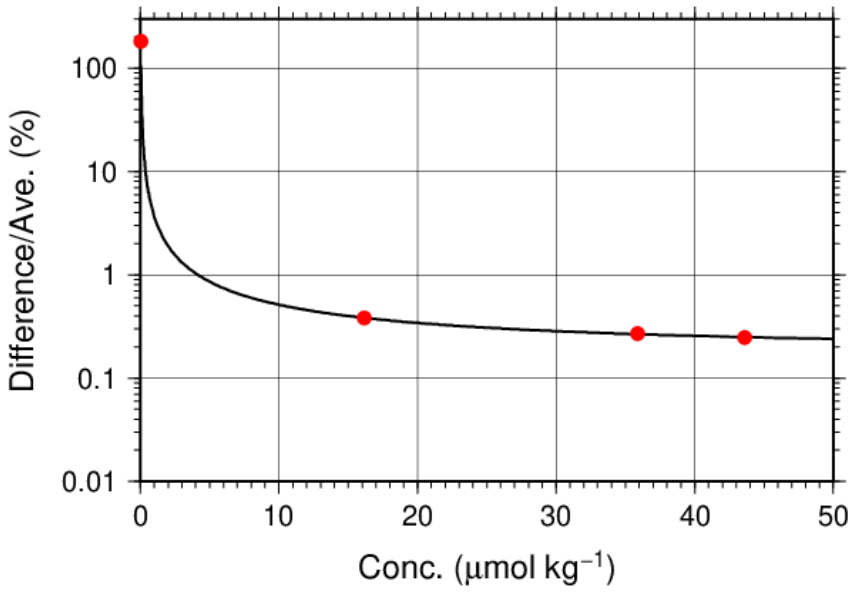

Figure C.4.18. Uncertainty of nitrate+nitrite associated with concentration level.

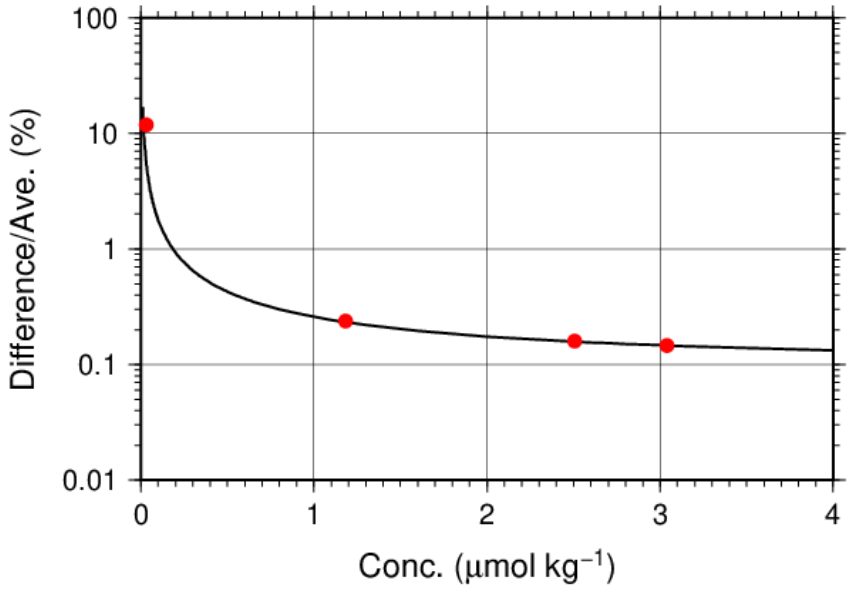

Figure C.4.19. Same as Figure C.4.18 but for phosphate.

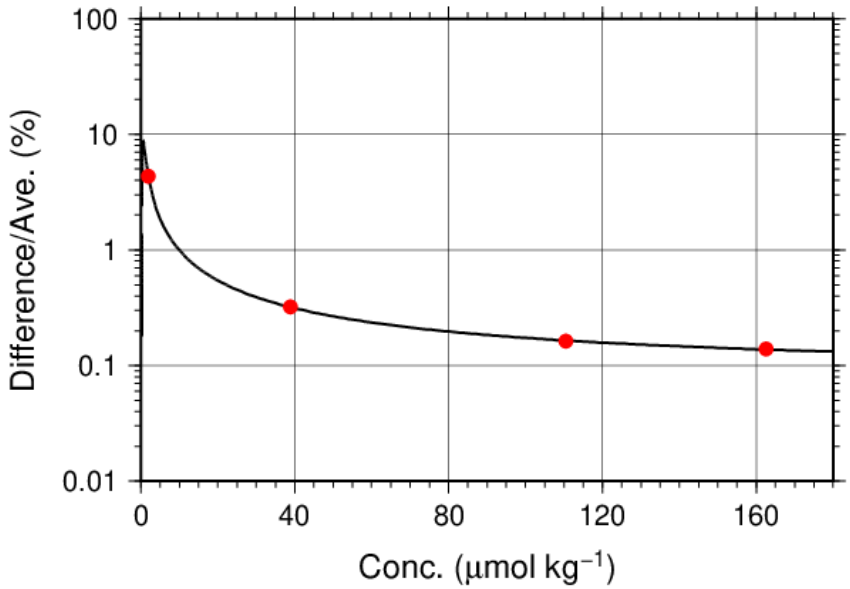

Figure C.4.20. Same as Figure C.4.18 but for silicate.

(8.2) Uncertainty of analysis between runs: U_s

Uncertainty of analysis among runs (U_s) was evaluated based on the coefficient of variation of measured concentrations of CRM-BZ with high concentration among the CRM lots throughout the cruise, as shown in subsection (7.2). The reason for using the CRM lot BZ to state U_s is to exclude the effect of uncertainty associated with lower concentration described previously. As is clear from the definition of U_c, U_s is equal to U_c at nutrients concentrations of lot BZ. It is important to note that U_s includes all of uncertainties during the measurements throughout stations, namely uncertainties of concentrations of in-house standard solutions

prepared for each run, uncertainties of slopes and intercepts of the calibration curve in each run if first order calibration curve applied, precision of measurement in a run (U_a), and between-bottle homogeneity of the CRM.

(8.3) Uncertainty of analysis in a run: U_a

Uncertainty of analysis in a run (U_a) was evaluated based on the coefficient of variation of repeated measurements of the "check standard" solution, as shown in subsection (7.3). The U_a reflects the conditions associated with chemistry of colorimetric measurement of nutrients, and stability of electronic and optical parts of the instrument throughout a run. Under a well-controlled condition of the measurements, U_a might show Poisson distribution with a mean as shown in Figures C.4.10–C.4.13 and Table C.4.7 and treated as a precision of measurement. U_a is a part of U_c at the concentration as stated in a previous section for U_c.
However, U_a may show larger value which was not expected from Poisson distribution of U_a due to the malfunction of the instruments, larger ambient temperature change, human errors in handling samples and chemistries and contaminations of samples in a run. In the cruise, we observed that U_a of our measurement was usually small and well-controlled in most runs as shown in Figures C.4.10–C.4.13 and Table C.4.7. However, in a few runs, U_a showed high values which were over the mean ± twice the standard deviations of U_a, suggesting that the measurement system might have some problems.

(8.4) Uncertainty of CRM concentration: U_r

In the certification of CRM, the uncertainty of CRM concentrations (U_r) was stated by the manufacturer (Table C.4.4) as expanded uncertainty at k=2. This expanded uncertainty reflects the uncertainty of the Japan Calibration Service System (JCSS) solutions, characterization in assignment, between-bottle homogeneity, and long term stability. We have ensured comparability between cruises by ensuring that at least two lots of CRMs overlap between cruises. In comparison of nutrient concentrations between cruises using KANSO CRMs in an organization, it was not necessary to include U_r in the conclusive uncertainty of concentration of measured samples because comparability of measurements was ensured in an organization as stated previously.

(8.5) Conclusive uncertainty of nutrient measurements of samples: U

To determine the conclusive uncertainty of nutrient measurements of samples (U), we use two functions depending on U_a value acquired at each run as follows:
When U_a was small and measurement was well-controlled condition, the conclusive uncertainty of nutrient measurements of samples, U, might be as below:

$$U = U_c. \qquad \text{(C4.5)}$$

When U_a was relative large and the measurement might have some problems, the conclusive uncertainty of nutrient measurements of samples, U, can be expanded as below:

$$U = \sqrt{U_c^2 + U_a^2}. \qquad \text{(C4.6)}$$

When U_a was relative large and the measurement might have some problems, the equation of U is defined as to include U_a to evaluate U, although U_a partly overlaps with U_c. It means that the equation overestimates the conclusive uncertainty of samples. On the other hand, for low concentration there is a possibility that the equation not only overestimates but also underestimates the conclusive uncertainty because the functional shape of U_c in lower concentration might not be the same and cannot be verified. However, we believe that the applying the above function might be better way to evaluate the conclusive uncertainty of nutrient measurements of samples because we can do realistic evaluation of uncertainties of nutrient concentrations of samples which were obtained under relatively unstable conditions, larger U_a as well as the evaluation of them under normal and good conditions of measurements of nutrients.

(9) Problems

Sensitivity drift occurred in measurements of phosphate after Stn.19 (Lat. 48-59.63 N / Long. 165-01.21 E, RF6263) and silicate after Stn.26 (Lat. 43-00.88 N / Long. 164-58.46 E, RF6270) due to an electrical trouble in colorimeters (Figure C.4.18). This problem continued to the end of the cruises. To correct this, we applied sensitivity correction for subdivided intervals using "check standard" concentrations which were occasionally measured in a run (see (7.3)), instead of the regular sensitivity correction for the whole span (Appendix A.3). However, this correction was insufficient. Therefore, these data were flagged as 3 (questionable).

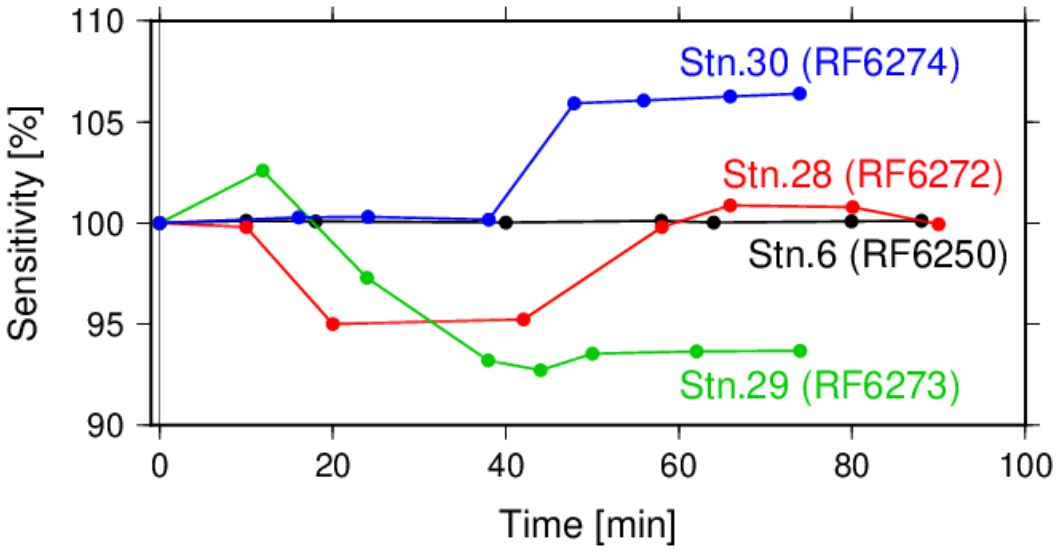

Figure C.4.18. Examples of temporal change in relative concentration of "check standard" in a run (sensitivity to initial one). Black color (Stn.6) indicates a measurement before the problem occurred.

Appendix

A1. Seawater sampling

Seawater samples were collected from 10-liters Niskin bottle attached CTD-system and a stainless steel bucket for the surface. Samples were drawn into 10 mL polymethylpenten vials using sample drawing tubes. The vials were rinsed three times before water filling and were capped immediately after the drawing.

No transfer was made and the vials were set on an auto sampler tray directly. Samples were analyzed immediately after collection.

A2. Measurement

(A2.1) General

Auto Analyzer III is based on Continuous Flow Analysis method and consists of sampler, pump, manifolds, and colorimeters. As a baseline, we used artificial seawater (ASW).

(A2.2) Nitrate+nitrite and nitrite

Nitrate+nitrite and nitrite were analyzed according to the modification method of Armstrong (1967). The sample nitrate was reduced to nitrite in a glass tube which was filled with granular cadmium coated with copper. The sample stream with its equivalent nitrite was treated with an acidic, sulfanilamide reagent and the nitrite forms nitrous acid which reacts with the sulfanilamide to produce a diazonium ion. N-1-naphthylethylene-diamine was added to the sample stream then coupled with the diazonium ion to produce a red, azo dye. With reduction of the nitrate to nitrite, sum of nitrate and nitrite were measured; without reduction, only nitrite was measured. Thus, for the nitrite analysis, no reduction was performed and the alkaline buffer was not necessary. The flow diagrams for each parameter are shown in Figures C.4.A1 and C.4.A2. If the reduction efficiency of the cadmium column became lower than 95 %, the column was replaced.

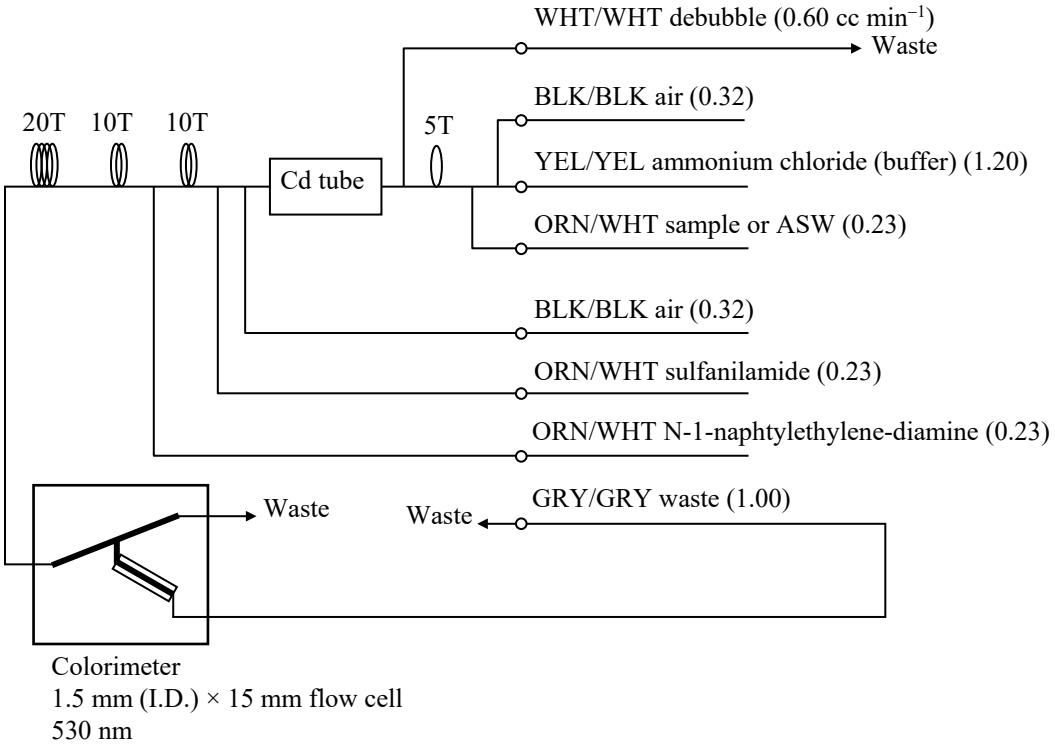

Figure C.4.A1. Nitrate+nitrite (ch. 1) flow diagram.

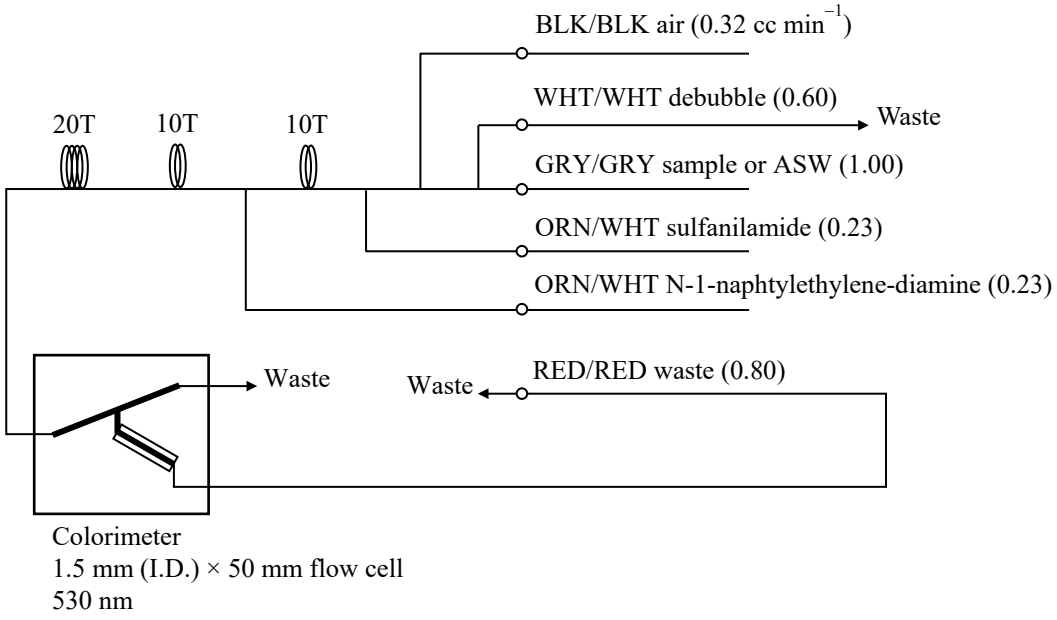

Figure C.4.A2. Nitrite (ch. 2) flow diagram.

(A2.3) Phosphate

The phosphate analysis was a modification of the procedure of Murphy and Riley (1962). Molybdic acid was added to the seawater sample to form phosphomolybdic acid which was in turn reduced to phosphomolybdous acid using L-ascorbic acid as the reductant. The flow diagram for phosphate is shown in Figure C.4.A3.

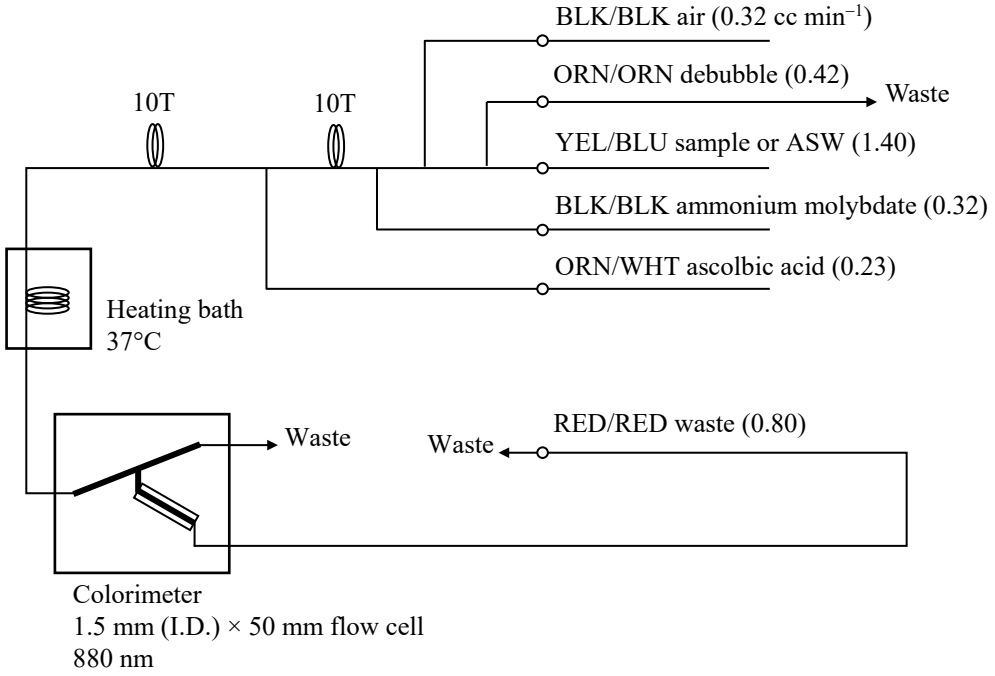

Figure C.4.A3. Phosphate (ch. 3) flow diagram.

(A2.4) Silicate

The silicate was analyzed according to the modification method of Grasshoff *et al.* (1983), wherein silicomolybdic acid was first formed from the silicate in the sample and added molybdic acid, then the silicomolybdic acid was reduced to silicomolybdous acid, or "molybdenum blue," using L-ascorbic acid as the reductant. The flow diagram for silicate is shown in Figure C.4.A4.

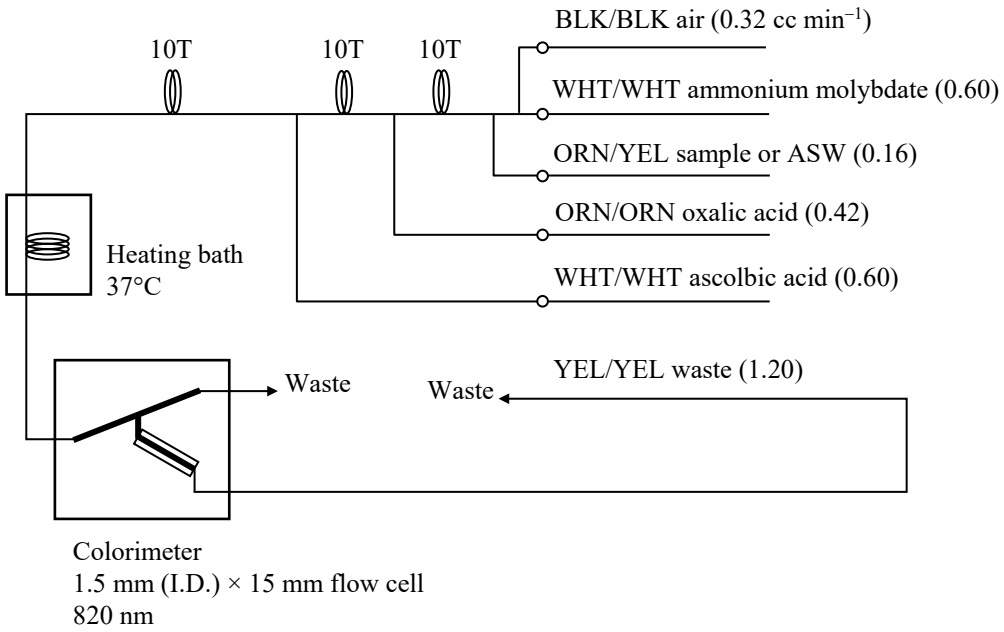

Figure C.4.A4. Silicate (ch. 4) flow diagram.

A3. Data processing

Raw data from Auto Analyzer III were recorded at 1-second interval and were treated as follows;

a. Check the shape of each peak and position of peak values taken, and then change the positions of peak values taken if necessary.
b. Baseline correction was done basically using liner regression.
c. Reagent blank correction was done basically using liner regression.
d. Carryover correction was applied to peak heights of each sample.
e. Sensitivity correction was applied to peak heights of each sample.
f. Refraction error correction was applied to peak heights of each seawater sample.
g. Calibration curves to get nutrients concentration were assumed quadratic expression.
h. Concentrations were converted from μmol L^{-1} to μmol kg^{-1} using seawater density.

A4. Reagents recipes

(A4.1) Nitrate+nitrite

Ammonium chloride (buffer), 0.7 μmol L^{-1} (0.04 % w/v);

Dissolve 190 g ammonium chloride, NH_4Cl, in ca. 5 L of DW, add about 5 mL ammonia(aq) to adjust pH of 8.2–8.5.

Sulfanilamide, 0.06 μmol L^{-1} (1 % w/v);

Dissolve 5 g sulfanilamide, 4-$NH_2C_6H_4SO_3H$, in 430 mL DW, add 70 mL concentrated HCl. After mixing, add 1 mL Brij-35 (22 % w/w).

N-1-naphtylethylene-diamine dihydrochloride (NEDA), 0.004 μmol L^{-1} (0.1 % w/v);

Dissolve 0.5 g NEDA, $C_{10}H_7NH_2CH_2CH_2NH_2 \cdot 2HCl$, in 500 mL DW.

(A4.2) Nitrite

Sulfanilamide, 0.06 μmol L^{-1} (1 % w/v); Shared from nitrate reagent.

N-1-naphtylethylene-diamine dihydrochloride (NEDA), 0.004 μmol L^{-1} (0.1 % w/v); Shared from nitrate reagent.

(A4.3) Phosphate

Ammonium molybdate, 0.005 μmol L^{-1} (0.6 % w/v);

Dissolve 3 g ammonium molybdate(VI) tetrahydrate, $(NH_4)_6Mo_7O_{24} \cdot 4H_2O$, and 0.05 g potassium antimonyl tartrate, $C_8H_4K_2O_{12}Sb_2 \cdot 3H_2O$, in 400 mL DW and add 40 mL concentrated H_2SO_4. After mixing, dilute the solution with DW to final volume of 500 mL and add 2 mL sodium dodecyl sulfate (15 % solution in water).

L(+)-ascorbic acid, 0.08 μmol L^{-1} (1.5 % w/v);

Dissolve 4.5 g L(+)-ascorbic acid, $C_6H_8O_6$, in 300 mL DW. After mixing, add 10 mL acetone. This reagent was freshly prepared before every measurement.

(A4.4) Silicate

Ammonium molydate, 0.005 μmol L^{-1} (0.6 % w/v);

Dissolve 3 g ammonium molybdate(VI) tetrahydrate, $(NH_4)_6Mo_7O_{24} \cdot 4H_2O$, in 500 mL DW and added concentrated 2 mL H_2SO_4. After mixing, add 2 mL sodium dodecyl sulfate (15 % solution in water).

Oxalic acid, 0.4 μmol L^{-1} (5 % w/v);

Dissolve 25 g oxalic acid dihydrate, $(COOH)_2 \cdot 2H_2O$, in 500 mL DW.

L(+)-ascorbic acid, 0.08 μmol L^{-1} (1.5 % w/v); Shared from phosphate reagent.

(A4.5) Baseline

Artificial seawater (salinity is ~34.7);

Dissolve 160.6 g sodium chloride, NaCl, 35.6 g magnesium sulfate heptahydrate, $MgSO_4 \cdot 7H_2O$, and 0.84 g sodium hydrogen carbonate, $NaHCO_3$, in 5 L DW.

References

Armstrong, F. A. J., C. R. Stearns and J. D. H. Strickland (1967), The measurement of upwelling and subsequent biological processes by means of the Technicon TM Autoanalyzer TM and associated equipment, *Deep-Sea Res.*, 14(3), 381–389.

DOE (1994), Handbook of methods for the analysis of the various parameters of the carbon dioxide system in sea water; version 2. *A. G. Dickson and C. Goyet (eds), ORNL/CDIAC-74*.

Grasshoff, K., Ehrhardt, M., Kremling K. et al. (1983), Methods of seawater analysis. 2nd rev, *Weinheim: Verlag Chemie, Germany, West.*

Murphy, J. and Riley, J.P. (1962), Analytica chimica *Acta*, *27, 31-36.*

Swift, J. H. (2010), Reference-quality water sample data: Notes on acquisition, record keeping, and evaluation. *IOCCP Report No.14, ICPO Pub. 134, 2010 ver.1*.

8. Phytopigments (chlorophyll-a and phaeopigment)

8 June 2020

(1) Personnel

RF18-05

Kazuhiro SAITO (GEMD/JMA)
Daisuke SASANO (GEMD/JMA)
Yoichi IMAI(GEMD/JMA)
Ryoma SUZUKI (GEMD/JMA)
Risa FUJIMOTO(GEMD/JMA)

RF18-06

Yoichi IMAI(GEMD/JMA)
Yoshihiro SHINODA(GEMD/JMA)
Ryoma SUZUKI (GEMD/JMA)
Takuya SASAKI(GEMD/JMA)
Takahiro OKA(GEMD/JMA)

(2) Station occupied

A total of 80 stations (RF 18-05 Leg 1: 21, Leg 2: 11, RF 18-06 Leg 1: 30, Leg 2: 18) were occupied for phytopigment measurements. Station location and sampling layers of phytopigment are shown in Figures C.5.1 and C.5.2.

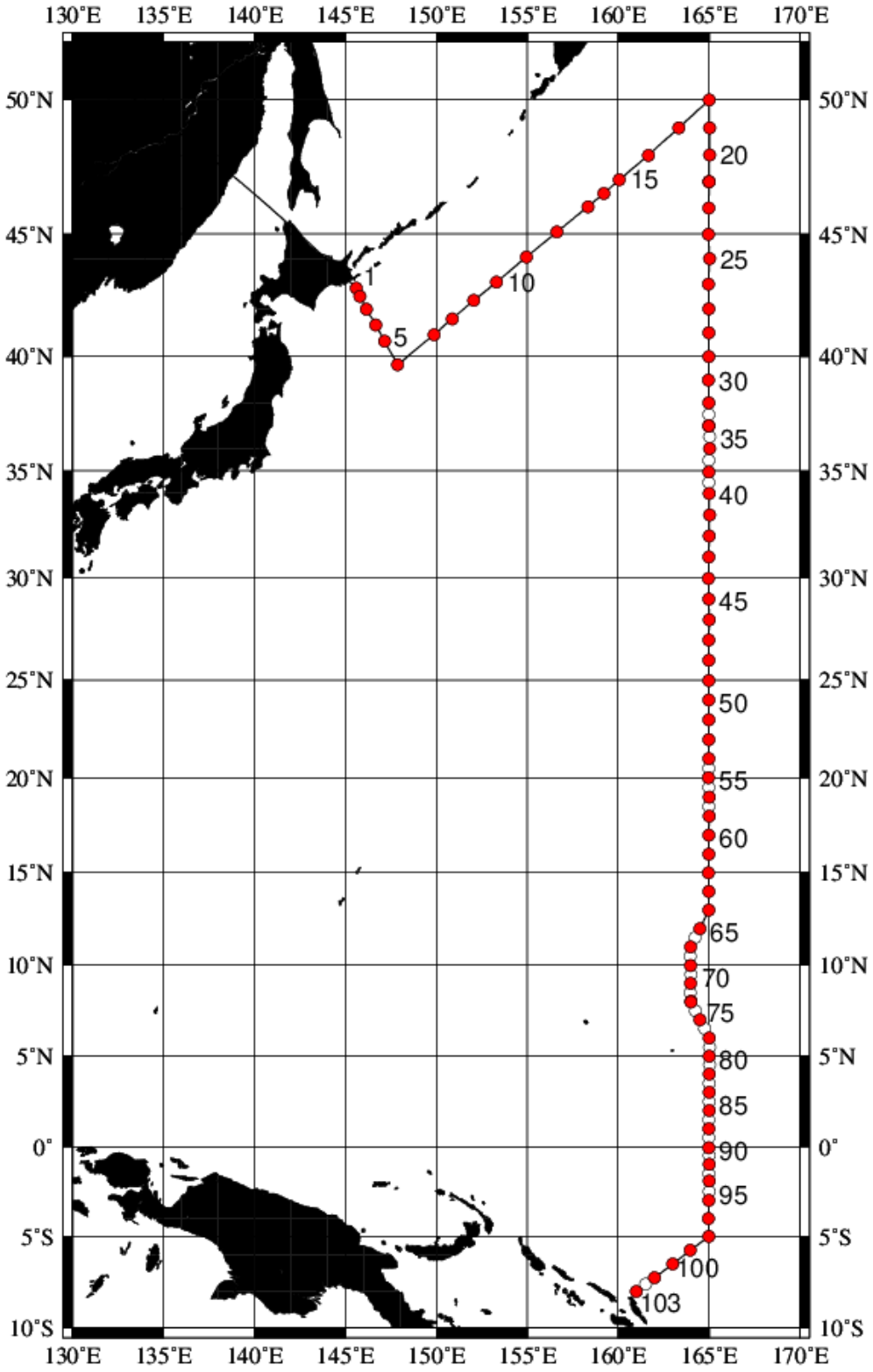

Figure C.5.1. Location of observation stations of chlorophyll-*a*. Closed and open circles indicate sampling and no-sampling stations, respectively.

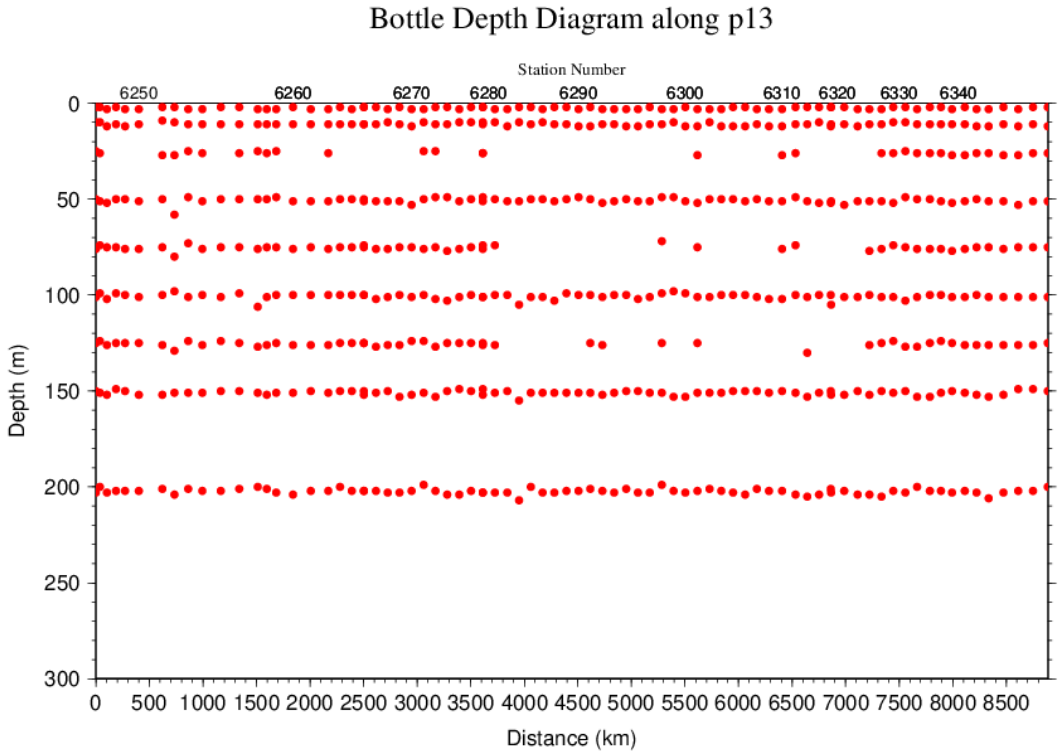

Figure C.5.2. Distance-depth distribution of sampling layers of chlorophyll-*a*.

(3) Reagents

N,N-dimethylformamide (DMF)
Hydrochloric acid (HCl), 0.5 mol L^{-1}
Chlorophyll-*a* standard from *Anacystis nidulans* algae (Sigma-Aldrich, United States)
Rhodamine WT (Turner Designs, United States)

(4) Instruments

Fluorometer: 10-AU (Turner Designs, United States)
Spectrophotometer: UV-1800 (Shimadzu, Japan)

(5) Standardization

(5.1) Determination of chlorophyll-*a* concentration of standard solution

To prepare the pure chlorophyll-*a* standard solution, reagent powder of chlorophyll-*a* standard was dissolved in DMF. A concentration of the chlorophyll-*a* solution was determined with the spectrophotometer as follows:

$$\text{chl. } a \text{ concentration } (\mu g\ mL^{-1}) = A_{chl} / a^{*}_{phy} \qquad (C5.1)$$

where A_{chl} is the difference between absorbance at 663.8 nm and 750 nm, and a^{*}_{phy} is specific absorption coefficient (UNESCO, 1994). The specific absorption coefficient is 88.74 L g^{-1} cm^{-1} (Porra *et al.*, 1989).

(5.2) Determination of R and f_{ph}

Before measurements, sensitivity of the fluorometer was calibrated with pure DMF and a rhodamine 1 ppm solution (diluted with deionized water).
The chlorophyll-*a* standard solution, whose concentration was precisely determined in subsection (5.1), was measured with the fluorometer, and after acidified with 1–2 drops 0.5 mol L^{-1} HCl the solution was also measured. The acidification coefficient (R) of the fluorometer was also calculated as the ratio of the unacidified and acidified readings of chlorophyll-*a* standard solution. The linear calibration factor (f_{ph}) of the fluorometer was calculated as the slope of the acidified reading against chlorophyll-*a* concentration. The R and f_{ph} in the cruise are shown in Table C.9.1.

Table C.9.1. R and f_{ph} in the cruises.

Cruises number	RF18-05	RF18-06
Acidification coefficient (R)	1.8707	1.8997
Linear calibration factor (f_{ph})	7.3470	6.2584

(6) Seawater sampling and measurement
Water samples were collected from 10-liters Niskin bottle attached the CTD-system and a stainless steel bucket for the surface. A 200 mL seawater sample was immediately filtered through 25 mm GF/F filters by low vacuum pressure below 15 cmHg, the particulate matter collected on the filter. Phytopigments were extracted in vial with 9 mL of DMF. The extracts were stored for 24 hours in the refrigerator at –30 °C until analysis.
After the extracts were put on the room temperature for at least one hour in the dark, the extracts were decanted from the vial to the cuvette. Fluorometer readings for each cuvette were taken before and after acidification with 1–2 drops 0.5 mol L^{-1} HCl. Chlorophyll-*a* and phaeopigment concentrations (μg mL^{-1}) in the sample are calculated as follows:

$$\text{chl } a \text{ conc.} = \frac{F_0 - F_a}{f_{ph} \cdot (R - 1)} \cdot \frac{v}{V} \qquad \text{(C5.2)}$$

$$\text{phaeo. conc.} = \frac{R \cdot F_0 - F_a}{f_{ph} \cdot (R - 1)} \cdot \frac{v}{V} \qquad \text{(C5.3)}$$

F_0: reading before acidification
F_a: reading after acidification
R: acidification coefficient (F_0/F_a) for pure chlorophyll-*a*
f_{ph}: linear calibration factor
v: extraction volume
V: sample volume.

(7) Quality control flag assignment
Quality flag value was assigned to oxygen measurements as shown in Table C.5.2, using the code defined in IOCCP Report No.14 (Swift, 2010).

Table C.5.2 Summary of assigned quality control flags.

Flag	Definition	Chl. *a*	Phaeo.

2	Good	616	616
3	Questionable	0	0
4	Bad (Faulty)	2	2
5	Not reported	1	1
	Total number	619	619

References

Porra, R. J., W. A. Thompson and P. E. Kriedemann (1989), Determination of accurate coefficients and simultaneous equations for assaying chlorophylls *a* and *b* extracted with four different solvents: verification of the concentration of chlorophyll standards by atomic absotption spectroscopy. *Biochem. Biophy. Acta,* 975, 384-394.

Swift, J. H. (2010), Reference-quality water sample data: Notes on acquisition, record keeping, and evaluation. *IOCCP Report No.14, ICPO Pub. 134, 2010 ver.1*.

UNESCO (1994), Protocols for the joint global ocean flux study (JGOFS) core measurements: Measurement of chlorophyll *a* and phaeopigments by fluorometric analysis, *IOC manuals and guides 29, Chapter 14.*

9. Total Dissolved Inorganic Carbon (DIC)

30 September 2023

(8) Personnel

HAMANA Minoru (RF18-05)
HORI Kasumi (RF18-05)
NAKAMURA Naoki (RF18-05)
AKAMATSU Mio (RF18-06)
MARUO Tetsuya (RF18-06)
TANIZAKI Chiho(RF18-06)

(9) Station occupied

A total of 78 stations (RF18-05 Leg 1: 19, RF18-05 Leg 2: 11, RF18-06 Leg 1: 30, RF18-06 Leg 2: 18) were occupied for total dissolved inorganic carbon (DIC). Station location and sampling layers of them are shown in Figures C.6.1 and C.6.2, respectively.

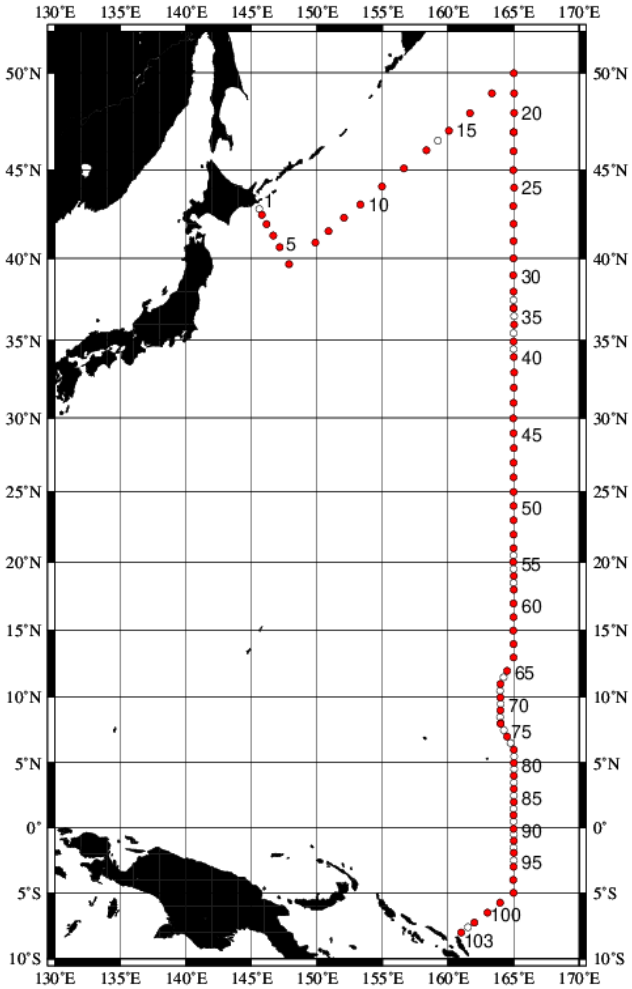

Figure C.6.1. Location of observation stations of DIC. Closed and open circles indicate sampling and no-sampling stations, respectively.

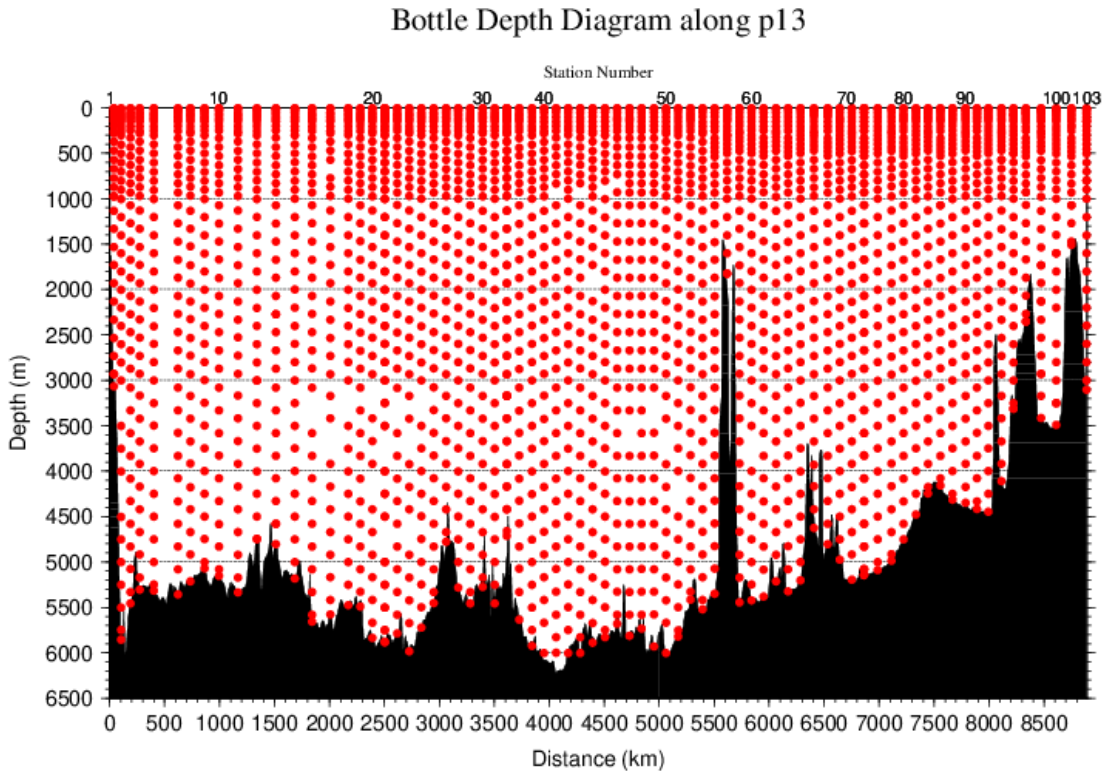

Figure C.6.2. Distance-depth distribution of sampling layers of DIC.

(10) Instrument

The measurement of DIC was carried out with DIC/TA analyzers (Nihon ANS Co. Ltd, Japan). We used two analyzers concurrently. These analyzers are designated as apparatus A and B.

(11) Sampling and measurement

Methods of seawater sampling, poisoning, measurement, and calculation of DIC concentrations were based on the Standard Operating Procedure (SOP) described in PICES Special Publication 3, SOP-2 (Dickson et al., 2007). DIC was determined by coulometric analysis (Johnson et al., 1985, 1987) using an automated CO_2 extraction unit and a coulometer. Details of sampling and measurement are shown in Appendix A1.

(12) Calibration

The concentration of DIC (C_T) in moles per kilogram (mol kg^{-1}) of seawater was calculated from the following equation:

$$C_T = N_S / (cV \cdot \rho_S) \qquad \text{(C6.1)}$$

where N_S is the counts of the coulometer (gC), cV is the calibration factor (gC (mol L^{-1})$^{-1}$), and ρ_S is density of seawater (kg L^{-1}), which is calculated from the salinity of the sample and the water temperature of the water-jacket for the sample pipette.

The values of cV were determined by measurements of Certified Reference Materials (CRMs) that were provided by Dr. Andrew G. Dickson of the Scripps Institution of Oceanography. Table C.6.1 provides information about the CRM batches used in this cruise.

Table C.6.1. Certified C_T and standard deviation of CRMs. Unit of C_T is μmol kg^{-1}. More information is available at the NOAA web site (https://www.ncei.noaa.gov/access/ocean-carbon-acidification-data-system/oceans/Dickson_CRM/batches.html).

Cruise	RF18-05	RF18-06
Batch number	168	174
C_T	2071.47±0.74	2050.56±0.62
Salinity	33.481	33.408

The CRM measurement was carried out at every station. After the cruise, a value of *cV* was assigned to each apparatus (A, B). Table C.6.2 summarizes the *cV* values. Figure C.6.3 shows details.

Table C.6.2. Assigned *cV* and its standard deviation for each apparatus during the cruise. Unit is gC $(mol\ L^{-1})^{-1}$.

Apparatus	Cruise	*cV*
A	RF18-05	0.191816±0.000245 (N=79)
	RF18-06 Leg 1	0.191534±0.000261 (N=66)
	RF18-06 Leg 2	0.191555±0.000220 (N=33)
B	RF18-05	0.192648±0.000303 (N=66)
	RF18-06 Leg 1	0.192653±0.000312 (N=65)
	RF18-06 Leg 2	0.192804±0.000244 (N=44)

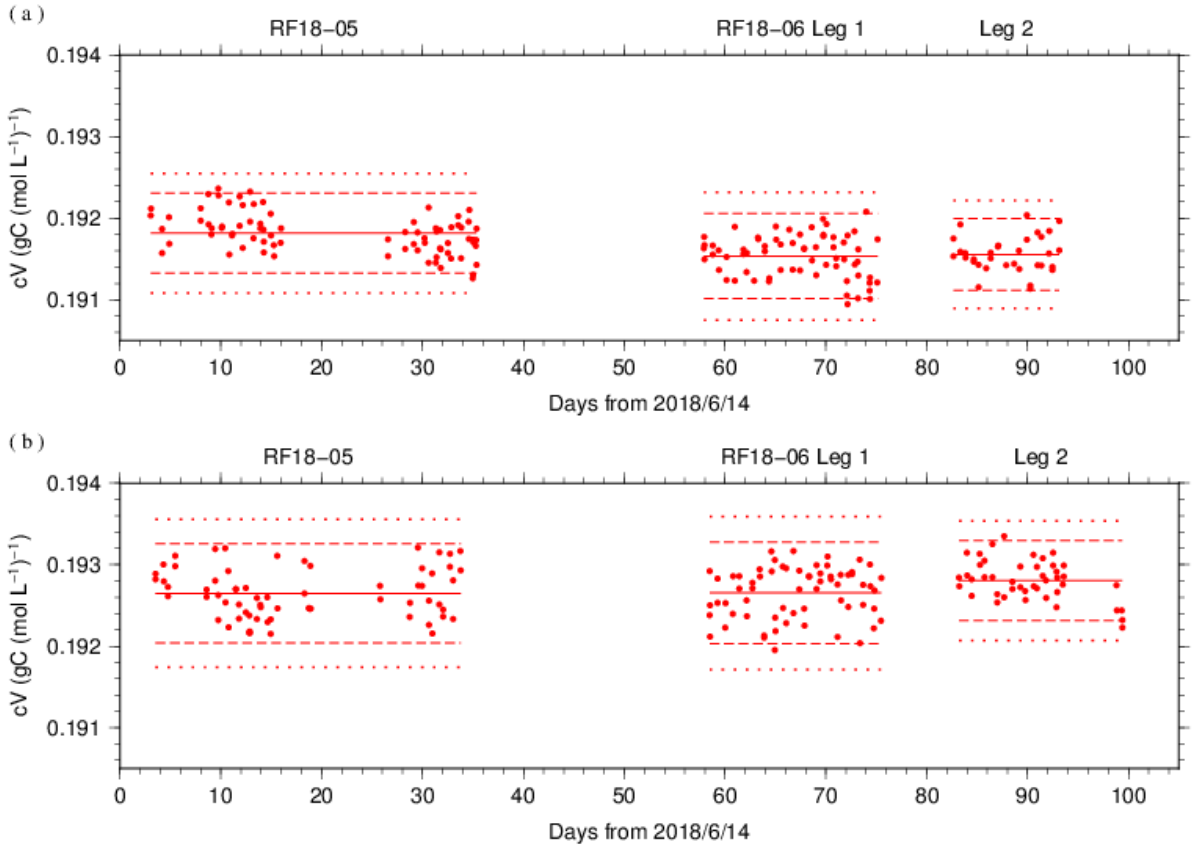

Figure C.6.3. Results of the cV at each station assigned for apparatus (a) A and (b) B. The solid, dashed, and dotted lines denote the mean, the mean ± twice the S.D., and the mean ± thrice the S.D. for all measurements, respectively.

The precisions of the cV is equated to its coefficient of variation (= S.D. / mean). They were 0.128 % for apparatus A in RF18-05, 0.136 % for apparatus A in RF18-06 Leg 1, 0.115 % for apparatus A in RF18-06 Leg 2, 0.157 % for apparatus B in RF18-05, 0.162 % for apparatus B in RF18-06 Leg 1 and 0.127 % for apparatus B in RF18-06 Leg 2. They correspond to 2.65 μmol kg^{-1}, 2.79 μmol kg^{-1}, 2.36 μmol kg^{-1}, 3.26 μmol kg^{-1}, 3.32 μmol kg^{-1} and 2.60 μmol kg^{-1} in C_T of CRM batch 168 (in RF18-05) and 174 (in RF18-06), respectively.

Finally, the value of C_T was multiplied by 1.00067 (= 300.2 / 300.0) to correct dilution effect induced by addition of 0.2 mL of mercury (II) chloride ($HgCl_2$) solution in a sampling bottle with a volume of ~300 mL.

(13) Quality Control

(6.1) Replicate and duplicate analyses

We took replicate (pair of water samples taken from a single Niskin bottle) and duplicate (pair of water samples taken from different Niskin bottles closed at the same depth) samples of DIC throughout the cruise. Table C.6.3 summarizes the results of the measurements with each apparatus. Figures C.6.4–C.6.5 show details of the results. The calculation of the standard deviation from the difference of sets of measurements was based on a procedure (SOP 23) in DOE (1994).

Table C.6.3. Summary of replicate and duplicate measurements. Unit is μmol kg^{-1}.

	Apparatus A	Apparatus B
Measurement	**Average magnitude of difference ± S.D.**	
Replicate	2.3±2.1 (N=103)	2.4±2.2 (N=92)
Duplicate	2.6±2.1 (N=15)	2.5±2.1 (N=12)

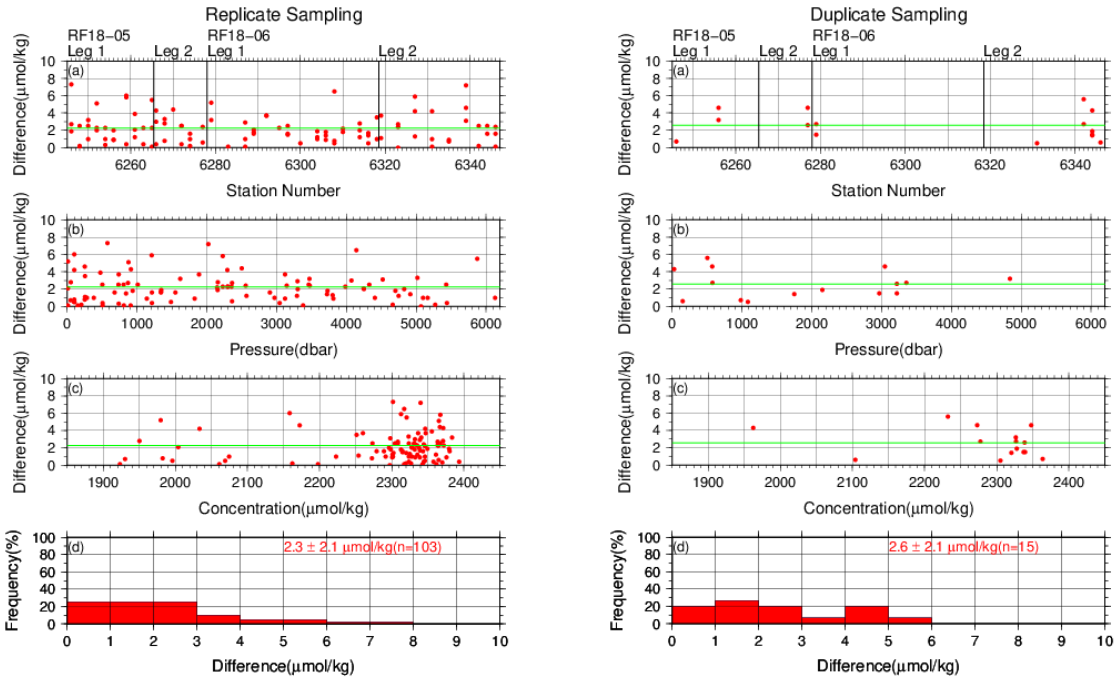

Figure C.6.4. Results of (left) replicate and (right) duplicate measurements during the cruise versus (a) station number, (b) pressure, and (c) C_T determined by apparatus A. The green lines denote the averages of the measurements. The bottom panels (d) show histograms of the measurements.

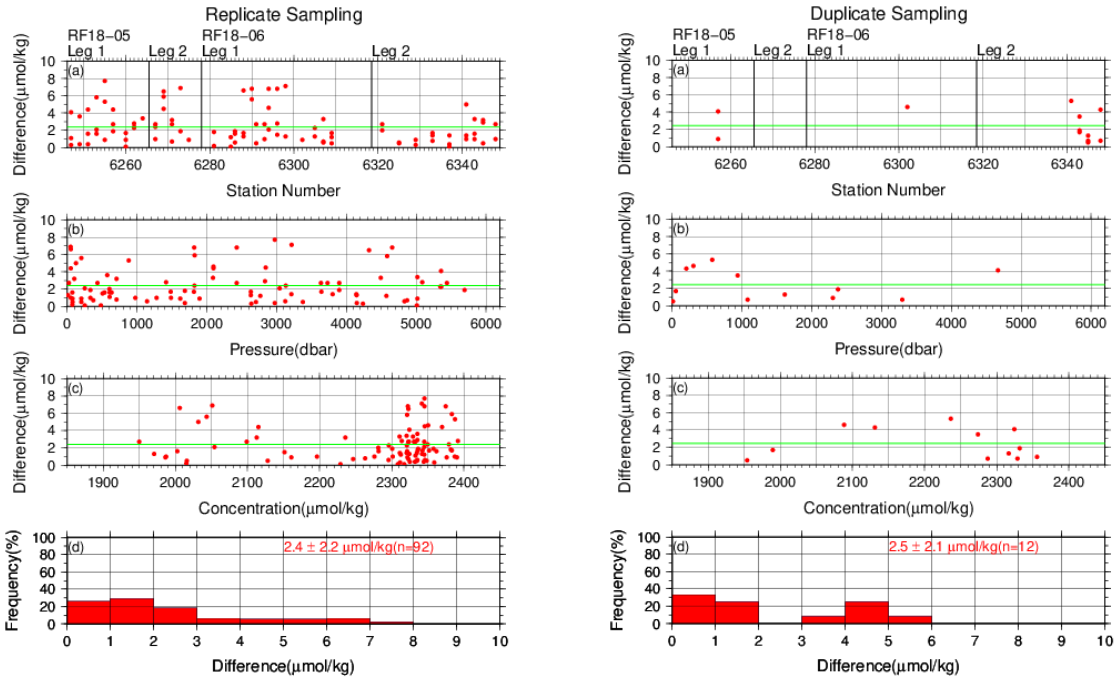

Figure C.6.5. Same as Figure C.6.4, but for apparatus B.

(6.2) Measurements of CRM and working reference materials

The precision of the measurements was monitored by using the CRMs and working reference materials bottled in our laboratory (Appendix A2). The CRM (batch 168 in RF18-05, 174 in RF18-06) and working reference material measurements were carried out at every station. At the beginning of the measurement of each station, we measured a working reference material and a CRM. If the results of these measurements were confirmed to be good, measurements on seawater samples were begun. At the end of a sequence of measurements at a station, another CRM bottle was measured. A CRM measurement was repeated twice from the same bottle. Table C.6.4 summarizes the differences in the repeated measurements of the CRMs, the mean C_T of the CRM measurements, and the mean C_T of the working reference material measurements. Figures C.6.6–C.6.8 show detailed results.

Table C.6.4. Summary of difference and mean of C_T in the repeated measurements of CRM and the mean C_T of the working reference material. These data are based on good measurements. Unit is μmol kg^{-1}.

Cruise	RF18-05		RF18-06	
Apparatus	**A**	**B**	**A**	**B**
Average magnitude of difference ± S.D. (CRM)	2.9±2.4 (N=39)	3.0±2.7 (N=33)	2.4±2.1 (N=44)	2.8±2.4 (N=51)
Mean Ave. ± S.D. (CRM)	2071.5±2.0 (N=39)	2071.5±2.7 (N=33)	2050.5±2.0 (N=46)	2050.6±2.3 (N=53)
Mean Ave. ± S.D. (Working reference material)	2080.9±1.9 (N=20)	2082.2±2.7 (N=17)	2082.6±1.5 (N=25)	2081.9±3.2 (N=30)

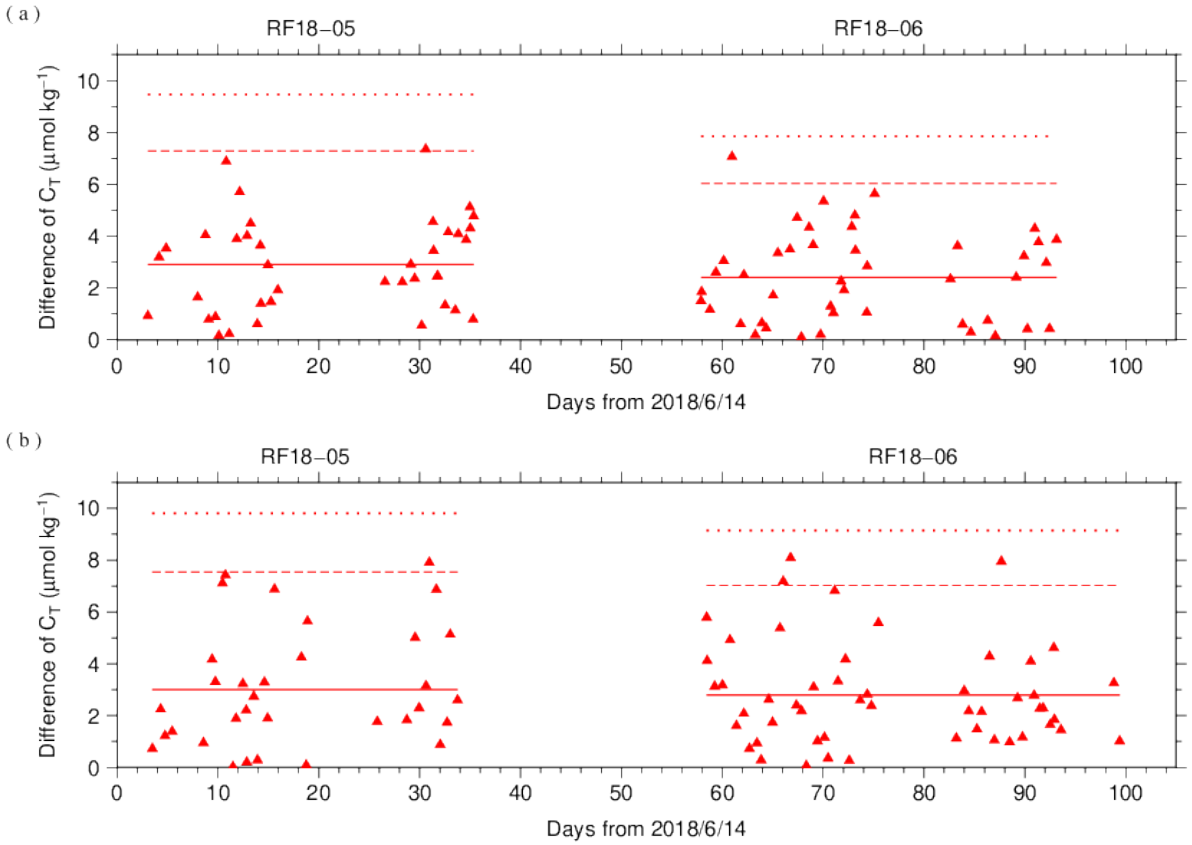

Figure C.6.6. The absolute difference (R) of C_T in repeated measurements of CRM determined by apparatus (a) A and (b) B. The solid line indicates the average of R ($\bar{R}$). The dashed and dotted lines denote the upper warning limit (2.512$\bar{R}$) and upper control limit (3.267$\bar{R}$), respectively (see Dickson et al., 2007).

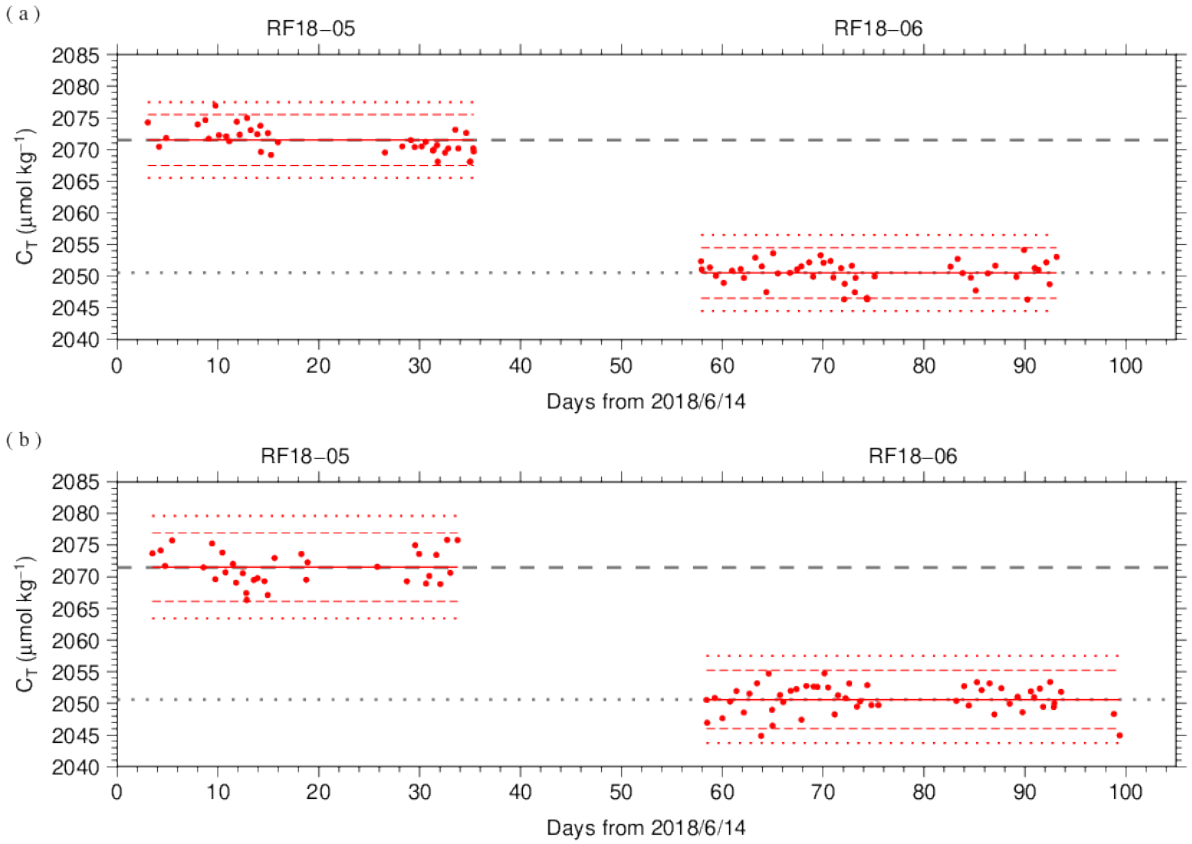

Figure C.6.7. The mean C_T of measurements of CRM. The panels show the results for apparatus (a) A and (b) B. The solid line indicates the mean of the measurements throughout the cruise. The dashed and dotted lines denote the upper/lower warning limit (mean ± 2S.D.) and the upper/lower control limit (mean ± 3S.D.), respectively. The gray dashed and dotted lines denote certified C_T of CRM batch 168 and 174.

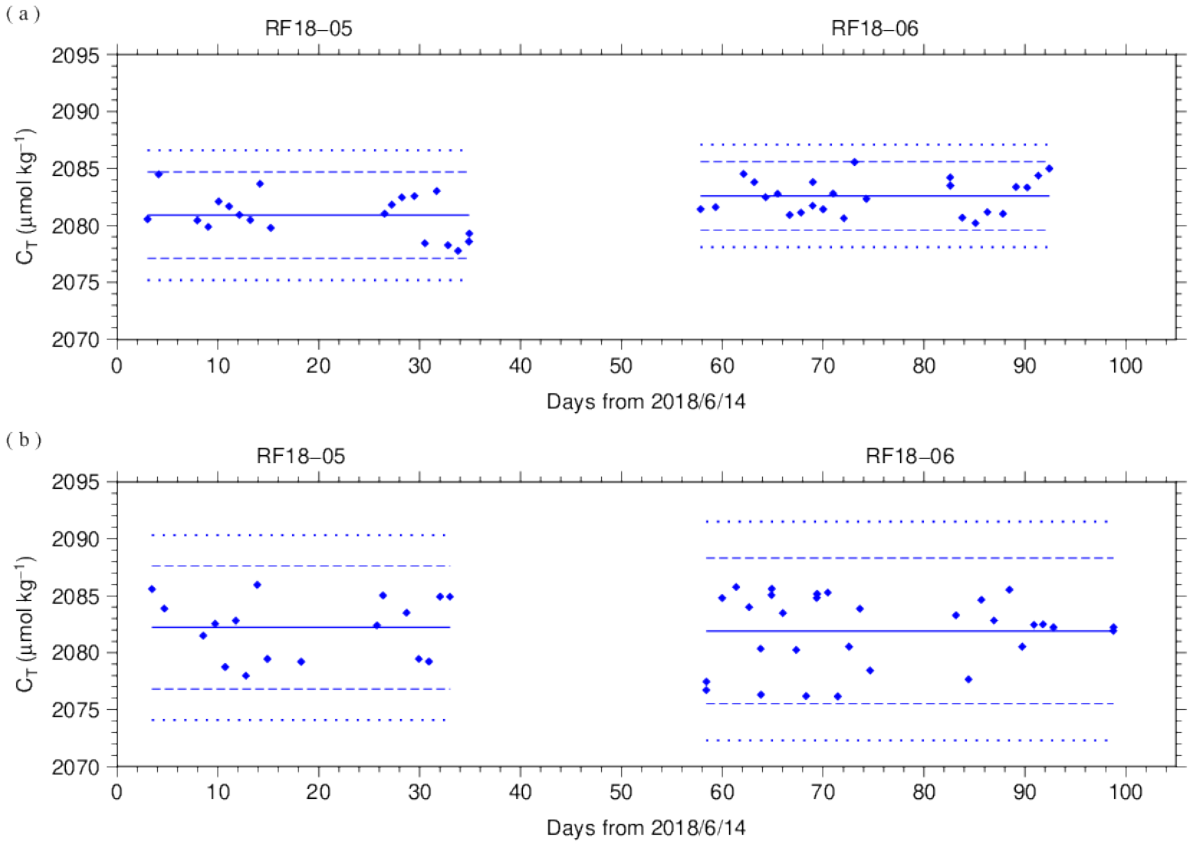

Figure C.6.8. Calculated C_T of working reference material measured by apparatus (a) A and (b) B. The solid, dashed and dotted lines are the same as in Figure C.6.7.

(6.3) Comparisons with other CRM batches

At every few stations, other CRM batches (165 in RF18-05, 164, 165 and 168 in RF18-06) were measured to provide comparisons with batch 168 (in RF18-05) and 174 (in RF18-06) to confirm the determination of C_T in our measurements. For these CRM measurements, C_T was calculated from the cV determined from batch 168 (in RF18-05) and 174 (in RF18-06) measurements. Figures C.6.9 show the differences between the calculated and certified C_T.

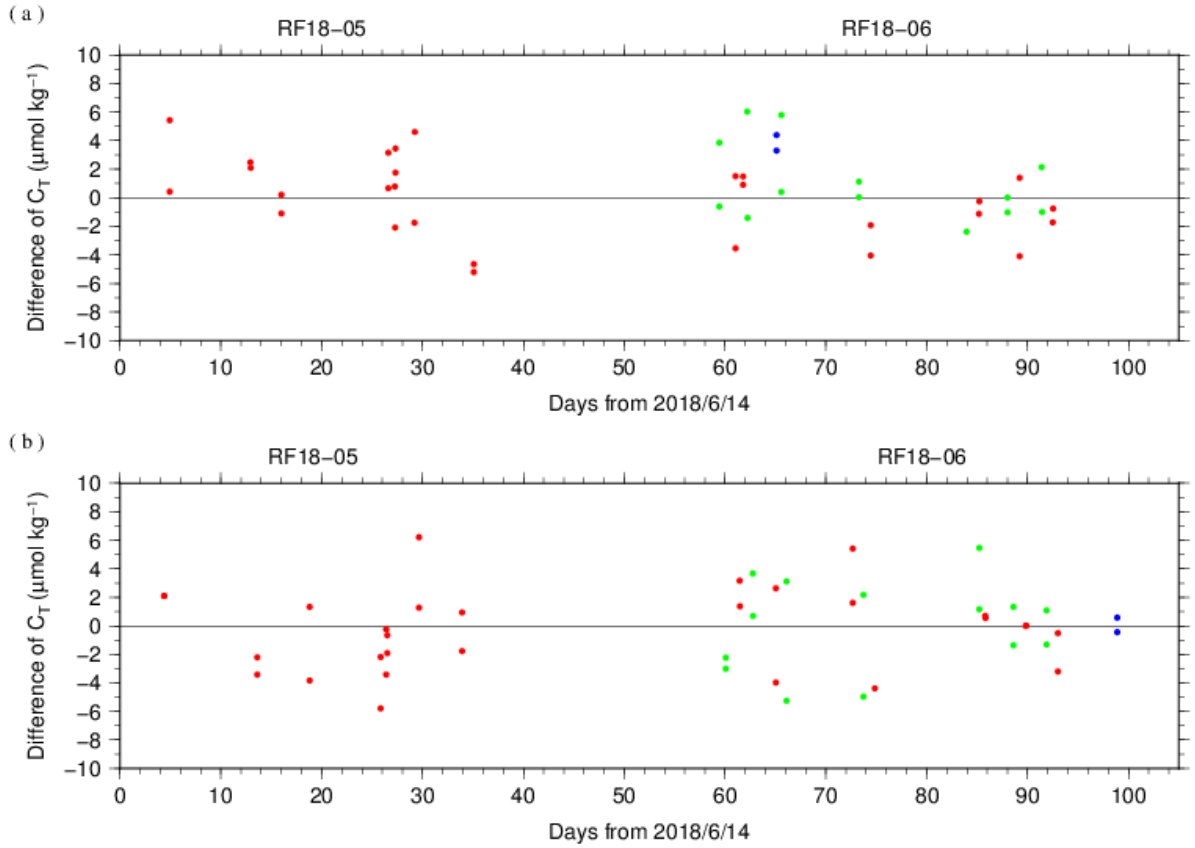

Figure C.6.9. The differences between the calculated C_T from batch 168 (in RF18-05) and 174 (in RF18-06) measurements and the certified C_T. The panels show the results for apparatus (a) A and (b) B. Colors indicate CRM batches; blue: 164, red: 165 and green: 168.

(6.4) Quality control flag assignment

A quality control flag value was assigned to the DIC measurements (Table C.6.5) using the code defined in the IOCCP Report No.14 (Swift, 2010).

Table C.6.5. Summary of assigned quality control flags.

Flag	Definition	Number of samples
2	Good	2575
3	Questionable	31
4	Bad (Faulty)	2
5	Not reported	1
6	Replicate measurements	195
	Total number of samples	2804

Appendix
A1. Methods
(A1.1) Seawater sampling
Seawater samples were collected from 10-liters Niskin bottles mounted on CTD-system and a stainless steel bucket for the surface. Samples for DIC/TA were transferred to Schott Duran® glass bottles (screw top) using sample drawing tubes. Bottles were filled smoothly from the bottom after overflowing double a volume while taking care of not entraining any bubbles, and lid temporarily with inner polyethylene cover and screw cap.
After all sampling finished, 2 mL of sample is removed from each bottle to make a headspace to allow thermal expansion, and then samples were poisoned with 0.2 mL of saturated $HgCl_2$ solution and covered tight again.

(A1.2) Measurement
The unit for DIC measurement in the coupled DIC/TA analyzer consists of a coulometer with a quartz coulometric titration cell, a CO_2 extraction unit and a reference gas injection unit. The CO_2 extraction unit, which is connected to a bottle of 20 % v/v phosphoric acid and a carrier N_2 gas supply, includes a sample pipette (approx. 12 mL) and a CO_2 extraction chamber, two thermoelectric cooling units and switching valves. The coulometric titration cell and the sample pipette are water-jacketed and are connected to a thermostated (25 °C) water bath. The automated procedures of DIC analysis in seawater were as follows (Ishii et al., 1998):

(a) Approximately 2 mL of 20 % v/v phosphoric acid was injected to an "extraction chamber", *i.e.*, a glass tube with a course glass frit placed near the bottom. Purified N_2 was then allowed to flow through the extraction chamber to purge CO_2 and other volatile acids dissolved in the phosphoric acid.

(b) A portion of sample seawater was delivered from the sample bottle into the sample pipette of CO_2 extraction unit by pressurizing the headspace in the sample bottle. After temperature of the pipette was recorded, the sample seawater was transferred into the extraction chamber and mixed with phosphoric acid to convert all carbonate species to CO_2 (aq).

(c) The acidified sample seawater was then stripped of CO_2 with a stream of purified N_2. After being dehumidified in a series of two thermoelectric cooling units, the evolved CO_2 in the N_2 stream was introduced into the carbon cathode solution in the coulometric titration cell and then CO_2 was electrically titrated.

A2. Working reference material recipe
The surface seawater in the western North Pacific was taken until at least a half year ago. Seawater was firstly filtered by membrane filter (0.45 μm-mesh) using magnetic pump and transfer into large tank. After first filtration finished, corrected seawater in the tank was processed in cycle filtration again for 3 hours and agitated in clean condition air for 6 hours. On the next day, agitated 5 minutes to remove small bubbles on the tank and transfer to Schott Duran® glass bottles as same method as samples (Appendix A1.1) except for overflowing a half of volume, not double. Created of headspace and poisoned with $HgCl_2$ was as same as samples, finally, sealed by ground glass stoppers lubricated with Apiezon® grease (L).

References
Dickson, A. G., C. L. Sabine, and J. R. Christian (Eds.) (2007), Guide to best practices for ocean CO_2 measurements. *PICES Special Publication 3*, 191 pp.

DOE (1994), Handbook of methods for the analysis of the various parameters of the carbon dioxide system in sea water; version 2. *A. G. Dickson and C. Goyet (eds), ORNL/CDIAC-74*.

Ishii, M., H. Y. Inoue, H. Matsueda, and E. Tanoue (1998), Close coupling between seasonal biological production and dynamics of dissolved inorganic carbon in the Indian Ocean sector and the western Pacific Ocean sector of the Antarctic Ocean, *Deep Sea Res*. *Part I*, **45**, 1187–1209, doi:10.1016/S0967-0637(98)00010-7.

Johnson, K. M., A. E. King and J. McN. Sieburth (1985), Coulometric TCO2 analyses for marine studies; an introduction. *Marine Chemistry*, **16**, 61–82.

Johnson, K. M., J. M. Sieburth, P. J. L. Williams and L. Brändström (1987), Coulometric total carbon dioxide analysis for marine studies: Automation and calibration. *Marine Chemistry*, **21**, 117–133.

Swift, J. H. (2010): Reference-quality water sample data, Notes on acquisition, record keeping, and evaluation. *IOCCP Report No.14, ICPO Pub.* **134**, 2010 ver.1.

10. Total Alkalinity (TA)

30 September 2023

(14) Personnel

HAMANA Minoru (RF18-05)
HORI Kasumi (RF18-05)
NAKAMURA Naoki (RF18-05)
AKAMATSU Mio (RF18-06)
MARUO Tetsuya (RF18-06)
TANIZAKI Chiho(RF18-06)

(15) Station occupied

A total of 78 stations (RF18-05 Leg 1: 19, RF18-05 Leg 2: 11, RF18-06 Leg 1: 30, RF18-06 Leg 2: 18) were occupied for total alkalinity (TA). Station location and sampling layers of them are shown in Figures C.7.1 and C.7.2, respectively.

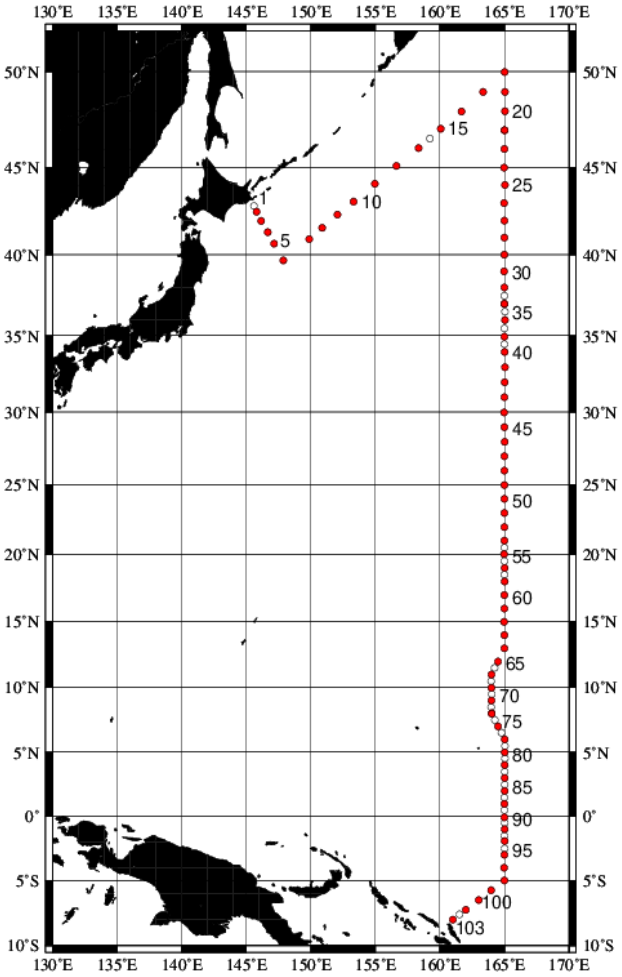

Figure C.7.1. Location of observation stations of TA. Closed and open circles indicate sampling and no-sampling stations, respectively.

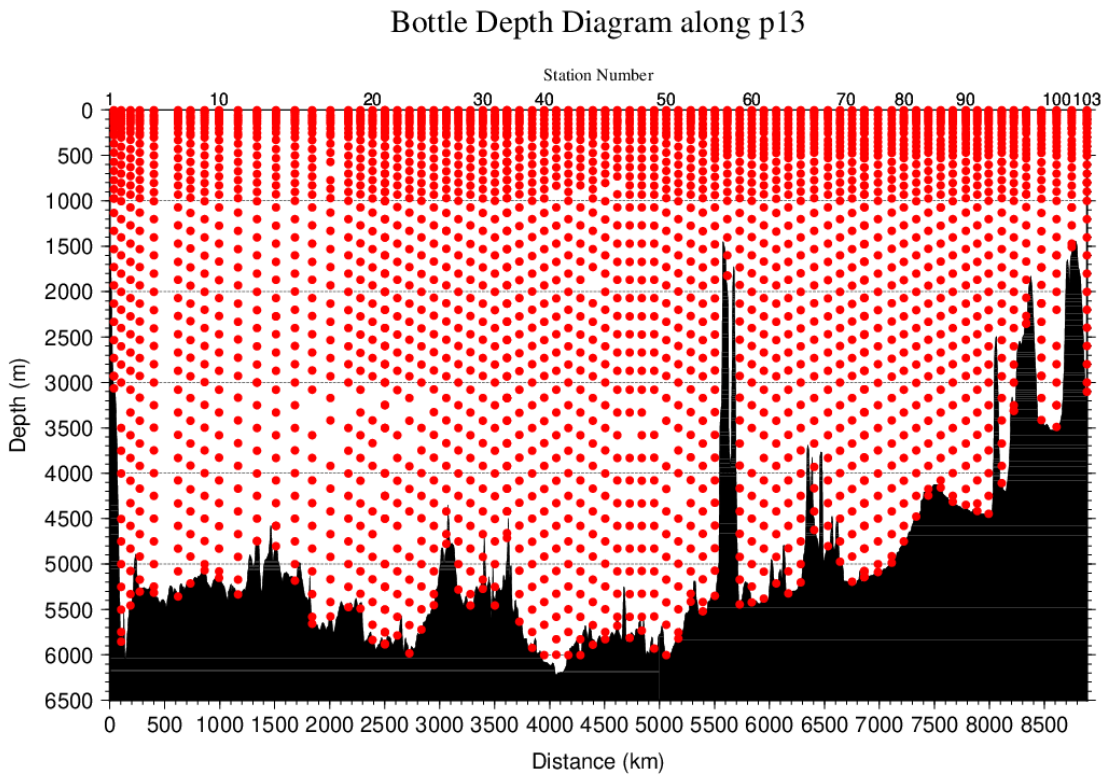

Figure C.7.2. Distance-depth distribution of sampling layers of TA.

(16) Instrument

The measurement of TA was carried out with DIC/TA analyzers (Nihon ANS Co. Ltd., Japan). The methodology that these analyzers use is based on an open titration cell. We used two analyzers concurrently. These analyzers are designated as apparatus A and B.

(17) Sampling and measurement

The procedure of seawater sampling of TA bottles and poisoning with mercury (II) chloride ($HgCl_2$) were based on the Standard Operating Procedure (SOP) described in PICES Special Publication 3 (Dickson et al., 2007). Details are shown in Appendix A1 in C.6.

TA measurement is based on a one-step volumetric addition of hydrochloric acid (HCl) to a known amount of sample seawater with prompt spectrophotometric measurement of excess acid using the sulfonephthalein indicator bromo cresol green sodium salt (BCG) (Breland and Byrne, 1993). We used a mixed solution of HCl, BCG, and sodium chloride (NaCl) as reagent. Details of measurement are shown in Appendix A1.

(18) Calculation

(5.1) Volume of sample seawater

The volumes of pipette V_S using in apparatus A and B was calibrated gravimetrically in our laboratory. Table C.7.1 shows the summary.

Table C.7.1. Summary of sample volumes of seawater V_S for TA measurements.

Apparatus	V_S / mL
A	42.8099
B	41.4764

(5.2) pH_T calculation in spectrophotometric measurement

The data of absorbance A and pipette temperature T (in °C) were processed to calculate pH_T (in total hydrogen ion scale; details shown in Appendix A1 in C.8) and the concentration of excess acid $[H^+]_T$ (mol kg^{-1}) in the following equations (C7.1)–(C7.3) (Yao and Byrne, 1998),

$$pH_T = -\log_{10}([H^+]_T)$$
$$= 4.2699 + 0.02578 \cdot (35 - S) + \log\{(R_{25} - 0.00131) / (2.3148 - 0.1299 \cdot R_{25})\} - \log(1 - 0.001005 \cdot S) \quad \text{(C7.1)}$$
$$R_{25} = R_T \cdot \{1 + 0.00909 \cdot (25 - T)\} \quad \text{(C7.2)}$$
$$R_T = \left(A_{616}^{SA} - A_{616}^{S} - A_{730}^{SA} + A_{730}^{S}\right) / \left(A_{444}^{SA} - A_{444}^{S} - A_{730}^{SA} + A_{730}^{S}\right). \quad \text{(C7.3)}$$

In the equation (C7.1), R_T is absorbance ratio at temperature T, R_{25} is absorbance ratio at temperature 25 °C and S is salinity. A_λ^S and A_λ^{SA} denote absorbance of seawater before and after acidification, respectively, at wavelength λ nm.

(5.3) TA calculation

The calculated $[H^+]_T$ was then combined with the volume of sample seawater V_S, the volume of titrant V_A added to the sample, and molarity of hydrochloric acid HCl_A (in mmol L^{-1}) in the titrant to determine to TA concentration A_T (in μmol kg^{-1}) as follows:

$$A_T = (-[H^+]_T \cdot (V_S + V_A) \cdot \rho_{SA} + HCl_A \cdot V_A) / (V_S \cdot \rho_S) \quad \text{(C7.4)}$$

ρ_S and ρ_{SA} denote the density of seawater sample before and after the addition of titrant, respectively. Here we assumed that ρ_{SA} is equal to ρ_S, since the density of titrant has been adjusted to that of seawater by adding NaCl and the volume of titrant (approx. 2.5 mL) is no more than approx. 6 % of seawater sample.

Finally, the value of A_T was multiplied by 1.00067 (= 300.2 / 300.0) to correct dilution effect in A_T induced by addition of $HgCl_2$ solution.

(19) Standardization of HCl reagent

HCl reagents were prepared in our laboratory (Appendix A2) and divided into bottles (HCl batches). HCl_A in the bottles were determined using measured CRMs provided by Dr. Andrew G. Dickson in Scripps Institution of Oceanography. Table C.7.2 provides information about the CRM batch used during this cruise.

Table C.7.2. Certified A_T and standard deviation of CRMs. Unit of A_T is μmol kg^{-1}. More information is available at the NOAA web site (https://www.ncei.noaa.gov/access/ocean-carbon-acidification-data-system/oceans/Dickson_CRM/batches.html).

Cruise	RF18-05	RF18-06
Batch number	168	174
A_T	2207.62±0.53	2212.23±0.68
Salinity	33.481	33.408

The CRM measurement was carried out at every station. The apparent HCl_A of the titrant was determined from CRM using equation (C7.4).
HCl_A was assigned for each HCl batches for each apparatus, as summarized in Table C.7.3 and detailed in Figure C.7.3.

Table C.7.3. Summary of assigned HCl_A for each HCl batches. The reported values are means and standard deviations. Unit is mmol L^{-1}.

Apparatus	Cruise	HCl Batch	HCl_A
A	RF18-05	A_1	49.7478±0.0269 (N=23)
		A_2	49.7202±0.0290 (N=36)
		A_3	50.0141±0.0252 (N=23)
		A_4	49.9653±0.0351 (N=24)
	RF18-06	A_5	50.1409±0.0254 (N=30)
		A_6	50.0380±0.0178 (N=27)
		A_7	50.0552±0.0257 (N=39)
		A_8	50.0423±0.0298 (N=29)
		A_9	50.0736±0.0190 (N=23)
B	RF18-05	B_1	49.7992±0.0249 (N=17)
		B_2	49.8025±0.0234 (N=42)
		B_3	50.0809±0.0303 (N=27)
	RF18-06	B_4	50.1107±0.0241 (N=28)
		B_5	49.9316±0.0462 (N=32)
		B_6	50.0398±0.0328 (N=31)
		B_7	50.0151±0.0284 (N=30)
		B_8	49.9723±0.0459 (N=41)

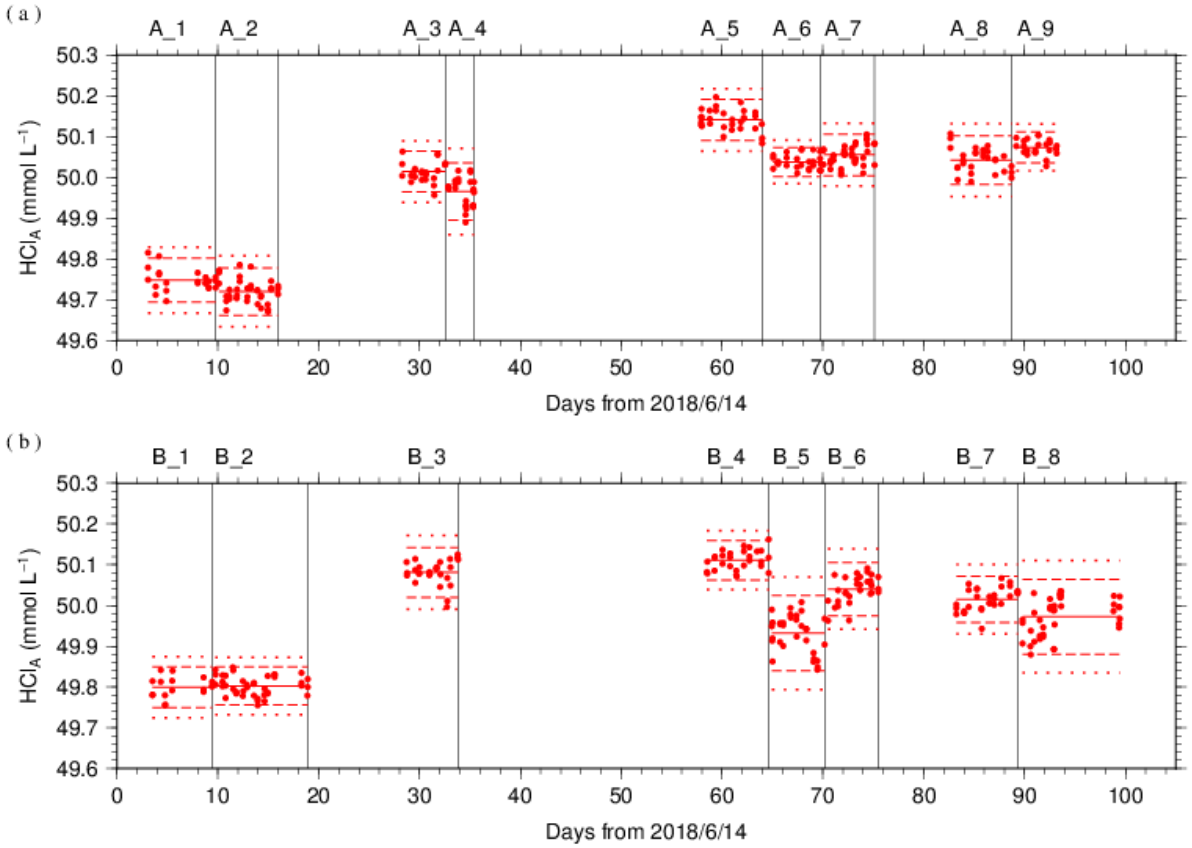

Figure C.7.3. Results of HCl_A measured by apparatus (a) A and (b) B. The HCl batch names are indicated at the top of each graph, and vertical lines denote the day when the HCl batch was switched. The red solid, dashed, and dotted lines denote the mean and the mean ± twice the S.D. and thrice the S.D. for each HCl batches, respectively.

The precisions of HCl_A, defined as the coefficient of variation (= S.D. / mean), were 0.0356–0.0702 % for apparatus A and 0.0470–0.0925 % for apparatus B. They correspond to 0.79–1.55 μmol kg^{-1} and 1.04–2.04 μmol kg^{-1} in A_T of CRM batch 168, respectively.

(20) Quality Control

(7.1) Replicate and duplicate analyses

We took replicate (pair of water samples taken from a single Niskin bottle) and duplicate (pair of water samples taken from different Niskin bottles closed at the same depth) samples of TA throughout the cruise. Table C.7.4 summarizes the results of the measurements with each apparatus. Figures C.7.4–C.7.5 show details of the results. The calculation of the standard deviation from the difference of sets of measurements was based on a procedure (SOP 23) in DOE (1994).

Table C.7.4. Summary of replicate and duplicate measurements. Unit is μmol kg^{-1}.

	Apparatus A	Apparatus B
Measurement	**Average magnitude of difference ± S.D.**	
Replicate	0.7±0.7 (N=119)	1.2±1.1 (N=111)
Duplicate	1.1±1.1 (N=17)	1.3±1.2 (N=13)

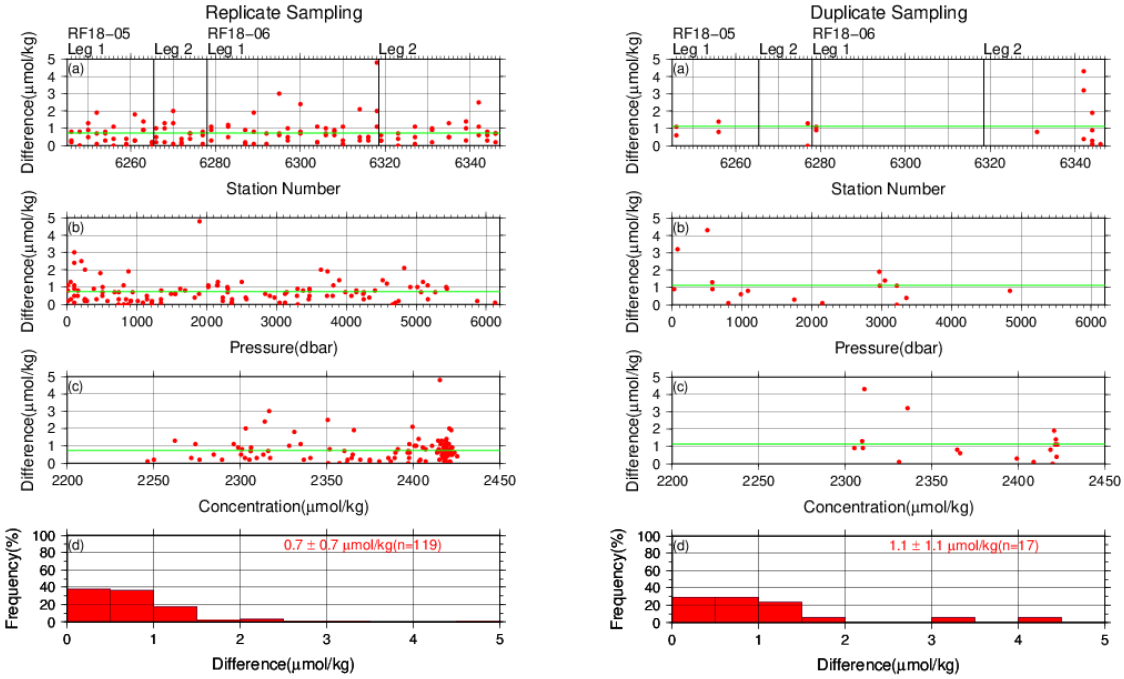

Figure C.7.4. Results of (left) replicate and (right) duplicate measurements during the cruise versus (a) station number, (b) pressure, and (c) A_T determined by apparatus A. The green lines denote the averages of the measurements. The bottom panels (d) show histograms of the measurements.

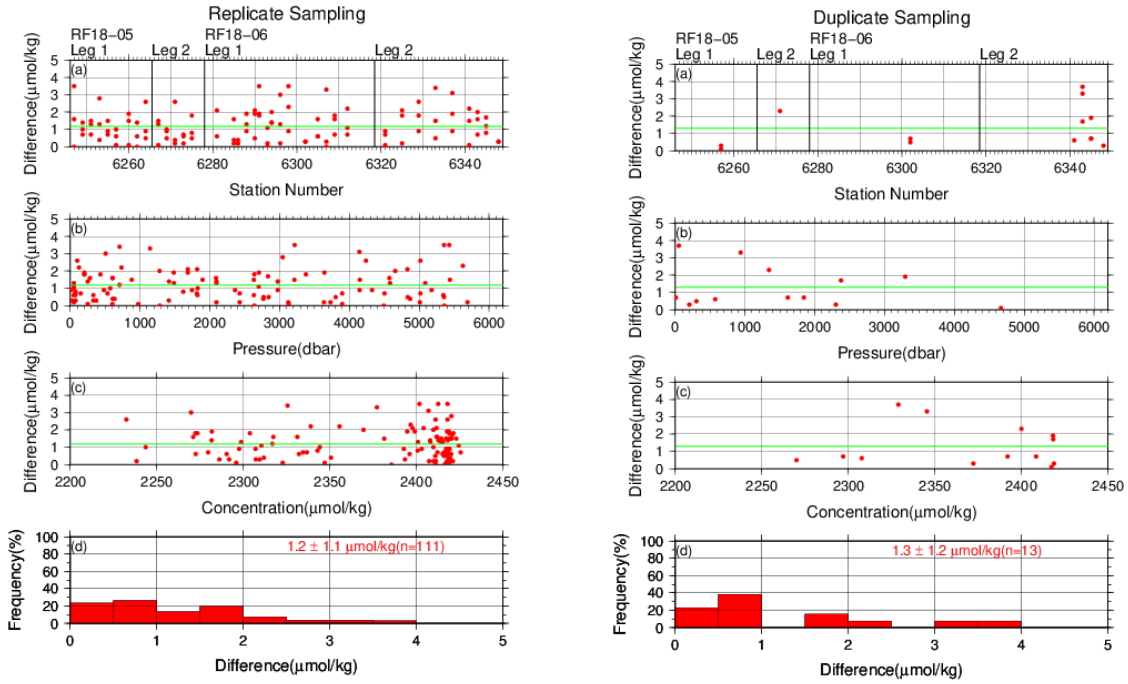

Figure C.7.5. Same as Figure C.7.4, but for apparatus B.

(7.2) Measurements of CRM and working reference materials

The precision of the measurements was monitored by using the CRMs and working reference materials bottled in our laboratory (Appendix A2 in C.6). The measurements of the CRMs and working reference materials were the same those used to measure DIC (see (6.2) in C.6), except that the CRM measurement was repeated 3 times from the same bottle. Table C.7.5 summarizes the differences in the repeated measurements of the CRMs, the mean A_T of the CRM measurements, and the mean A_T of the working reference material measurements. Figures C.7.6–C.7.8 show detailed results.

Table C.7.5. Summary of difference and mean of A_T in the repeated measurements of CRM and the mean A_T of the working reference material. These data are based on good measurements. Unit is μmol kg^{-1}.

Cruise	HCl Batch	Average magnitude of difference ± S.D. (CRM)	Mean Ave. ± S.D. (CRM)	Mean Ave. ± S.D. (Working reference material)
RF18-05	A_1	1.1±0.8 (N=8)	2207.7±1.1 (N=8)	2312.1±1.0 (N=3)
	A_2	0.9±0.7 (N=12)	2207.6±1.2 (N=12)	2310.9±1.4 (N=6)
	A_3	0.9±0.7 (N=8)	2207.7±1.0 (N=8)	2310.5±0.9 (N=5)
	A_4	0.8±0.6 (N=8)	2207.6±1.6 (N=8)	2311.8±1.6 (N=5)
RF18-06	A_5	1.2±0.9 (N=10)	2212.2±0.9 (N=10)	2313.9±0.8 (N=7)
	A_6	1.0±0.7 (N=9)	2212.2±0.5 (N=9)	2314.2±0.8 (N=6)
	A_7	0.8±0.6 (N=13)	2212.2±1.1 (N=13)	2313.4±0.9 (N=5)
	A_8	1.0±0.7 (N=10)	2212.2±1.3 (N=10)	2313.5±1.0 (N=6)
	A_9	0.9±0.7 (N=8)	2212.2±0.7 (N=8)	2313.2±0.3 (N=4)
RF18-05	B_1	1.0±0.8 (N=6)	2207.5±1.0 (N=6)	2314.3±0.9 (N=3)
	B_2	0.9±0.7 (N=14)	2207.6±0.9 (N=14)	2312.7±0.9 (N=7)
	B_3	1.1±1.0 (N=9)	2207.6±1.1 (N=9)	2313.9±1.6 (N=5)
RF18-06	B_4	1.2±0.9 (N=9)	2212.3±0.8 (N=9)	2313.9±1.1 (N=7)
	B_5	1.6±1.3 (N=11)	2212.2±1.9 (N=11)	2314.3±2.1 (N=9)
	B_6	1.5±1.2 (N=11)	2212.3±1.3 (N=11)	2314.2±2.2 (N=5)
	B_7	0.9±0.8 (N=10)	2212.2±1.1 (N=10)	2314.4±1.3 (N=5)
	B_8	1.5±1.2 (N=14)	2212.2±1.9 (N=14)	2314.2±2.0 (N=6)

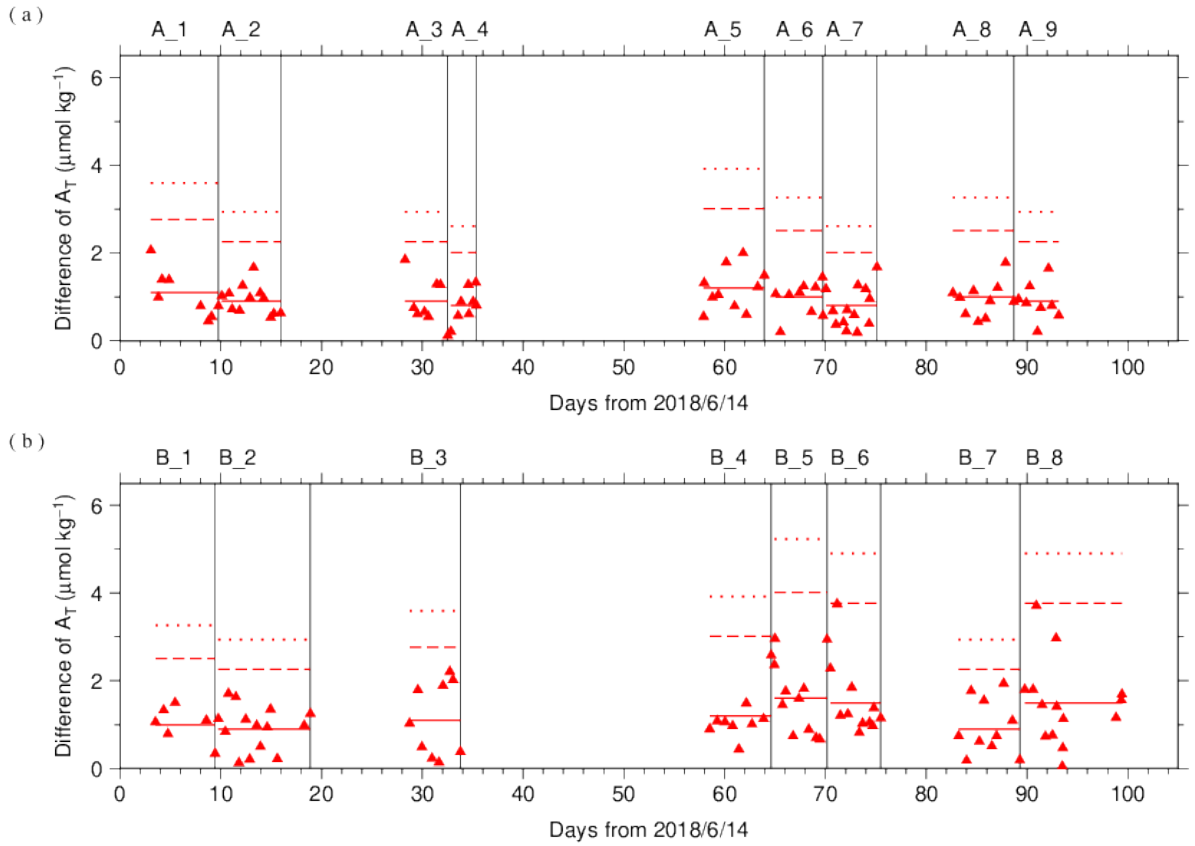

Figure C.7.6. The absolute difference (R) of A_T in repeated measurements of CRM determined by apparatus (a) A and (b) B. The solid line indicates the average of R ($\bar{R}$). The dashed and dotted lines denote the upper warning limit ($2.512\bar{R}$) and upper control limit ($3.267\bar{R}$), respectively (see Dickson et al., 2007).

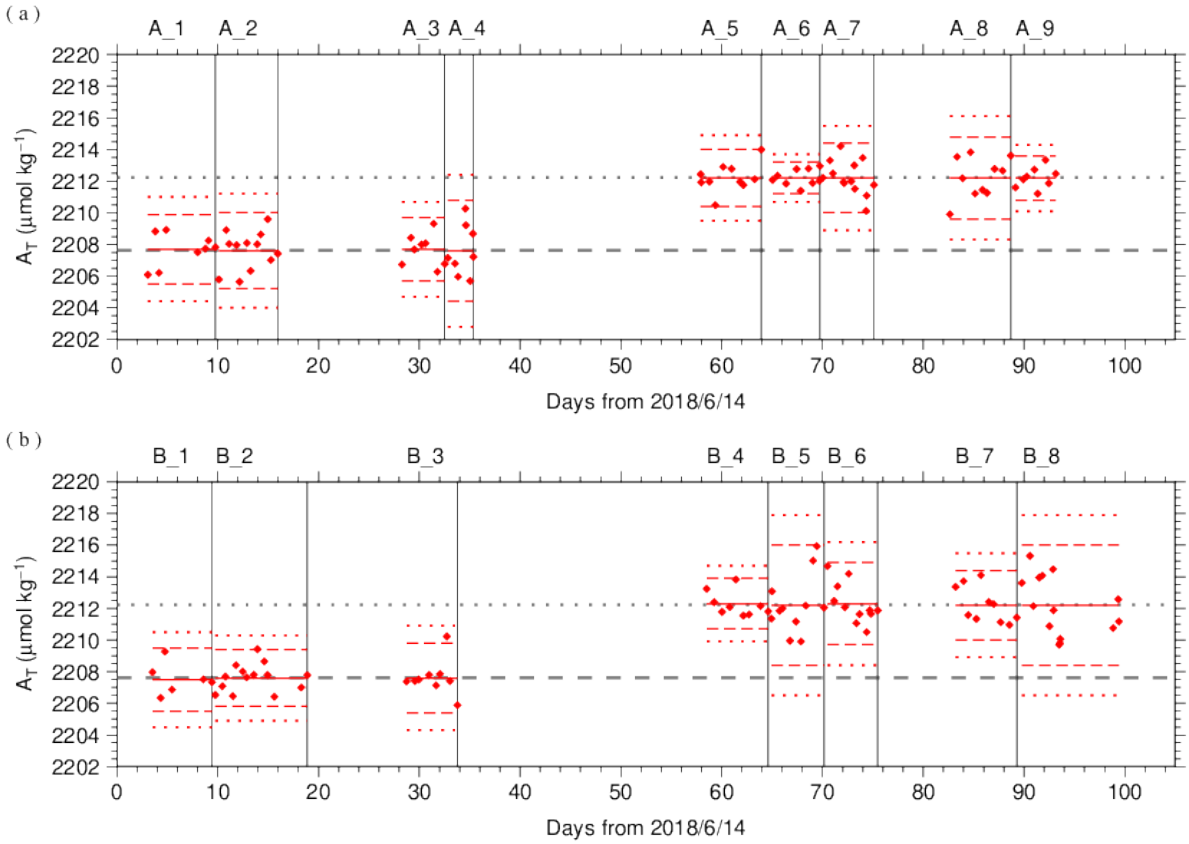

Figure C.7.7. The mean A_T of measurements of CRM. The panels show the results for apparatus (a) A and (b) B. The solid line indicates the mean of the measurements. The dashed and dotted lines denote the upper/lower warning limit (mean ± 2S.D.) and the upper/lower control limit (mean ± 3S.D.), respectively. The gray dashed and dotted lines denote certified A_T of CRM batch 168 and 174. The labels at the top of the graph and vertical lines have the same meaning as in Figure C.7.3.

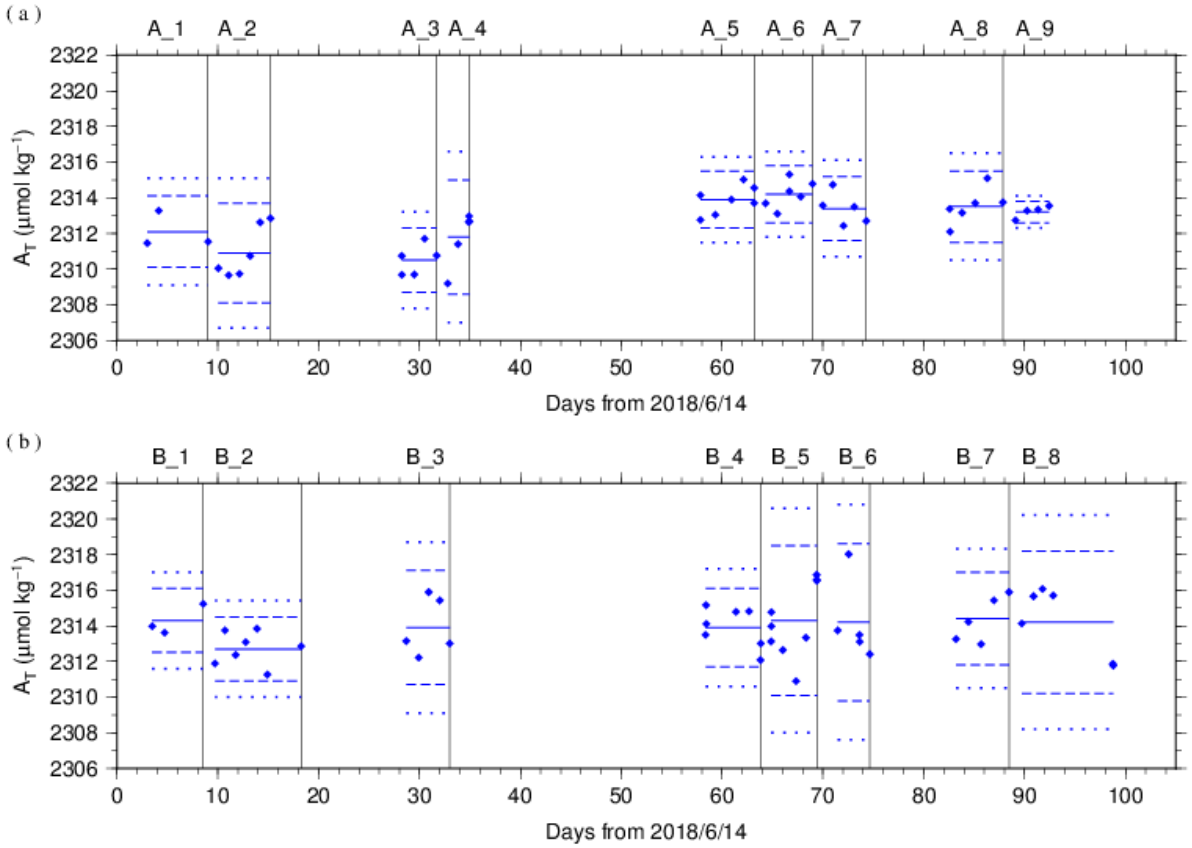

Figure C.7.8. Calculated A_T of working reference material measured by apparatus (a) A and (b) B. The solid, dashed and dotted lines have the same meaning as in Figure C.7.7. The labels at the top of the graph and vertical lines have the same meaning as in Figure C.7.3.

(7.3) Comparisons with other CRM batches

At every few stations, other CRM batches (165 in RF18-05, 164, 165 and 168 in RF18-06) were measured to provide comparisons with batch 168 (in RF18-05) and 174 (in RF18-06) to confirm the determination of A_T in our measurements. For these CRM measurements, A_T was calculated from HCl_A determined from batch 168 (in RF18-05) and 174 (in RF18-06) measurements. Figures C.7.9 show the differences between the calculated and certified A_T.

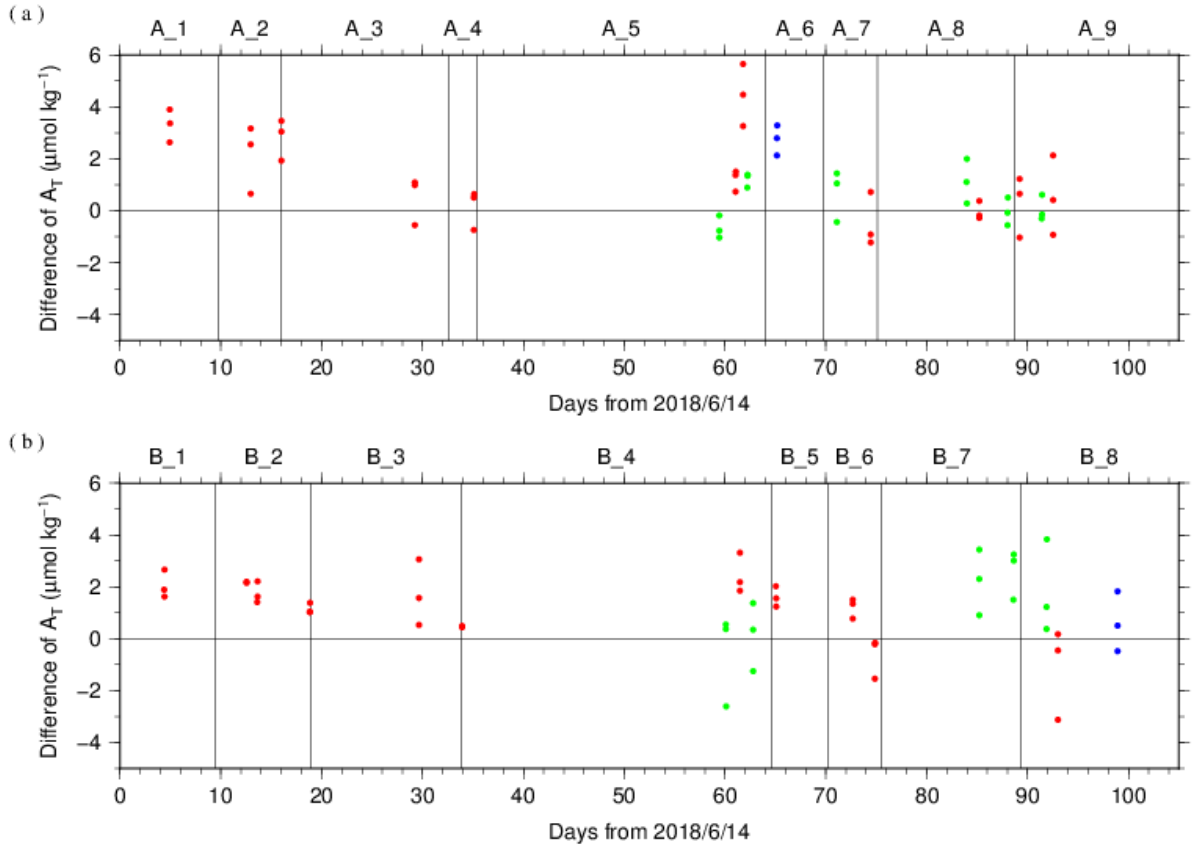

Figure C.7.9. The differences between the calculated A_T from batch 168 (in RF18-05) and 174 (in RF18-06) measurements and the certified A_T. The panels show the results for apparatus (a) A and (b) B. The labels at the top of the graph and vertical lines have the same meaning as in Figure C.7.3. Colors indicate CRM batches; blue: 164, red: 165 and green: 168.

(7.4) Quality control flag assignment

A quality control flag value was assigned to the TA measurements (Table C.7.6) using the code defined in the IOCCP Report No.14 (Swift, 2010).

Table C.7.6. Summary of assigned quality control flags.

Flag	Definition	Number of samples
2	Good	2562
3	Questionable	9
4	Bad (Faulty)	2
5	Not reported	1
6	Replicate measurements	230
Total number of samples		2804

Appendix
A1. Methods
(A1.1) Measurement

The unit for TA measurements in the coupled DIC/TA analyzer consists of sample treatment unit with a calibrated sample pipette and an open titration cell that are water-jacketed and connected to a thermostated water bath (25 °C), an auto syringe connected to reagent bottle of titrant stored at 25 °C, and a double-beam spectrophotometric system with two CCD image sensor spectrometers combined with a high power Xenon lamp. The mixture of 0.05 N HCl and 40 μmol L^{-1} BCG in 0.65 M NaCl solution was used as reagent to automatically titrate the sample as follows:

(a) A portion of sample seawater was delivered into the sample pipette (approx. 42 mL) following sample delivery into the DIC unit for a measurement. After the temperature in the pipette was recorded, the sample was transferred into a cylindrical quartz cell.

(b) An absorption spectrum of sample seawater in the visible light domain was then measured, and the absorbances were recorded at wavelengths of 444 nm, 509 nm, 616 nm, and 730 nm as well as the temperature in the cell.

(c) The titrant that contains HCl was added to the sample seawater by the auto syringe so that pH of sample seawater altered in the range between 3.85 and 4.05.

(d) While the acidified sample was being stirred, the evolved CO_2 was purged with the stream of purified N_2 bubbled into the sample at approx. 200 mL min^{-1} for 5 minutes.

(e) After the bubbled sample steadied down for 1 minute, the absorbance of BCG in the sample was measured in the same way as described in (b), and pH (in total hydrogen ion scale, pH_T) of the acidified seawater was precisely determined spectrophotometrically.

A2. HCl reagents recipes

0.05 N HCl and 40 μmol L^{-1} BCG in 0.65 M NaCl solution

Dissolve 0.30 g of BCG and 190 g of NaCl in roughly 1.5 L of deionized water (DW) in a 5 L flask, and slowly add 200 mL concentrated HCl. After the powders completely dissolved, dilute with DW to a final volume of 5 L.

References

Breland II, J. A. and R. H. Byrne (1993), Spectrophotometric procedures for determination of sea water alkalinity using bromocresol green, *Deep-Sea Res. I*, 470, 629–641.

Dickson, A. G., C. L. Sabine, and J. R. Christian (Eds.) (2007), Guide to best practices for ocean CO_2 measurements. PICES Special Publication 3, 191 pp.

DOE (1994), Handbook of methods for the analysis of the various parameters of the carbon dioxide system in sea water; version 2. *A. G. Dickson and C. Goyet (eds), ORNL/CDIAC-74*.

Yao, W. and R. H. Byrne (1998), Simplified seawater alkalinity analysis: Use of linear array spectrometers. *Deep-Sea Res. I*, 45, 1383–1392.

Swift, J. H. (2010): Reference-quality water sample data, Notes on acquisition, record keeping, and evaluation. *IOCCP Report No.**14**, ICPO Pub. 134, 2010 ver.1.*

11. pH

30 September 2023

(21) Personnel

HAMANA Minoru (RF18-05)
HORI Kasumi (RF18-05)
NAKAMURA Naoki (RF18-05)
AKAMATSU Mio (RF18-06)
MARUO Tetsuya (RF18-06)
TANIZAKI Chiho(RF18-06)

(22) Station occupied

A total of 78 stations (RF18-05 Leg 1: 19, RF18-05 Leg 2: 11, RF18-06 Leg 1: 30, RF18-06 Leg 2: 18) were occupied for pH. Station location and sampling layers of them are shown in Figures C.8.1 and C.8.2, respectively.

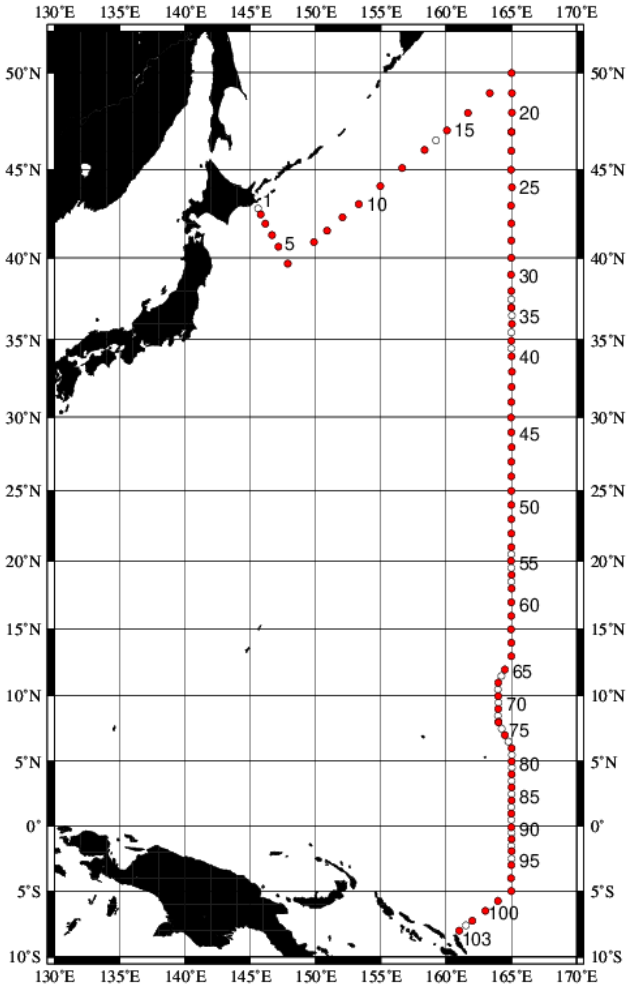

Figure C.8.1. Location of observation stations of pH. Closed and open circles indicate sampling and no-sampling stations, respectively.

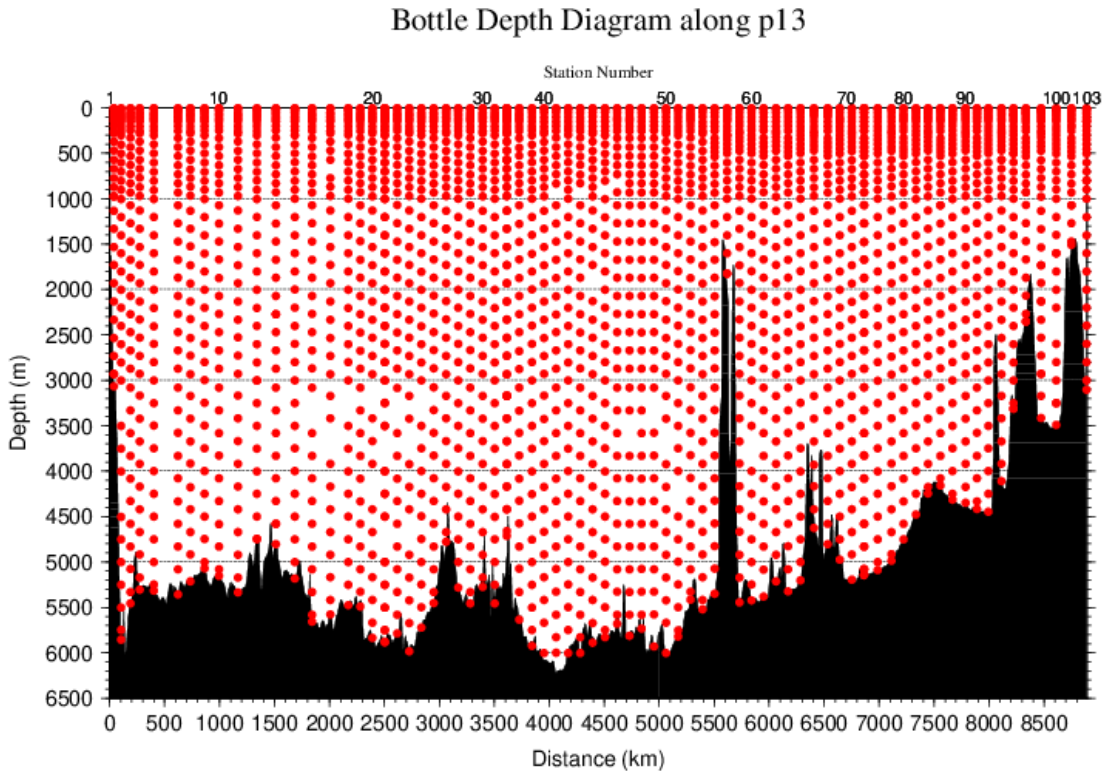

Figure C.8.2. Distance-depth distribution of sampling layers of pH.

(23) Instrument

The measurement of pH was carried out with a pH analyzer (Nihon ANS Co. Ltd, Japan).

(24) Sampling and measurement

Methods of seawater sampling, poisoning, spectrophotometric measurements using the indicator dye *m*-cresol purple (hereafter *m*CP) and calculation of pH_T (on the total hydrogen ion scale; Appendix A1) were based on Saito et al. (2008). The pH_T is calculated from absorbance ratio (R) with the following equations,

$$pH_T = pK_2 + \log_{10}\{(R - 0.0069)/(2.222 - 0.1331 \cdot R)\} \quad \text{(C8.1)}$$

$$R = \left(A_{578}^{SD} - A_{578}^{S} - A_{730}^{SD} + A_{730}^{S}\right)/\left(A_{434}^{SD} - A_{434}^{S} - A_{730}^{SD} + A_{730}^{S}\right) \quad \text{(C8.2)}$$

where pK_2 is the acid dissociation constant of *m*CP,

$$pK_2 = 1245.69/T + 3.8322 + 0.00211 \cdot (35 - S) \quad \text{(C8.3)}$$

(293 K $\leq T \leq$ 303 K, 30 $\leq S \leq$ 37).

A_λ^S and A_λ^{SD} in equation (C8.2) are absorbance of seawater itself and dye plus seawater, respectively, at wavelength λ (nm). The value of pK_2 in equation (C8.3) is expressed as a function of temperature T (in Kelvin) and salinity S (in psu). Finally, pH_T is reported as the value at temperature of 25 °C. Details are shown in Appendix A1.

(25) pH perturbation caused by addition of *m*-cresol purple solution

The *m*CP solution using as indicator dye was prepared in our laboratory (Appendix A2) and was subdivided into some bottles (*m*CP batches) that attached to the apparatus. The injection of *m*CP solution perturbs the sample pH_T slightly because the acid-base equilibrium of the seawater is disrupted by the addition of the dye acid-base pair (Dickson et al., 2007).

Before applying R to the equation (C8.1), the measured R in the sample was corrected to that value expected to be unperturbed by the addition of the dye (Dickson et al., 2007; Clayton and Byrne, 1993). The magnitude of the perturbation (ΔR) was calculated empirically from that by the second addition of the dye and absorbance ratio measurement as follows:

$$\Delta R = R_2 - R_1, \qquad \text{(C8.4)}$$

where R_1 and R_2 are the absorbance ratio after the initial addition of dye solution in the sample measurement and after the second addition in the experimental measurement, respectively. Because the value of ΔR depends on the pH_T of sample, we expressed ΔR as a quadratic function of R_1 based on experimental ΔR measurement obtained at this cruise as follows:

$$\Delta R = \mathrm{C}_2 \times R_1^2 + \mathrm{C}_1 \times R_1 + \mathrm{C}_0. \qquad \text{(C8.5)}$$

In each measurement for a station, ΔR was measured for about 10 samples from various depths to obtain wide range of R_1 and experimental ΔR data. For each *m*CP batch bottle, coefficients (C_0, C_1 and C_2) were calculated by equation (C8.5), and ΔR was evaluated for each R_1. The coefficients for each *m*CP batch are showed in Table C.8.1. The plots and function curves are illustrated in Figure C.8.3.

Table C.8.1. Summary of coefficients; C_2, C_1 and C_0 in $\Delta R = \mathrm{C}_2 \times R_1^2 + \mathrm{C}_1 \times R_1 + \mathrm{C}_0$.

Stations	*m*CP batch	C_2	C_1	C_0
2–21	1	−7.25669E−03	−4.10134E−03	9.57174E−03
22–33	2	−2.58107E−03	−9.14504E−03	1.01108E−02
34–64	3	−5.40236E−04	−1.51472E−02	1.51998E−02
65–103	4	7.18411E−05	−1.79396E−02	1.59564E−02

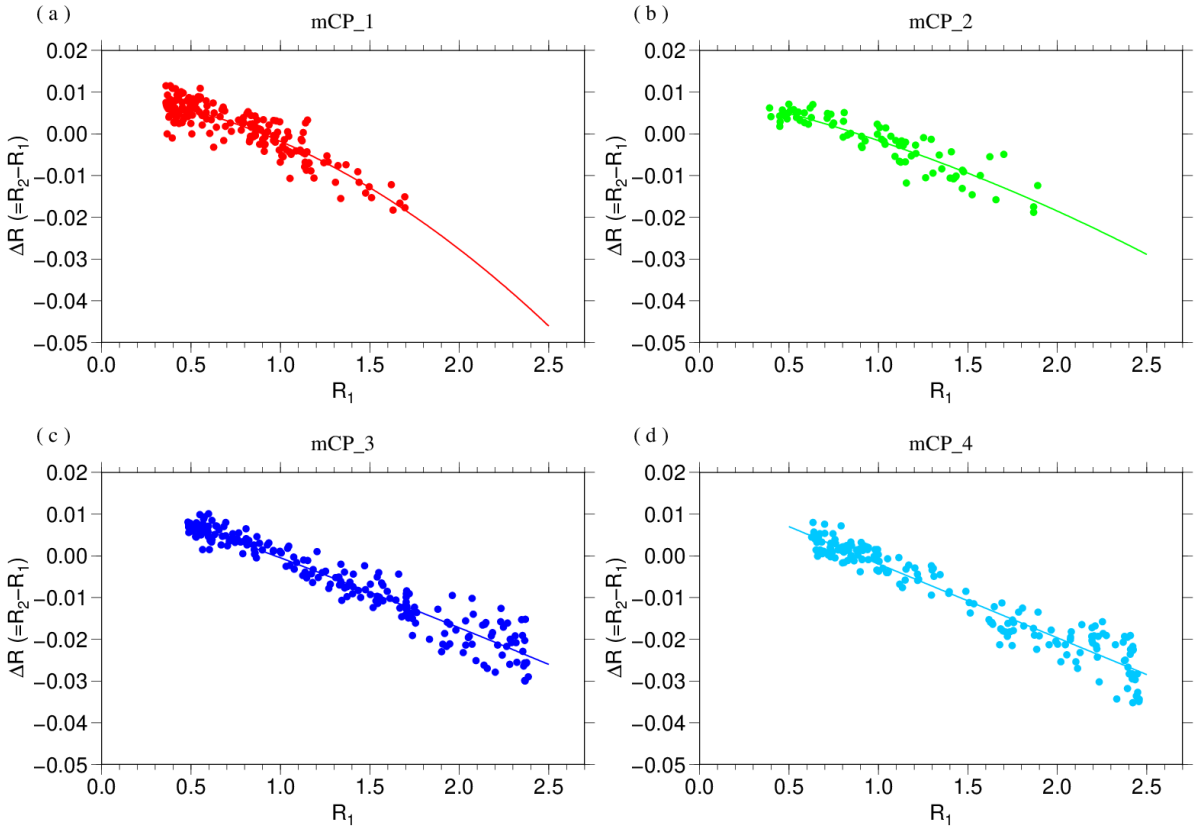

Figure C.8.3. The function curve of the ΔR (= $R_2 - R_1$) vs R_1 for (a) first, (b) second, (c) third and (d) fourth *m*CP batch of solution shown in Table C.8.1.

(26) Quality Control

(6.1) Replicate and duplicate analyses

We took replicate (pair of water samples taken from a single Niskin bottle) and duplicate (pair of water samples taken from different Niskin bottles closed at the same depth) samples for pH_T determination throughout the cruise. Table C.8.2 summarizes the results of the measurements. Figure C.8.4 shows details of the results. The calculation of the standard deviation from the difference of sets of measurements was based on a procedure (SOP 23) in DOE (1994).

Table C.8.2. Summary of replicate and duplicate measurements of pH_T.

Measurement	Average magnitude of difference ± S.D.
Replicate	0.0017±0.0015 (N=220)
Duplicate	0.0018±0.0015 (N=30)

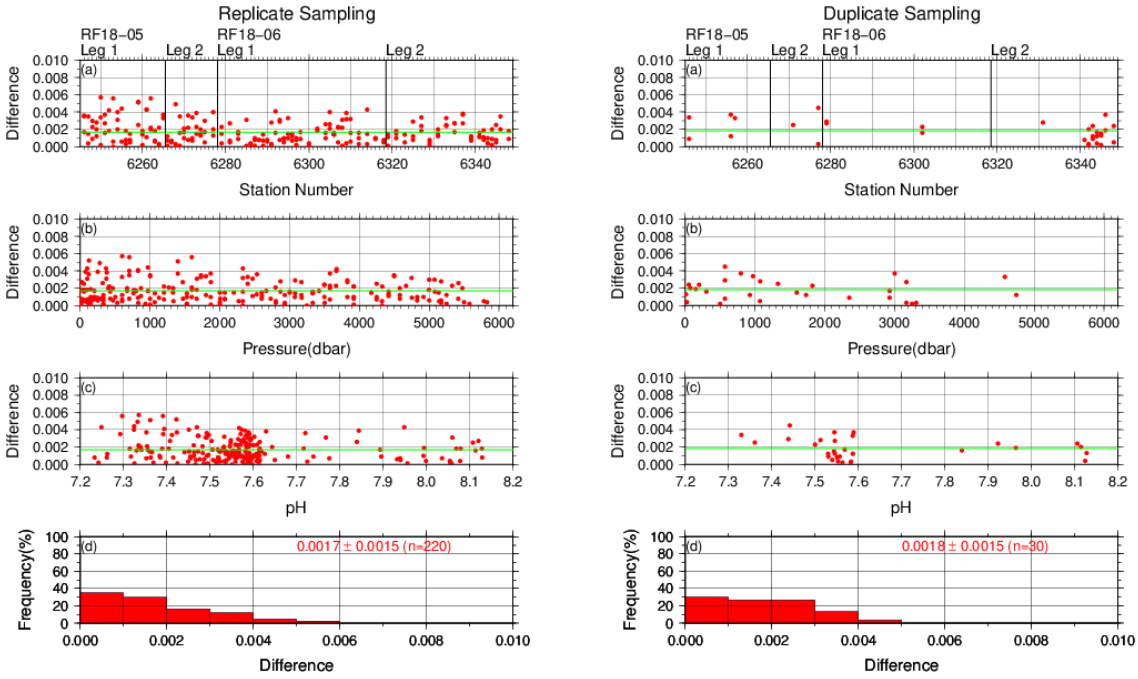

Figure C.8.4. Results of (left) replicate and (right) duplicate measurements during the cruise versus (a) station number, (b) pressure and (c) pH_T. The green lines denote the averages of the measurements. The bottom panels (d) show histograms of the measurements.

(6.2) Measurements of CRM and working reference materials

The precision of the measurements was monitored by using the CRMs and working reference materials bottled in our laboratory (Appendix A2 in C.6). Although the pH_T value of the CRM was not assigned, it could be calculated from certified parameters of DIC and TA (https://www.ncei.noaa.gov/access/ocean-carbon-acidification-data-system/oceans/Dickson_CRM/batches.html) based on the chemical equilibrium of the carbonate system (Lueker et al., 2000). The pH_T of the CRMs (batch 168 and 174) were calculated to be 7.7359 and 7.8002. Working reference material measurements were carried out first at every station. If the results of the measurements were confirmed to be good, measurements on seawater samples were begun. CRM (batch 168 in RF18-05 and 174 in RF18-06) measurements were done at every few (about 3) stations. The measurement for seawater sample and working reference material was made once for a single bottle, and that for CRM was made twice. Table C.8.3 summarizes the means of difference of pH_T between two measurements and pH_T values for a CRM bottle and the means of the pH_T value for a working reference material for each *m*CP batch. Figures C.8.5–C.8.7 show detailed results.

Table C.8.3. Summary of difference and means of the pH_T values for two measurements for a CRM bottle, and mean of pH_T for a working reference material, which was calculated with data with good measurements.

Cruise	*m*CP Batch	Magnitude of difference Ave. ± S.D. (CRM)	Mean Ave. ± S.D. (CRM)	Mean Ave. ± S.D. (Working reference material)
RF18-05	1	0.0013±0.0010 (N=7)	7.7309±0.0032 (N=7)	7.9191±0.0023 (N=21)
	2	0.0017±0.0016 (N=2)	7.7356±0.0050 (N=2)	7.9213±0.0029 (N=13)
RF18-06	3	0.0013±0.0011 (N=9)	7.7985±0.0020 (N=9)	7.9182±0.0013 (N=23)
	4	0.0020±0.0016 (N=9)	7.7998±0.0019 (N=9)	7.9190±0.0013 (N=26)

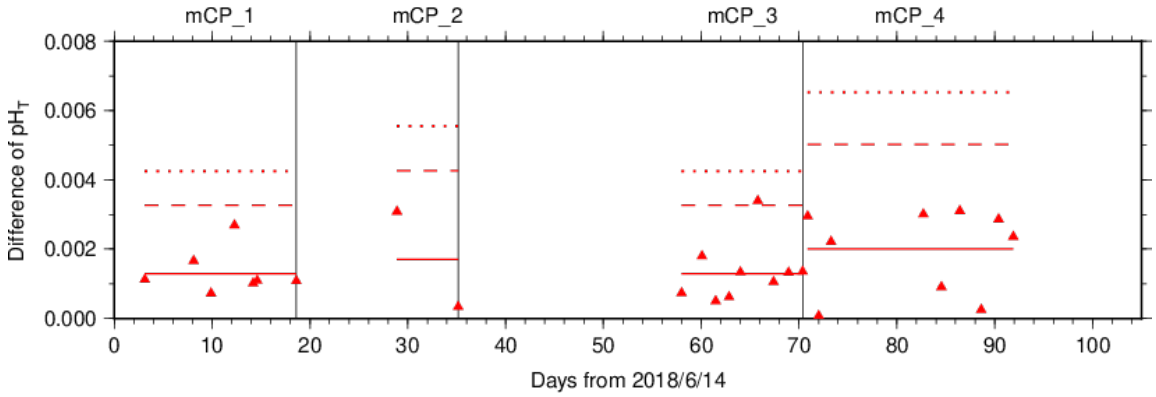

Figure C.8.5. The absolute difference (R) of pH_T between two measurements of a CRM bottle. The *m*CP batch names are shown above the graph, and vertical lines denote the day *m*CP batches were changed. The solid, dashed and dotted lines denote the average range ($\bar{R}$), upper warning limit ($2.512\bar{R}$) and upper control limit ($3.267\bar{R}$) for each *m*CP batch bottle, respectively (see Dickson et al., 2007).

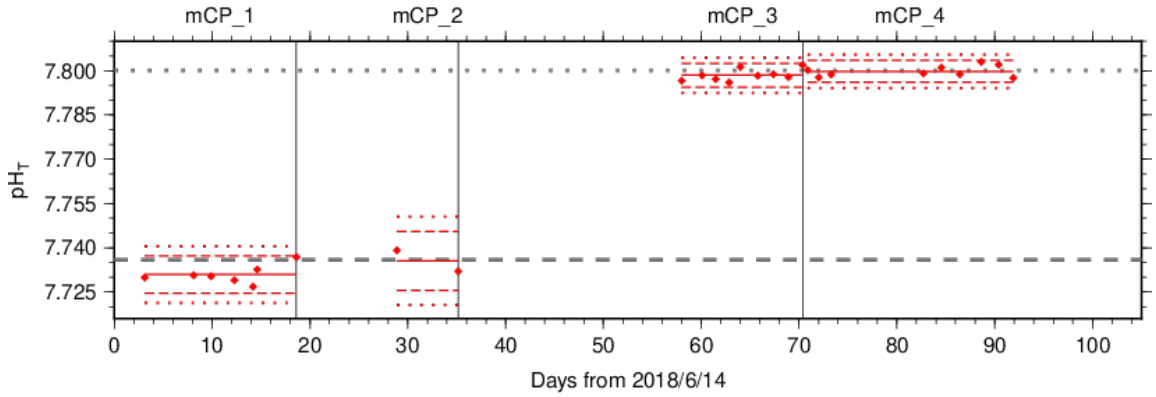

Figure C.8.6. The mean of pH_T values between two measurements of a CRM bottle. The *m*CP batch names are shown above the graph, and vertical lines denote the day when the *m*CP batch was changed. The solid, dashed, and dotted lines denote the mean of measurements, upper/lower warning limit (mean ± 2S.D.), and upper/lower control limit (mean ± 3S.D.) for each *m*CP batch

bottle, respectively (see Dickson et al., 2007). The gray dashed and dotted lines denote pH_T of CRM batch 168 and 174 calculated from certified parameters.

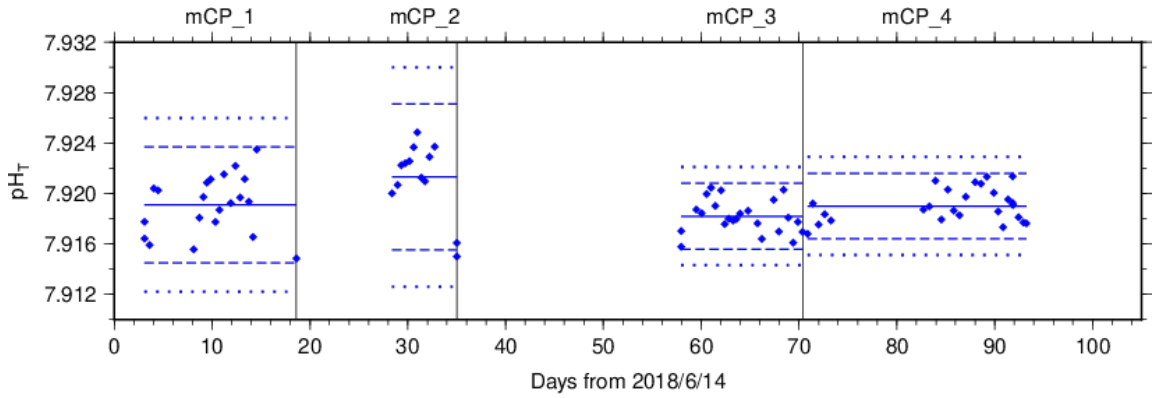

Figure C.8.7. Same as C.8.6, but for working reference material.

(6.3) Quality control flag assignment

A quality control flag value was assigned to the pH measurements (Table C.8.4) using the code defined in the IOCCP Report No.14 (Swift, 2010).

Table C.8.4. Summary of assigned quality control flags.

Flag	Definition	Number of samples
2	Good	2575
3	Questionable	7
4	Bad (Faulty)	2
5	Not reported	0
6	Replicate measurements	220
	Total number of samples	2804

(6.4) Comparison at cross-stations during the cruise

There were cross-stations during the cruise located at 47˚N/165˚E (in RF18-05), 37˚N/165˚E (in RF18-05 and RF18-06) and 8˚N/164˚E (in RF18-06). At these points, hydrocast sampling for pH_T was conducted two times at interval of 14 days (Stns.21 and 22), 25 days (Stns.33 and 34) and 9 days (Stns.73 and 74). These profiles are shown in Figure C.8.8.

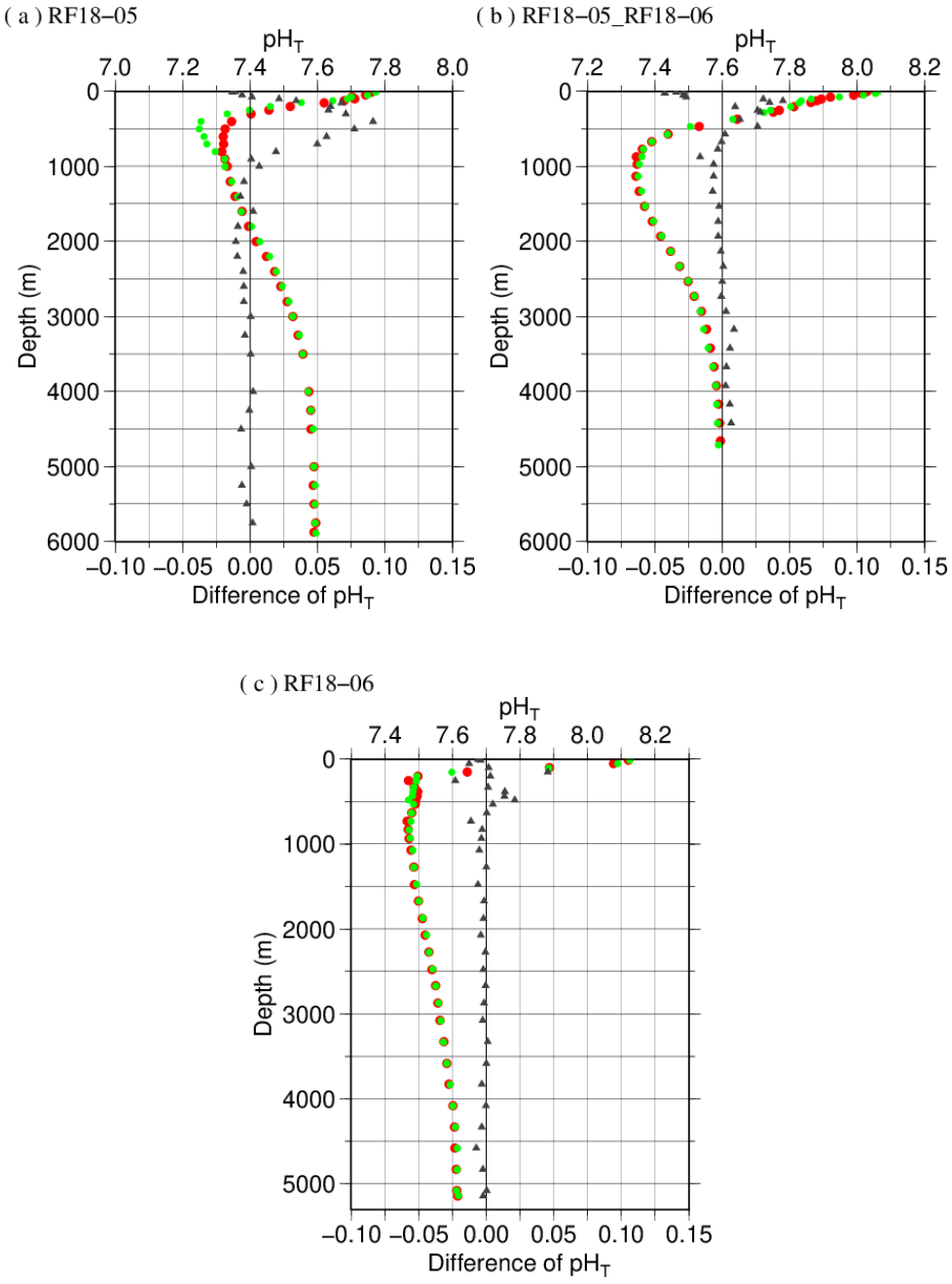

Figure C.8.8. Comparison of pH$_T$ observed at same location in different legs of the cruise: (a) 47˚N/165˚E (in RF18-05), (b) 37˚N/165˚E (in RF18-05 and RF18-06) and (c) 8˚N/164˚E (in RF18-06). The red and green circles denote former (Stns.21, 33, and 73) and latter (Stns.22, 34, and 74) stations, respectively. Triangles denote the difference in pH$_T$ measured at same depth in different legs.

(6.5) Comparison at cross-stations of WHP cruises

We compared pH$_T$ data of this cruise and other WHP cruises by JMA, Japan Agency for Marine-Earth Science and Technology (JAMSTEC) and Scripps Institution of Oceanography (SIO) at

cross points. Summary of the comparisons are shown in Figure C.8.9(a) for cross point with WHP-P4 line (around 9˚N/164˚E), Figure C.8.9(b) for cross point with WHP-P3 line (around 24˚N/165˚E), Figure C.8.9(c) for cross point with WHP-P2 line (around 30˚N/165˚E), Figure C.8.9(d) for cross point with WHP-40N line (around 40˚N/165˚E) and Figure C.8.9(e) for cross point with WHP-P1 line (around 47˚N/160˚E). Data of other cruises are downloaded from the CCHDO web site (https://cchdo.ucsd.edu).

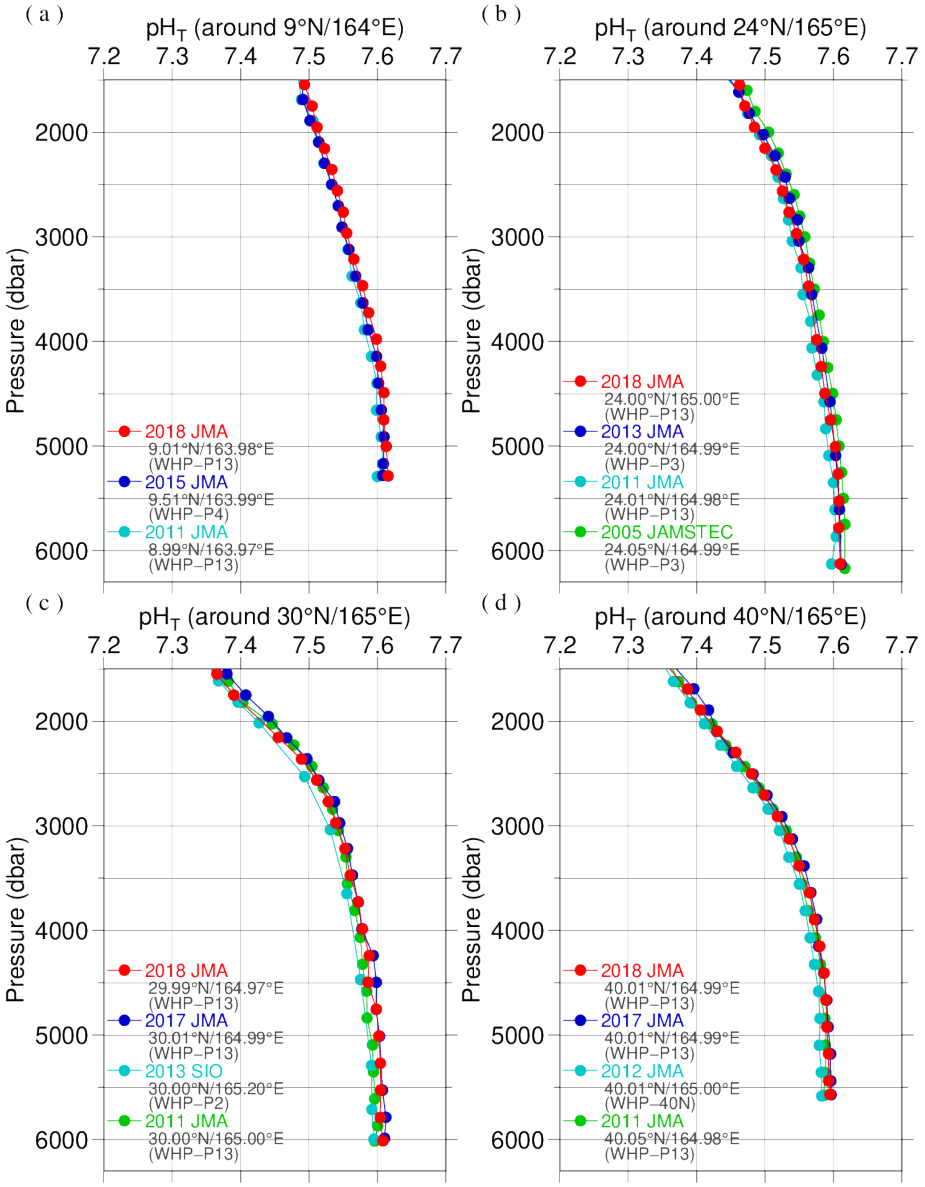

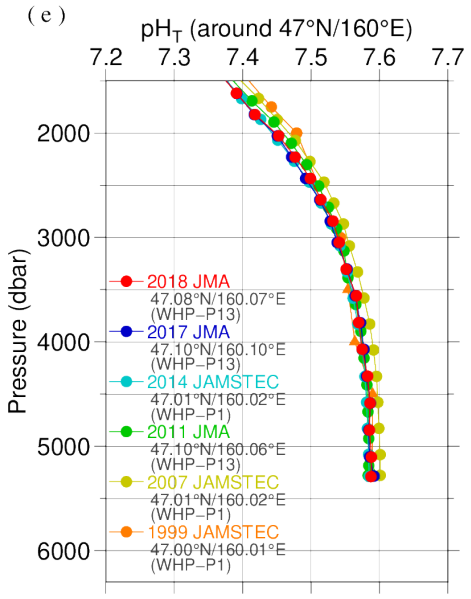

Figure C.8.9. Comparison of pH$_T$ profiles at (a) 9˚N/165˚E (cross point with WHP-P4 line), (b) 24˚N/165˚E (cross point with WHP-P3 line), (c) 30˚N/165˚E (cross point with WHP-P2 line), (d) 40˚N/165˚E (cross point with WHP-40N line) and (e) 47˚N/160˚E (cross point with WHP-P1 line). Circles and triangles denote good and questionable values, respectively. The red ones show this cruise.

(27) Appendix

A1. Methods

(A1.1) Seawater sampling

Seawater samples were collected from 10-liters Niskin bottles mounted on CTD-system and a stainless steel bucket for the surface. Samples for pH were transferred to Schott Duran® glass bottles using sample drawing tubes. Bottles were filled smoothly from the bottom after overflowing double a volume while taking care of not entraining any bubbles, and lid temporarily with ground glass stoppers.

After all sampling finished, 2 mL of sample is removed from each bottle to make a headspace to allow thermal expansion. Although the procedure is differed from Standard Operating Procedure (SOP) described in PICES Special Publication 3, SOP-2 (Dickson, 2007), poisoned with 0.2 mL of saturated $HgCl_2$ solution to prevent change in pH_T caused by biological activity. Finally, samples were sealed with ground glass stoppers lubricated with Apiezon® grease (L).

(A1.2) Measurement

Custom-made pH analyzer (2009 model; Nihon ANS) was prepared and operated in the cruise. The analyzer comprised of a sample dispensing unit, a pre-treatment unit combined with an automated syringe, and two (sample and reference) spectrophotometers combined with a high power xenon light source. Spectrophotometric cell was made of quartz tube that has figure of "U". This cell was covered with stainless bellows tube to keep the external surface dry and for total light to reflect in the tube. The temperature of the cell was regulated to 25.0 ± 0.1 °C by means of immersing the cell into the thermostat bath, where the both ends of bellows tube located above the water surface of the bath. Spectrophotometer, cell and light source were connected with optical fiber.

The analysis procedure was as follows:

a) Seawater was ejected from a sample loop.

b) A portion of sample was introduced into a sample loop including spectrophotometric cell. The spectrophotometric cell was flushed two times with sample in order to remove air bubbles.

c) An absorption spectrum of seawater in the visible light range was measured. Absorbance at wavelengths of 434 nm, 488 nm, 578 nm and 730 nm as well as cell temperature were recorded. To eject air bubbles from the cell, the sample was moved four times and the absorbance was recorded at each stop.

d) 10 µl of indicator *m*CP was injected to the loop.

e) Circulating 2 minutes 40 seconds through the loop tube, seawater sample and indicator dye was mixed together.

f) Absorbance of *m*CP plus seawater was measured in the same way described above (c).

(A1.3) Calculation

In order to state clearly the scale of pH, we mention "pH_T" that is defined by equation (C8.A1.3.1),

$$pH_T = -\log_{10}([H^+]_T/C^0) \qquad \text{(C8.A1.3.1)}$$

where $[H^+]_T$ denotes the concentration of hydrogen ion expressed in the total hydrogen ion scale. $[H^+]_T = [H^+]_F\left(1 + [SO_4]_T/K_{HSO_4^-}\right)$, where $[H^+]_F$ is the concentration of free hydrogen ion, $[SO_4]_T$ is the total concentration of sulphate ion and $K_{HSO_4^-}$ is acid dissociation constant of hydrogen sulphate ion (Dickson, 1990). C^0 is the standard value of concentration (1 mole per kilogram of seawater, mol kg^{-1}). The pH_T was reported as the value at temperature of 25 °C in "total hydrogen ion scale".

pH_T was calculated from the measured absorbance (A) based on the following equations (C8.A1.3.2) and (C8.A1.3.3), which are the same as (C8.1) and (C8.2), respectively.

$$\begin{aligned} pH_T &= pK_2 + \log_{10}([I^{2-}]/[HI^-]) \\ &= pK_2 + \log_{10}\{(R - 0.0069)/(2.222 - 0.1331 \cdot R)\} \end{aligned} \qquad \text{(C8.A1.3.2)}$$

$$R = \left(A_{578}^{SD} - A_{578}^{S} - A_{730}^{SD} + A_{730}^{S}\right)/\left(A_{434}^{SD} - A_{434}^{S} - A_{730}^{SD} + A_{730}^{S}\right) \qquad \text{(C8.A1.3.3)}$$

where pK_2 is the acid dissociation constant of *m*CP. $[I^{2-}]$ / $[HI^-]$ is the ratio of *m*CP base form (I^{2-}) concentration over acid form (HI^-) concentration which is calculated from the corrected absorbance ratio (R) shown in the section 8(5) and the ratios of extinction coefficients (Clayton and Byrne, 1993). A_λ^S and A_λ^{SD} in equation (C8.A1.3.3) are absorbance of seawater itself and dye plus seawater, respectively, at wavelength λ (nm). The value of pK_2 ($= -\log_{10}(K_2/k^0)$, k^0 = 1 mol kg^{-1}) had also been expressed as a function of temperature T (in Kelvin) and salinity S (in psu) by Clayton and Byrne (1993), but the calculated value has been subsequently corrected by 0.0047 on the basis of a reported pH_T value accounting for "tris" buffer (DelValls and Dickson, 1998):

$$\begin{aligned} pK_2 &= pK_2(\text{Clayton \& Byrne, 1993}) + 0.0047 \\ &= 1245.69/T + 3.8322 + 0.00211 \cdot (35 - S). \\ &\quad (293\ \text{K} \le T \le 303\ \text{K},\ 30 \le S \le 37) \end{aligned} \qquad \text{(C8.A1.3.4)}$$

Finally, pH_T determined at a temperature t ($pH_T(t)$, with t in °C) was corrected to the pH_T at 25.00 °C ($pH_T(25)$) with the following equation (Saito et al., 2008).

$$\begin{aligned} &(pH_T(t) - pH_T(25))/(t - 25.00) \\ &= (2.00170 - 0.735594 \cdot pH_T(25) + 0.0896112 \cdot pH_T(25)^2 - 0.00364656 \cdot pH_T(25)^3). \end{aligned} \qquad \text{(C8.A1.3.5)}$$

A2. pH indicator

Indicator *m*-cresol purple (*m*CP) solution

Add 0.67 g *m*CP to 500 mL deionized water (DW) in a borosilicate glass flask. Pour DW slowly into flask to weight of 1 kg (*m*CP + DW), and mix well to dissolve *m*CP. Regulate the pH (free hydrogen ion scale) of indicator solution to 7.9±0.1 by small amount of diluted NaOH solution (approx. 0.25 mol L^{-1}) if the pH was out of the range. The pH of indicator solution was monitored using glass electrode pH meter. The reagent had not been refining.

References

Clayton T.D. and R.H. Byrne 1993. Spectrophotometric seawater pH measurements: total hydrogen ion concentration scale calibration of m-cresol purple and at-sea results. *Deep-Sea Res. I*, **40**, 2115–2129.

DelValls, T. A and A. G. Dickson, 1998. The pH of buffers based on 2-amino-2-hydroxymethyl-1,3-propanediol ('tris') in synthetic sea water. *Deep-Sea Res. I*, **45**, 1541-1554.

Dickson, A.G. 1990. Standard potential of the reaction: AgCl(s) + 1/2 H2(g) = Ag(s) + HCl(aq), and the standard acidity constant of the ion HSO_4^- in synthetic sea water from 273.15 to 318.15 K. *J. Chem. Thermodynamics*, **22**, 113–127.

Dickson, A.G., Sabine, C.L. and Christian, J.R. (Eds.) 2007. Guide to best practices for ocean CO_2 measurements. *PICES Special Publication* 3, 191 pp.

Lueker, T.J, A.G. Dickson and C.D. Keeling, 2000. Ocean pCO_2 calculated from dissolved inorganic carbon, alkalinity, and equations for K_1 and K_2: validation based on laboratory measurements of CO_2 in gas and seawater at equilibrium. *Marine Chem.*, **70**, 105-119.

Saito, S., M. Ishii, T. Midorikawa and H.Y. Inoue 2008. Precise Spectrophotometric Measurement of Seawater pH_T with an Automated Apparatus using a Flow Cell in a Closed Circuit. *Technical Reports of Meteorological Research Institute*, **57**, 1–28.

Swift, J. H. (2010): Reference-quality water sample data, Notes on acquisition, record keeping, and evaluation. *IOCCP Report No.**14**, ICPO Pub. 134, 2010 ver.1*